



HAL
open science

Human locomotion analysis, classification and modeling of normal and pathological vertical ground reaction force signals in elderly

Rami Alkhatib

► **To cite this version:**

Rami Alkhatib. Human locomotion analysis, classification and modeling of normal and pathological vertical ground reaction force signals in elderly. Signal and Image Processing. Université de Lyon, 2016. English. NNT: 2016LYSES029 . tel-01907758

HAL Id: tel-01907758

<https://theses.hal.science/tel-01907758>

Submitted on 29 Oct 2018

HAL is a multi-disciplinary open access archive for the deposit and dissemination of scientific research documents, whether they are published or not. The documents may come from teaching and research institutions in France or abroad, or from public or private research centers.

L'archive ouverte pluridisciplinaire **HAL**, est destinée au dépôt et à la diffusion de documents scientifiques de niveau recherche, publiés ou non, émanant des établissements d'enseignement et de recherche français ou étrangers, des laboratoires publics ou privés.



N°d'ordre NNT : xxx

THESE de DOCTORAT DE L'UNIVERSITE DE LYON
opérée au sein de
Laboratoire d'Analyse des Signaux et Processus Industriels

Ecole Doctorale N° accréditation (Ed SIS n° 488)
JEAN MONNET SAINT-ETIENNE UNIVERSITY, LASPI

Spécialité de doctorat : Sciences Ingénierie, Santé
Discipline : Image, Vision, Signal

Soutenue publiquement/à huis clos le 12/07/2016, par :
AL Khatib Rami

**Analyse, classification et modélisation
de la locomotion humaine : application
a des signaux GRF sur une population
âgée**

Devant le jury composé de :

Guillet, Francois	PU	Universite' Jean Monnet St Etienne	Président
Carrault, Guy	PU	Universite' de Rennes, Laboratoire LTSI, Inserm U 1099	Rapporteur
Nait-Ali Amine	PU	Universite' Paris Est Créteil Val de Marne	Rapporteur
Achour- Crawford Emilie	MCF	Universite' Jean Monnet St Etienne	Examineur
Chkeir Aly	MCF	Universite' Technologique Troyes	Examineur
EL Badaoui Mohamed	PU	Universite' Jean Monnet St Etienne, IUT	Directeur
Diab Mohamad	MCF	Universite' Rafik Hariri - Liban	Co-directeur
Corbier Christophe	MCF	Universite' Jean Monnet St Etienne, IUT	Co-encadrant

ACKNOWLEDGMENT

First and Foremost I would like to thank my advisors Pr. Mohamed El Badaoui and Dr.Christophe Corbier. I appreciate all their effort and contributions of time and ideas to make my Ph.D. experience productive and stimulating. They have contributed to my personal and professional time in my academic career.

Second, I would like to thank Dr.Mohammed Diab for the wealth of experience and valuable insights shared with me via focus valuable group discussions. I will always remember the days and nights that he spent in helping me to accomplish this final work. I'd like also to extend my thanks to Dr.Bassam who provided me with a valuable revision and comments on the whole work.

I would like to acknowledge honorary Rafik Hariri University, the place I have finished my Masters degree, the area where I am currently conduct my studies and research , the occupation where I work and the residence where I live.

For this dissertation I would like also to thank my reading committee members for their time and comments.

Lastly, I would like to thank my family, my students, my instructors and my friends, certainly Mr.Samir Berjoui and Dr.Rached Zantout (My Instructor), for all their love and encouragement. For my brothers and my sisters Amal and Hayat who gave me inspiration, for my parents who raised me with a love of science and supported me in all my pursuits. Thank you.

UN RÉSUMÉ DE LA THÈSE DE

Rami Alkhatib

for

Doctor of Philosophy

Titre de la thèse: Analyse, classification et modélisation de la locomotion humaine : application a des signaux GRF sur une population âgée

La marche est définie par des séquences de gestes cycliques et répétées. Il a été déjà montré que la vitesse et la variabilité de ces séquences peuvent révéler des aptitudes ou des défaillances motrices. L'originalité de ce travail est alors d'analyser et de caractériser les foulées de sujets âgés à partir des signaux de pression issus de semelles instrumentées lors de la marche, au moyen d'outils de traitement du signal. Une étude préliminaire, sur les signaux de pression générés lors de la marche, nous a permis de mettre en évidence le caractère cyclo-stationnaire de ces signaux. Ces paramètres sont testées sur une population de 47 sujets.

Tout d'abord, nous avons commencé par un prétraitement des signaux et nous avons montré dans la première de cette thèse que le filtrage peut éliminer une partie vitale du signal. C'est pourquoi un filtre adaptatif basé sur la décomposition en mode empirique a été conçu. Les points de retournement ont été filtrés ensuite en utilisant une technique temps-fréquence appelée «synochronosqueezing». Nous avons également montré que le contenu des signaux de force de marche est fortement affecté par des paramètres

inquantifiables tels que les tâches cognitives qui les rendent difficiles à normaliser. C'est pourquoi les paramètres extraits de nos signaux sont tous dérivés par une comparaison inter-sujet. Par exemple, nous a assimilé la différence dans la répartition de poids entre les pieds. Il est également recommandé dans ce travail de choisir le centre des capteurs plutôt que de compter sur la somme des forces issues du réseau de capteurs pour la classification.

Ensuite, on a montré que l'hypothèse de la marche équilibrée et déséquilibrée peut améliorer les résultats de la classification. Le potentiel de cette hypothèse est montré à l'aide de la répartition du poids ainsi que le produit de l'âge \times vitesse dans le premier classificateur et la corrélation dans le second classificateur. Une simulation de la série temporelle de VGRF basé sur une version modifiée du modèle de Markov non stationnaire, du premier ordre est ensuite dérivée. Ce modèle prédit les allures chez les sujets normaux et suffisamment pour les allures des sujets de Parkinson.

On a trouvé que les trois modes: temps, fréquence et espace sont très utiles pour l'analyse des signaux de force, c'est pourquoi l'analyse de facteurs parallèles est introduite comme étant une méthode de tenseur qui peut être utilisée dans la future.

AN ABSTRACT OF THE THESIS OF

Rami Alkhatib

for

Doctor of Philosophy

Title of Thesis: Human Locomotion Analysis, Classification and Modeling of Normal and Pathological Vertical Ground Reaction Force Signals in Elderly

Walking is defined as sequences of repetitive cyclic gestures. It was already shown that the speed and the variability of these sequences can reveal abilities or motorskill failures. The originality of this work is to analyze and characterize the steps of elderly persons by using pressure signals. In a preliminary study, we showed that pressure signals are characterized by cyclostationarity. In this study, we intend to exploit the non-stationarity of the signals in a search for new indicators that can help in gait signal classification between normal and Parkinson subjects in the elderly population. These parameters are tested on a population of 47 subjects.

First, we started with preprocessing the vertical ground reaction force (VGRF) signals and showed in this first part of the thesis that filtering can remove a vital part of the signal. That is why an adaptive filter based on empirical mode decomposition (EMD) was built. Turning points are filtered using synchrosqueezing of time-frequency representations of the signal. We also showed that the content of gait force signals is highly affected by unquantifiable parameter such as cognitive tasks which make them hard to be normalized. That is why features being extracted are derived from inter-subject

comparison. For example we equated the difference in the load distribution between feet. It is also recommended in this work to choose the mid-sensor rather than relying on summation of forces from array of sensors for classification purposes.

A hypothesis of balanced and unbalanced gait is verified to be potential in improving the classification accuracy. The power of this hypothesis is shown by using the load distribution and Age \times Speed in the first classifier and the correlation in the second classifier. A time series simulation of VGFR based on a modified version of nonstationary-Markov model of first order is derived. This model successfully predict gaits in normal subjects and fairly did in Parkinson's gait.

We found out that the three modes: time, frequency and space are helpful in analyzing force signals that is why parallel factor analysis is introduced as a tensor method to be used in a future work.

TABLE OF CONTENTS

AKNOWLEDGMENTS	v
ABSTRACT	vi
TABLE OF CONTENTS	x
LIST OF FIGURES	xv
LIST OF TABLES	xx

Chapter	Page
GENERAL INTRODUCTION	1
1. LITERATURE REVIEW	5
1.1 Definition of Human Locomotion	5
1.2 Biomechanics Point of View	7
1.3 Gait Analysis	10
1.3.1 Biometrics	12
1.3.2 Stride Interval.....	13
1.3.3 GRF and Pressure	14
1.4 Preprocessing	17
1.4.1 Normalization.....	17
1.4.2 Filtering.....	19
1.5 Classification	23

1.6 Falls risk assessment, prediction, and detection	25
1.7 Research Motivation	29
1.8 Research Objective	31
2. METHODOLOGY AND TECHNIQUES	33
2.1 Gait Data Description.....	33
2.2 Data Transformation Techniques.....	35
2.2.1 Fourier Transform	35
2.2.2 Time-Frequency Transforms.....	38
2.2.2.a Short Time Fourier Transform (STFT)	39
2.2.2.b Wavelet Transform (WT).....	40
2.2.2.c Hilbert-Haung Transformation	41
2.3 Synchrosqueezing of Time-Frequency Transforms	46
2.4 Modelling	47
2.5 Feature Selection Techniques: ROC.....	49
2.6 Classification Techniques	50
2.6.1 Logistic Regression	50
2.6.2 Principle Component Analysis (PCA).....	52
2.6.3 Discriminant Analysis	53
2.6.4 k-Nearest Neighbors Algorithm (K-NN).....	55
2.7 General Definitions.....	56
3. ANALYSIS & CLASSIFICATION OF VGRF SIGNALS	59
3.1 Filtering	59
3.1.1 Synchrosqueezing Characterize Non-Stationary Signals	68
3.1.2 Turning Points Filtering.....	71

3.1.3 Effect of Dual Task on Gait: Instances where Normalization Fails	72
3.2 Treating the Total VGRF	76
3.2.1 Indications from Hilbert spectrum applied to the raw signal.....	76
3.2.2 Normal and Parkinson	78
3.2.3 IMF General Property.....	79
3.2.4 Zero Crossing effect of each IMF on training accuracy	81
3.3 Frequency Content Analysis.....	83
3.3.1 System’s Frequency Nonlinearity	83
3.3.2 Frequency content	84
3.3.3 Difference between Normal and Parkinson	86
3.4 Analysis of Sensor’s Array.....	88
3.5 Sensor Selection.....	91
3.5.1 Features Used	92
3.5.2 Testing: Features Evaluation by ROC	93
3.5.3 Verification	97
3.5.4 A simple feature of the mid-sensor	98
3.6 Classification Methodology.....	99
3.7 Observations and Methods	100
3.7.1 Center of pressure path	100
3.7.2 Load Distribution	103
3.7.3 Speed and Age.....	107
3.7.4 Correlation	108
3.8 Investigation and Results.....	110
3.9 Discussion and Future Work	114

4. MODELLING OF VGRF	118
4.1 Introduction	118
4.2 Analysis and Motivation	119
4.3 VGRF Analysis for Normal Subject	122
4.4 VGRF Analysis for Parkinson Subject	123
4.5 Modelling Insight into One stride	125
4.6 Periodizing VGRF Signals	128
4.7 Time Series Comparison	131
4.8 Periodgram Comparison.....	132
4.9 Hypothesis	133
4.10 First Order Markov Model	134
4.11 Nonstationarity of VGRF	134
4.12 First Order Markov Model of VGRF with Non-stationarity	135
4.13 Modified First Order Markov Model of VGRF with Non-stationarity.....	136
4.14 Prediction of one step ahead in “Normal” & “Parkinson”	138
4.15 Discussion and Conclusion.....	139
 5. GENERAL CONCLUSION AND PERSPECTIVES	 142
5.1 Summary: The Main Results of this Research	142
5.2 Introduction to the Future Work	145
5.3 PARAFAC Outcomes	148
5.4 PARAFAC Summarizes Information from Multi-Sensors	152
5.4.1 Space Mode.....	154
5.4.2 Time Mode.....	156
5.4.3 Frequency Mode.....	156

5.5 PARAFAC Classify both Normal and Parkinson.....	157
5.6 Discussion.....	159
REFERENCES	160
LIST OF PUBLICATIONS	170

LIST OF FIGURES

Figure	Page
1.1 Phases of walking cycle.....	7
1.2 Standard conceptual models of legged locomotion.....	8
1.3 Angular momentum is conserved around the point of impact.	9
1.4 Limit cycle trajectory for kneed walker.....	10
1.5 Forces during the stance phase.....	14
1.6 Example of Gait Variables.....	19
1.7 Falls injury pyramid.....	28
2.1 Sensor’s position as distributed underneath both feet	34
2.2 Sample of VGRF data captured by the eight sensors underneath the left foot. The red curve represent their summation	34
2.3 Flowchart of Empirical Mode Decomposition algorithm.....	43
2.5 Maximizing the variance of the projection in the residual subspace.....	52
2.6 Flowchart for the K-NN.....	56
2.7 The first row plot is for stationary signal and the rest corresponds for non-stationary signal.....	57
3.1 Vertical GRF vector during Gait Cycle	60
3.2 Ground Reaction Force filtering by second order Butterworth filter of 25 Hz shows a vital part being attenuated colored in red.	60
3.3 During Heel strike, the measured VGRF consist of horizontal frictional component ...	61
3.4 loading response and the push-off are circled.....	63
3.5 Adaptive filter	64

3.6 The first raw is the original signal,Seven IMFs plus the trend are plotted	66
3.7 Segments colored in black are being omitted	67
3.8 STFT and its time averaged applied on the assumed signal $x(t)$	69
3.9 Synchrosqueezed STFT and its time averaged applied on the assumed signal $x(t)$	69
3.10 synchrosqueezed short time Fourier transform	71
3.11 Time Averaged Synchrosqueezed STFT	73
3.12 Synchro squeezed STFT for total VGR signal extracted from the gait of Parkinson subject on both walking conditions	74
3.13 Hilbert spectrum of the VGRF for a normal subject.	76
3.14 Hilbert spectrum of the raw signal corresponding for a control subject.....	77
3.15 Hilbert spectrum of the raw signal corresponding for patient with idiopathic PD	77
3.16 Mean frequency V.S. Zero Crossing for IMF2 of all 47 subjects.	79
3.17 The power of frequency content present in tVGRF and the summed amplitude is different from the summation of frequencies for sensor's VGRF.	79
3.18 STFT plot and upper plot is time averaged STFT	84
3.19 Amplitude of time averaged STFT amplitude for all 8 sensor underneath right foot for a normal subject. The strikes corresponds to frequency tVGRF	84
3.20 Amplitude of time averaged short time Fourier transform - Gaussian.....	85
3.21 Amplitude of time averaged wavelet transform – Lognorm.....	86
3.22 Eigenvalue versus its component number for Left foot sensors in a normal subject ...	89
3.23 Maximum Eigenvalues being computed at different time lags for left sensor to right foot sensors (Red), left sensor to Left foot sensors (Blue), and black indicates when computed for all sensors as one matrix.	90
3.24 Skewness ability in discrimination between Normal and Parkinson Gait using ROC curve.	93

3.25 Skewness is extracted from the total force from sensors located under the right foot and its performance in binary classification is evaluated using ROC curve	95
3.26 The most important locations to acquire data for Gait analysis.	96
3.27 Skewness and Median Frequency are extracted from signals of sensor 5 in mid-foot	97
3.28 Standard deviation versus mean for an abnormal subject upon midsensor located in the right foot.	98
3.29 Path of COP over 30 consecutive steps underneath the right foot for two Parkinson gait subjects. The right columns represent their mean and their standard deviations	100
3.30 Path of COP over 30 consecutive steps underneath the right foot for a Normal gait subject. The right column represent their mean (in blue) and their standard deviations ...	101
3.31 Flowchart of gait classification	104
3.32 Load Distribution underneath both feet in Normal and Parkinson Gaits	105
3.33 Scatter plot with two marginal histograms to envision the association between Speed (m/sec) and Age (years).....	106
3.34 Box plots of Speed in Normal and Parkinson Gait.....	107
3.35 Scatter plot of correlations between right and left foot at sensors 5 and 7. A comparison between Normal and Parkinson Gait (all dataset).	108
3.36 Box plots of Speed in Normal and Parkinson Gait.....	109
3.37 Decision boundary between balanced and unbalanced gait.....	110
3.38 Illustration for test set with respect to decision boundary obtained.	111
3.39 Decision boundary between the two groups of balanced gait based on correlation between right and left foot at sensors 5 and 7.....	113
3.40 Decision tree for the used algorithm.....	115
3.41 Gait Signature.....	116
4.1 Sample of VGRF	119

4.2 Correlogram of VGRF.....	120
4.3 PACF of VGRF.....	120
4.4 Sample and Partial Autocorrelation for a Normal subject.....	121
4.5 Sample and Partial Autocorrelation for a Parkinson subject.....	122
4.6 Sample and Partial Autocorrelation for VGRF signal differenced two times.....	123
4.7 Sample and Partial Autocorrelation for VGRF signal differenced two times.....	123
4.8 Linearity in the plot of current values versus past values in VGRF's data for midsensor on a single step. In this case the difference is one time lag.....	125
4.9 Linearity in the plot of current values versus past values in VGRF's data for midsensor given the 2 min signal.....	126
4.10 Step Isolation of VGRF stance phases at the heel. They are saved over 89 samples equivalent to 0.89 seconds.....	127
4.11 Power Spectrum of the new generated signal.....	128
4.12 Sample Autocorrelation Function.....	128
4.13 Partial Autocorrelation Function.....	129
4.14 Stance phases being isolated from VGRF extracted from the heel sensor underneath the left foot of a normal gait subject and their contour plot.....	130
4.15 Stance phases being isolated from VGRF extracted from the heel sensor underneath the left foot of a Parkinson gait subject and their contour plot.....	130
4.16 Power Spectrum for both altered signals of Normal and Parkinson gait subject.....	132
4.17 Data generated by markov-Model V.S. Raw Experimental Data.....	136
4.18 Data generated by the modified Markov-Model V.S. Raw Experimental Data.....	138
4.19 Algorithm for Modified Markov Model.....	139
4.20 Forecasting Normal and Parkinson Gaits.....	140
5.1 PARAFAC a special case of 2-way PCA.....	147

5.2 Foot being segmented into 5 locations	149
5.3 PARAFAC Model of a randomly chosen subject. Mode#1, 2 and 3 reflect the footedness, time domain signal and the type of foot strike respectively	150
5.4 PARAFAC Model of a randomly chosen subject. Mode#1, 2 and 3 reflect the footedness, time domain signal and the type of foot strike respectively	151
5.5 PARAFAC Model for the same gait obtained in Fig.6.3 but only with the heel and toe sensors	152
5.6 PARAFAC Model for the same gait obtained in Fig.6.3 but only with the heel and toe sensors	154
5.7 PARAFAC Model for the all sensors underneath both feet.	155
5.8 First component after conducting the PARAFAC Model for the all sensors underneath both feet	156
5.9 Loadings Under both Feet for a normal subject and Parkinson subject	157
5.10 VGRF component both Feet for a normal subject and Parkinson subject	148
5.11 Loadings Under both Feet for a normal subject and Parkinson subject	149
5.12 PARAFAC Model conducted on both normal and Parkinson subject over all foot locations	150
5.13 PARAFAC Model conducted on both normal and Parkinson subject under the inner arch of the left foot	160

LIST OF TABLES

Table	Page
1.1 Common falls risk factors.....	28
1.2 fatal falls in numbers	29
2.1 Comparison between various techniques used to analyze our VGRF signals	38
3.1 Intrinsic mode function characteristics	66
3.2 The percentage of certain number of IMFs present in raw signal.....	80
3.2 Omitted IMF effect on training accuracy	82
3.3 Energy percentage compared to the total energy of the original signal, except for Residue	82
3.4 Frequency content	86
3.5 ROC evaluation of skewness among all sensors.....	96
3.6 Balanced vs. Unbalanced Gait- Subjects	113

General Introduction

Why and how do we move? For thousands of years we have been thinking about such question. Still we do not have a very clear idea about the motor act itself. Movement ecology is then developed by biologists to come up with explanations about how limbs move in seconds and how the body dynamic per minutes in addition to the locations being traveled per day. Such a study involves the participation of engineers to explain motion, cognitive scientists to handle navigation, neuroscientist and so on. Newton's law states that acceleration are a cause of forces being applied against environment. Those forces are carried by appendages, limbs,... However, these appendages have to travel with body at the time they asserting forces and transmitting forces from ground to body. As a result definitely there will be oscillation. And if this is the case, they must oscillate in a very tight coordination. This requires a very complicated feedback loops to be understood by engineers and biologists. In other words, enough intelligence is built into our muscles. They function as motors and even as brakes and certainly as springs. What if this intelligence is baked into the whole body?

Understanding human locomotion will inspire us in building robotic passively walking toys, develop a Prosthetics leg exoskeleton robot, improve athletic performance, identification of people for security purposes, diagnose specific pathologies, researching new rehabilitative tools in the treatment of mobility-limiting conditions, motion planning and control problems for under actuated robots and many more.

Our first objective as presented in this thesis is to differentiate normal human gait from abnormal gait, particularly in aged people. This would enhance the ability to figure out gait parameters that could lead to falling if they are subjected to alteration. We will focus only on one kinematic parameter which is by examining the amount of VGRF produced by each foot contacting the ground. To achieve our goals, statistical analysis and modeling are being conducted. There have been numerous studies involving research and development, for detecting falls exhibited by the elderly. Studying and exploiting the nonstationary properties of vertical ground reaction provide an insight into the neural function and the neural control of walking which would be altered by changes associated with aging and the presence of certain diseases.

This thesis is structured as follows:

Chapter 1 provides a definition of human gait bounded to bipedal locomotion. Then biomechanics point of view is presented to inspire our research thinking. Gait analysis techniques are collected as the state of the art of biometrics, stride interval, ground reaction forces and pressures. Since preprocessing is a fundamental step in any signal contaminated with noise, filtering and normalizing techniques are expressed. Moreover, an intuition for classification techniques is presented to classify normal from pathological gaits. Finally, fall risk assessments and their prediction and detection are introduced before we offered our research motivation and objectives.

Chapter 2 delivers data transformation techniques like Fourier transform, wavelet transform and others are presented. Then synchrosqueezing of time- frequency transformations is expressed with its advantages. In addition, receiver operator characteristic is explained as one of

the feature selection techniques. Some of the classification methods used in this thesis are explained. One mathematical modelling technique of the signal is also presented to enhance our understanding of the signal. We end with general definitions that would enrich our empathetic of the reminder of this work.

Chapter 3 provides an intuition of how synchrosqueezing of time-frequency transforms enriches the detection of non-stationarity evidenced with higher resolution behavior and in particular augments signal separation. Most importantly, the effect of cognitive task on gait is clearly pointed out in the context of signal preprocessing. It is also beneficial to extract frequency content of signals certainly the instantaneous frequencies and study their properties in both walking conditions (usual walking and walking while examining cognitive tasks) to inspect if there is a difference in both normal and Parkinson subject.

Various sensory network architectures were designed to capture the most of the biomechanics of walking and running in subjects. In fact, sensor distribution in such designs is crucial and should be delicately treated, knowing that we have continuously varying centers of pressure (COP). That being observed that the sensor located at the inner arch of the sole of the foot (i.e. at mid foot) holds the most relevant information needed for better classification between balanced and unbalanced gait in comparison to other sensor positions, this contradicts the traditional research that only focuses on the summation of the array of signals. It forms a foundation in manufacturing the insole data acquisition system. Then a classification between normal and Parkinson is implemented based on hypothesis of balanced and unbalanced gaits which are ultimately verified.

Chapter 4 mainly focuses on the main statistical component and basis in Gait-GRF analysis. The ultimate objective is to identify model of VGRF in addition to generate and forecast one step ahead VGRF. In fact, a time series simulation of VGRF based on a modified version of nonstationary-Markov model of first order is exposed. An estimate of a normal and Parkinson gait is conducted to spot out a difference between them.

Chapter 5 is a concluding chapter. In this chapter, we emphasize future perspectives in gait analysis. In fact by using multiway analysis mainly parallel factor analysis (PARAFAC), we can verify easily the previous results and deliver more insight about the dataset. Moreover, a comparison between normal and Parkinson is being presented on time, space and frequency modes of PARAFAC. The feasibility of classification using PARAFAC is just introduced.

To conclude, we end up with a summary of the overall results for each path of study, before presenting the research perspectives associated with this work.

CHAPTER 1

LITERATURE REVIEW

Human locomotor system is a complex and higher level of cognitive functioning and dynamical system [1], a rule for time evolution on state space [2]. Very often, state of dynamical systems is described in terms of variables by a set of differential equations. The objective behind this mathematical model is to predict future states giving the past and the present states or to diagnose the past states that led to the present state or in contrary to provide theory for this physical phenomenon [3]. However, gait analysis, the study of locomotion, can be considered to be high stochastic so that the person walk with minimum energy expenditure and then the sequence of observations could infer some features. In addition, time series analysis and its transforms and distributions forms superior to mathematical modeling since we are starting from experimental data. Therefore, is it possible to identify people based on the analysis of their walking gait and thus to predict falls in elderly?

1.1 Definition of Human Locomotion

Human gait is a manner or style of walking and a suited medical term to describe human locomotion [4]. Walking gait defined as sequences of repetitive cyclic gestures as it consists of both periodic movement of each foot from one position of support to a next position of support. In addition, support of body is done by sufficient ground reaction forces applied through the feet [5]. This bipedal locomotion is enhanced by different parts of body like bones, muscle, nervous system and others. Consequently, each limb contributes to braking and propulsive forces, to maintain

balance, as well as they contribute to the forward velocity and to vertical support forces of body [6]. Therefore, any defect in one of those parts may lead to a pathological gait. However, those patients still be able to correct their gait before unexpected fall occurring. In the other hand, physiology alteration and disability including cardiovascular changes and mental health [7] such that problems in cortical processing of information as in dementia could also result in falling [1]. In addition, gait can be affected by a function of many other variables such as aging [8], weight, disease that can deteriorate the correlation in stride interval [9], injuries, skeletal structure, muscular activity, limb lengths, bone structures, etc... [10].

Usual walking cycle shown in Fig.1.1 is made up of three main phases:

- Stance Phase: The foot is on contact with the ground (60 % of gait cycle)
 - o Heel Strike (HS)
 - o Foot Flat (FF)
 - o Mid-stance (MS)
 - o Heel off (HO)
 - o Toe off (TO)
- Swing Phase: The other foot is in air and thus not in touch with ground (40 % of gait cycle).
- Double support: Both foot are in contact with ground (12 % of gait cycle)

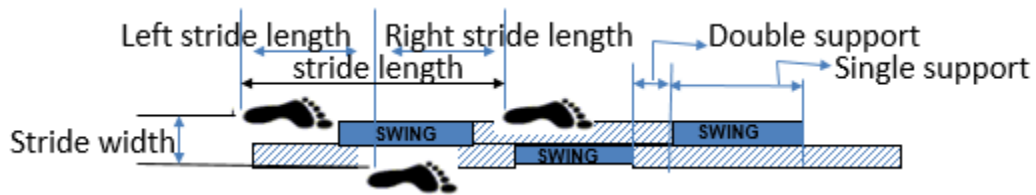


Figure 1.1. Phases of walking cycle

1.2 Biomechanics point of view

Human gait is a legged mobile type of motion where the dynamics and energy management is a main concern. First, those will enable the human body to direct the ground reaction forces (a specific force as it is a force per mass) to outcome a forward movement or redirect them to jump up or even to lead subject to fall and so on. That is why we are interested in the timing, amplitude of forces and the coordination of leg patterns that will definitely give a variety of VGRF signals. Such a variety will give different styles of locomotion. Second, through our legs we can feel the environment and this is so called proprioception. For instance, when we in a stance phase the body need to be in a given posture not to burn any more energy by exerting extra forces on the ground [1]. During push off, the foot pushes against ground and the GRF pushes back against foot. If insufficient traction occur by creating a virtual pin joint, a foot will slide back ward. This can only be achieved by sensing forces of the ground through legs and hips to get balanced and efficient foot to ground contact. However, we must spend energy to get into our ends. Specific power that result on how to move energy from one form into another can be thought as the speed at which a GRF can be sustained resulting in a stable energetic display called basins. For illustration, basins of attraction places energy at its lowest states.

In biomechanics, we look at the behavioral components by modeling the human walking by so called templates to give a simplest model that describes the target behavior and then embed them into a higher dimensional physical system so called anchor. In addition, we also focus on physical components that's corresponds to the materials and their compliance properties, structures and energy needed by our actuator muscles. For instance, walking can be thought as a vaulting over inverted pendulum executing compass gait as shown in Fig. 1.2[1]:

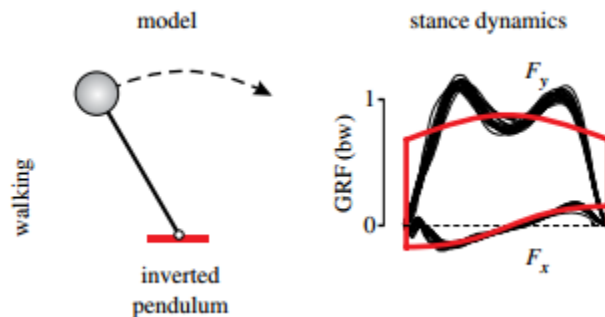


Figure 1.2 Standard conceptual models of legged locomotion. The inverted pendulum is a standard model for walking. The model-predicted stance dynamics (red lines) fit experimental data (black traces recorded from human treadmill walking). Horizontal and vertical ground reaction force (GRF) normalized to body weight (bw).

Therefore human walking results from complex dynamical interactions between the subject whom is made up of complex multi-link mechanism and environment [12]. In above model, it is clear that part of mechanical energy is pertained from one stride to the next stride. Then the massless model can be derived as in equation (1.1) based on D'Alembert principle:

$$\begin{aligned}
X &= X_{com} - \frac{\ddot{x}z}{\ddot{z} + g} \\
Y &= Y_{com} - \frac{\ddot{y}z}{\ddot{z} + g}
\end{aligned}
\tag{1.1}$$

The center of mass is denoted by “com” and has the coordinates (X_{com}, Y_{com}) . The dynamic equation is then given by equation (1.2):

$$\ddot{\theta} = \frac{g}{L} \sin \theta
\tag{1.2}$$

During foot collision as shown in Fig.1.3, the angular momentum around the point of collision at time just before the next foot collides with the ground is $L(t^-) = -ml^2\dot{\theta}(t^-) \cos(2\alpha)$.

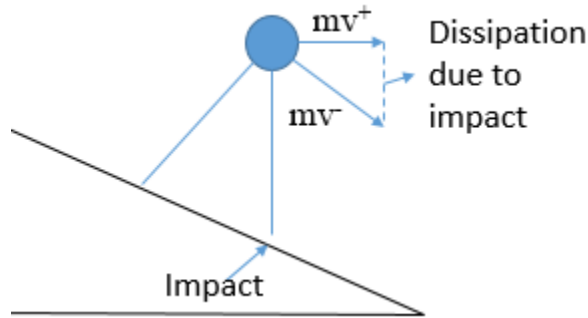


Figure1.3: Angular momentum is conserved around the point of impact

The angular momentum at the same point immediately after the collision is

$$L(t^+) = -ml^2\dot{\theta}(t^+)
\tag{1.3}$$

Assuming angular momentum is conserved, this collision causes an instantaneous loss of velocity:

$$\dot{\theta}(t^+) = \dot{\theta}(t^-) \cos(2\alpha)
\tag{1.4}$$

Different models being adopted to understand how the foot impacts the ground in addition to understanding how humans walk. Fig.1.4 is another way of analysis. However, we will not delve too much in this domain throughout this thesis and we can handle this in a future work.

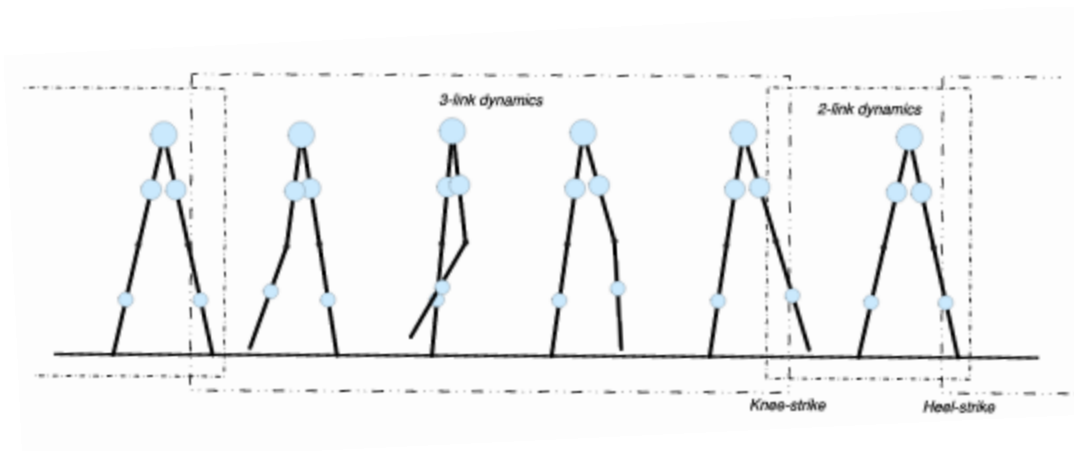


Figure 1.4: Limit cycle trajectory for kneed walker

1.3 Gait Analysis

Gait analysis is used in many applications including the improvement of sports techniques and performance, assisting disabilities by improving rehabilitation programs, the planning and assessment of surgical outcomes, and the recognition of gaits due to falls-risk in the elderly [13].

The human locomotor system is a dynamical system, a rule for time evolution on state space [14]. Very often, the state of dynamical systems is described in terms of variables by a set of differential equations. The objective behind this mathematical object is to predict future states given the past and the present states or to diagnose the past states that led to the present state or in contrary to provide theory for this physical phenomenon [15]. However, gait analysis can be considered to be highly stochastic where the sequence of observations could infer some features.

Human body requires a continuous contact with the ground during walking and thus GRF formed as reflections of various forces that the entire body examine during gait. VGRF holds the major amplitude and thus has been a topic of interest for many scientists certainly when dealing with its peak value [16]. They are highly correlated to bone growth and strength [17]. Their profile is also proved to examine gait mechanics of powered exoskeleton-assisted walking and reflections to the amount of loading given that subjects are of different level of assist and with different weights and cadences [18]. In addition, VGRFs capture various parameters with no need to measure them. For instance, The peak vertical ground reaction force shows a linear relationship with drop height [16]. Furthermore, they are used in diagnosing the effectiveness of surgeries at knee and hip, neuromuscular impairments like in Parkinson's disease, analyses of injury risk, assessment of falling risk, biomechanics and so on [14].

Human walking is produced based on all information acquired from the environment that would affect the walking pattern. With the help of the central nervous system, humans will fit their walk to maximize their stability. Understanding the internal forces inside human body are not limited to rehabilitation, prosthesis design, biomechanics, robotics modelling, sports [16] and others, but exceed to cover sensor validation when it comes to real implementation of gait system. However those forces are hardly measurable [19]. An alternative was to use external forces that are readily observable (experimental data) that serves as an input for musculoskeletal modelling (computer based simulation) to estimate those in vivo forces. This is the potential of inverse dynamic analysis. Having then the VGRF mathematically modelled introduces some inconsistency stemmed from the boundary conditions.

It was proven that each person has a specific and unique gait pattern [11]. It has been used in biometrics as gait information acquired to identify individuals, differentiating between normal and patient subjects, orthoses and prostheses devices for rehabilitation, and assessing fall risk among subjects as this study concerns, where elderly are our apprehension. Gait analysis can be done using different techniques. For example, gait variability considered as a quantifiable feature of walking in clinically relevant syndromes, such as falling, frailty, and neuro-degenerative disease [7]. Moreover, biometrics, stride interval, ground reaction force (GRF), pressure which is our focus are used in gait analysis. Other forces like gravitational force, muscular force and forces of momentum considered also forces of gait. Such biomechanical parameters and others like heel velocity and cadence could give a great insight into gait analysis.

1.3.1 Biometrics

In biometrics (the recognition of people by their physiological or behavioral characteristics), person's walking can be recognized from the non-stationary in the distribution of 2D image features relationships over time which are represented as points in a space of probability functions (SoPF) using standard pattern recognition techniques such as the principle component analysis (PCA) that is applied over probability functions [20]. As gait is considered a behavioral biometric, dynamic features extracted from different parts of the body can be perceived from a distance without personal contact [10].

1.3.2 Stride Interval

Studying stride interval data can also be used in analysis of human locomotion [7]. One of the techniques used is recurrent plots and recurrent quantification. The main advantage of the recurrence plots over another widely used techniques as for example Fourier analysis, is that they preserve both temporal and spatial dependence in the time series. Their analysis shows that the gait maturation data are mixed of high dimensional deterministic and stochastic process with maturation signals become more stochastic. The gait analysis of neurodegenerative diseased people show high stride interval with low speed and increased instability. According to a study, patterns in the recurrence plot of stride interval variability differentiate healthy from diseased, young from old [21]. It's also shown that normal gait exhibits long range correlation in stride interval and its deterioration implies an aging or disease [22]. However, it's worth mentioning that subjects who underwent a Physical Rehabilitation Program (PRP) for four consecutive weeks, the coefficient of variation (CV) improved in Parkinson disease (PD) and remained constant and smaller for control one. Unfortunately, there was no statistically significant difference between groups [23]. The dynamics of gait examine alterations in the fractal pattern with healthy aged [7].

Some other result based on wavelet denoising based on Inertial Measurement Unit (IMU) that measure both gravitational acceleration vector and acceleration due to body movement. This lead to two factors of gait and postural characteristics: double-support time and postural transition times. And their variation in elderly indicates instability [24].

1.3.3 GRF and Pressure

As mentioned, GRF provides significant information in differentiating between normal walking and pathologic gait [25]. Accordingly, disorder in gait implies that a subject is patient. Pathological gait is then can be used for clinical purposes. GRF is generated initially by a nerve impulse in central nervous system [5]. GRF is a “*reflection of the total mass-times-acceleration product of all body segments and therefore represents the total of all net muscle and gravitational force actions at each instant of time over the stance phase*”[26 ,27]. This force can be measured in 3-D, three axis as shown in Fig.1.5 [28]: mediolateral (F_x) , anterior-posterior force component (F_z) in the sagittal plane, and longitudinal (F_y) [29].

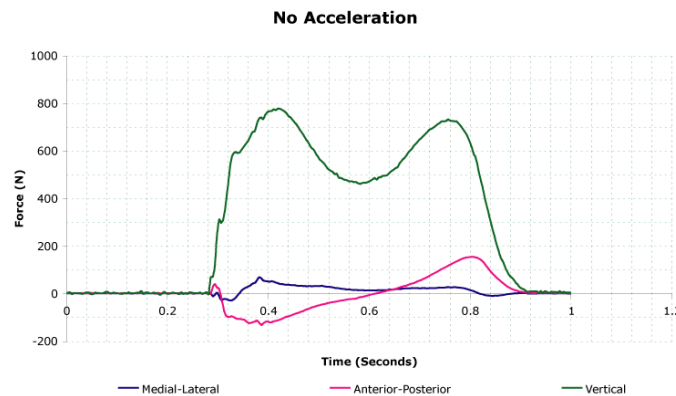


Figure 1.5. Forces during the stance phase

The vertical (F_y) GRF has a characteristic double hump. The first hump appears at heel contact, showing a rapid rise to a value in excess of body weight as full weight bearing takes place and the body's downward velocity is being arrested. Then, as the knee flexes during midstance, the plate is partially unloaded and F_z drops below body weight. At push-off the plantar flexors are active, causing a second force peak greater than body weight, which

demonstrates that the body's center of mass is being accelerated upwards to increase its upward velocity. Finally the weight drops to zero as the opposite limb takes up the body weight. Therefore, the vertical component of GRF which is our concern can be classified into M-shaped and non-M-shaped. This classification is correlated with both gait parameters and functional performance as the pain component of the Japan Orthopaedic Association (JOA) score [30]. In addition, the type of foot contact with the ground could also affect the shape of VGRF. Knowing that, VGRF has no significant differences between the left and right foot during walking and not affected by the sex of normal subjects [30]. Unfortunately, the vertical load curve has been found to be unreliable as a clinical measure [31]. In contrary, vertical GRF has been shown to be reliable and repeatable feature of gait [30]. Cyclostationary modeling of GRF signal where it's periodically varying statistics and its contribution to PSD (Power Spectrum Density) is used to characterize the gait and running assessment where during locomotion, parameters vary from step to step. The PSD analysis of GRF signal indicates the presence of periodic part and the presence of resonance frequency. The cyclic spectra before and after fatigue shows that the amplitude of the spectral correlation density (SCD) is more after fatigue which is due to the tiredness of the runner. Therefore step fluctuation signal increases after fatigue i.e. the frequency of the step become more random [32]. In addition, the first two principal component coefficients of GRF are used to differentiate between normal and patient with lower limb fracture and how the later coefficients moves toward the normal region after the linear separator with a rehabilitation treatment [33]. A further study proposed a score to quantify the abnormality of gait where two, four and six PCCs were used to obtain the standard distance (D) and using the six sigma have the best accuracy of 96.1%. The study

shows that D decreased for that fracture group after rehabilitation (FGA). In addition, FG subjects had positive PCC while control group (CG) subjects presented negative values [34]. GRF measured during a run on a treadmill is also used to characterize the runner's step and its analysis is based on cyclostationary to model signals with periodically varying statistics, instead of assuming it statistically stationary signal features [32]. Separation results of GRF signal using Blind Source Separation (BSS) as to separate multiple sources mixed through an unknown mixing system using spatial diversity which is given by system outputs offers good results in separation of the contribution of each leg [35]. Some results also shows that the frequency components difference of the GRF may not significantly recorded. For instance, t-tests were used to examine the frequency content of all three components of the ground reaction force in patients with Essential Tremor (ET) and PD and results are not significantly different from each other [6]. It also revealed no significant difference in the vertical GRF between young and elderly females. Where a significantly higher frequency content in elderly compared with young females in the anterior–posterior direction [36]. However, one can reduce the effect of determinants by taking one component of the force. For illustration, aging differences were not detected in vertical direction of GRF using the frequency domain analysis in both elderly and young [36]. The maximum peak value in vertical GRF is observed to be high in parkinsons group and was not observed in healthy. In addition, a trouble in damping down vertical axis perturbation occurs in PD subjects [29].

Pressure can also be used in the gait analysis and therefore to detect falls in elderly that may cause serious injuries. The center of pressure is shown to be the neuromuscular response

to imbalances of the body's center of gravity. The comparison between left and right leg during normal gait cycle shows a high similarity [31].

1.4 Preprocessing

Before using data for any purpose, preprocessing must be performed on the data to remove any undesirable characteristics that were produced during acquisition. For instance, normalization and filtering of the signals are being pointed out in the scope of others work.

1.4.1 Normalization

If one variable is to be normalized to another variable, it is important to understand the relation between them [37]. For instance correlation coefficients are normalized to fall between zero and one which makes them insensitive to the variations in the gain of the data acquisition process. However, in our case, the variable scales are similar and therefore one can use covariance instead to compare between two variables. In a large number of studies, Division normalization of GRF data were successful. Such kind of normalization occurs through dividing the data by parameters like body weight (BW) [25], [27], [38], [39] body mass [29], body weight x height (BWH), and body weight x leg length (BWL) [34]. Others investigate the power curve normalization, and offset normalization on peak GRF to normalize data at all variables [40]. Power curve and offset normalization, however, were effective at normalizing all variables, “therefore, when attempting to normalize GRF and joint moments, perhaps nonlinear or offset methods should be implemented” [40]. In another study that takes running into consideration shows that normalizing peak forces by linearly scaling to body weight is not an appropriate

method. It also has been documented that normalizing VGRF signals through dividing by body weight to the power (BW^α), where α is the exponent of the best fit power curve equation, effectively eliminates the influence of the body weight on the data set [37]. In contrast one could also found that GRFs were normalized to body weight (BW) and % stance phase [38]. And as the GRF is normalized by body height in some studies, a different constraint is also normalized by the same parameter, for instance the distance parameters of stride length and step width were normalized for the height of the subject [30]. In addition, the distribution of number of falls, DST, CV step length and CV stride time variables were also found to be normalized using log transformations [41].

Normalizing VGRF by the mass is not an accurate practice since the body will be moving in the three directions making it difficult to compute the mass that contributes to the vertical force. The 26 bones that are forming the foot will act as a rigid lever and termed as supination. However this is possible during the stance phase where all body is most likely be supported by a single foot but still need more investigation. Nonetheless, since the viscoelastic properties of the shoe affect the load rate [29], diseases that reduces level chemical mediator production by neurons that are essential on movement coordination [42], and other parameters like age and height as shown in Fig.1.6 includes examples of variable that could interfere in gait ground reaction force.

Many others are complicated enough to be estimated in a quantifiable way like when having emotional and psychological case.

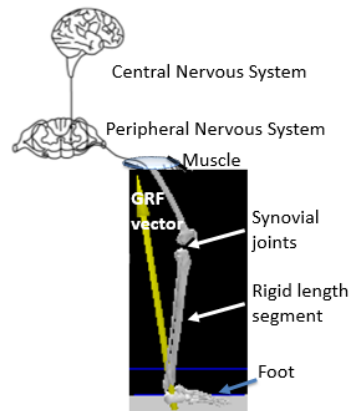


Figure 1.6: Example of Gait Variables

That is why normalization is a topic that needs accurate dealing that help in avoiding us from handling data in a wrong way and therefore result in erroneous interpretations. Some questions that rises: Is there a need for normalization? Why? When? And How? In addition to what appropriate elucidation restrictions one should follow. It is enough to remember that during heel contact the body weight begins to shift into stance limb.

1.4.2 Filtering

Filtering removes any unwanted disturbance in any signal GRF data. For instance, the presence of noise can totally mask the true information in data. In addition, it's significant to eliminate sources of variation on the measured VGRF like the influence of mediolateral and anterior-posterior variations.

Butterworth low pass filter of second order with 20 Hz cut-off frequency is used to smoothen GRF data because during walking on treadmill, white noise existed due to vibrations and motion artifact [27]. Fourth-order low-pass Butterworth filter with a cutoff frequency of 100 Hz used to smooth the data before analysis in another study [37]. In addition, further study used

GRF data after being filtered at 50 Hz with a second order low pass Butterworth filter [21]. The vertical GRF is low passed filtered with a cut-off frequency 15 Hz to reduce measurement noise according to another article [29]. While other studies consider the reservation GRF data as being filtered using a 7 point moving average [38]. GRF data were also filtered with a cutoff frequency of 75 Hz [21]. However, in another study GRF data were filtered using a low-pass filter with 50 Hz cutoff frequency [23]. In a further study, 13-point moving average low-pass filter with a cut-off frequency of 33.3Hz was used to filter the GRF data [43]. Moreover, GRFs were low-pass filtered using a fourth-order, zero-lag Butterworth filter with a 20 Hz cutoff frequency in alternative study[39]. A second order Butterworth filter with a 6 Hz cut-off frequency is being used in a different study [44]. However, it was recorded that the frequency content of ground reaction during walking for both vertical and lateral components to be less than 9 Hz. While in running the vertical is less than 10 Hz and for the lateral component was at frequencies less than 17 Hz [44]. In order to eliminate noise and not affecting the data, a fourth order low passed Butterworth nonrecursive filter with 25 Hz cutoff frequency is chosen to be 25 Hz at the former study [44]. Such kind of filtering without relying on a given basis may remove components of the actual movements [45].

Antonsson's database composed of two categories, runners and walkers. He studied 30 foot contacts from 12 subjects. By applying FFT spectral power analysis of these force records, 99% of the integrated power content of VGRF signals below 9 Hz. For running, 99% of the integrated power content of the VGRF signals was at frequencies less than 10 Hz [27, 38]. Furthermore, the amplitudes above 10 Hz are recorded to be less than 5 % of the fundamental frequency. 2 % above

20 Hz and all amplitudes more than 1 % are delimited below 50 Hz. 99.5 % frequency in VGRF is recorded to be 6.39 ± 2.31 Hz in Parkinson subjects. The median frequency is found 0.45 ± 0.09 Hz and the bandwidth is said to be 1.23 ± 0.29 Hz. A difference is found in frequency content when compared to healthy subjects [39]. After averaging the VGRF signals of PD subjects, the power of high frequency is lower and the first and second peak's amplitude are lower than normal subjects with a delayed occurrence of the first peak. The average power is between 0.5 Hz and 1.5 Hz is logged in PD [29].

These results helped in the process of selecting the appropriate filter that is the fourth order Butterworth filter with a 25Hz cutoff frequency. This filter appeared to eliminate 99% of the noise while retaining all of the important components of the signal [38]. Another research done in the University of Nebrashka Omaha has discussed the effect of multiple sclerosis on the frequency content in VGRF during walking by applying Fourier transform on the signals. Wurdeman et al. results showed that patients with multiple sclerosis had significantly lower than 99.5% frequency ($P= 0.006$) and median frequency ($P<0.001$) in the vertical ground reaction force. The lower frequency content suggests lesser vertical oscillation of the center of gravity [40]. Analysis of the frequency content may potentially serve to provide earlier diagnostic assessment of this debilitating disease [40].

Likewise, frequency content of various body movement is recorded to be less than 20 Hz where 99% of the FFT spectrum is contained below 15Hz in walking signals [40]. However as a majority of the signal existed below 10 Hz as shown by Simon et al, at the heel contact a peak appeared with frequency content of 10-75 Hz. Giakis and Baltzopoulos indicated that 95 % of

signal's amplitude is within the first 15 harmonics up to 20.27 Hz [30]. Vertical GRF impact peak is assumed within 8-50 Hz given that it will visually absent in time domain for forefoot running and a suggestion of an overlap between impact and active peak frequencies do exist [35]. Moreover, the standards for testing prosthetic components required for ankle-foot in order to study the fatigue process are by applying alternating forces within 0.5-3Hz as given by the international organization for standardization [36].

1.5 Classification

Many studies examined the exceptional ability of humans to develop internal models of environmental dynamics by learning different motor tasks. Those models related to walking could be updated by providing unexpected environmental force perturbations [40]. Studies show that one limb is responsible for transferring and supporting body weight while the contralateral limb is responsible for providing propulsion. For instance, the limb dominance shows a great impact on VGRF and COP [47]. Symmetrical foot loading patterns are recorded in normal gait. It is found that Mediolateral (F_x) and vertical (F_z) forces have no significant difference. This asymmetry becomes significant in pathological gait at fast walking [48].

Numerous variables interfere in gait ground reaction force such as age and height. The viscoelastic properties of the shoe is another parameter that affect the load rate [49]. Diseases that reduce level chemical mediator production by neurons are also examples that mark movement coordination [42]. Many of them are complicated enough to be estimated in a quantifiable way like when having emotional and psychological cases.

The preferred walking speed of many humans is around 1.4 m/s. This forms a sign of independence and mobility [50]. The speed selection in elderly tends to be slow. This is a usual prominent characteristic in Parkinson subjects caused by degeneration of central nervous system and decrease in ability to control the locomotors system. Gait variability is shown to increase with slower walking speed in addition to age. However, elderly with gait disability have a tendency to walk more slowly to improve their dynamic stability regardless of increasing gait variability that is known to increase risk of falling [51]. Walking speed could minimize metabolic energy costs which is associated to aerobic capacity that is correlated with aging [52]. Furthermore, there is a need to distinguish the effect of walking speed from the effect of age on gait variability. In trunk roll angle, Age \times Speed displays a crucial interaction. Research results indicate that variations in gait variability occur in healthy normal aging [53]. Likewise, the foot clearance is too small in elderly. This could be reflected by the COP variation underneath the foot. Certainly, patients with idiopathic Parkinson Disease (PD) have gait disturbance marked by postural instability, slow walking in addition to shuffling and a difficulty in initiating steps [54]. Such disturbance could lead subject to lose stability and fall. Consequently, Gait variability in addition to other factors associated with aging is correlated to risk of falling in elderly [53]. Injuries in elderly, due to falling have turned out to be very serious with the increase in the life expectancy and aging in population [55].

On the other hand, one of the studies shows that the first two principal component coefficients of GRF can be used to differentiate between normal and patient with lower limb fracture and indicate how the later coefficients moves toward the normal region after the linear

separator with a rehabilitation treatment [25]. A further study proposed a score to quantify the abnormality of gait where two, four and six principle component coefficients (PCCs) were used to obtain the standard distance (D) and using the six have the best accuracy of 96.1%. The study shows that D decreased for that fracture group after rehabilitation (FGA). In addition, fracture group subjects had positive PCCs while control group subjects presented negative values [1].

An artificial neural network (ANN) has been used successfully used to diagnosis correctly 10 out of 10 PD patients and 9 out of 10 healthy subjects [37]. The average power between 0.5 Hz and 1.5 Hz and between 1.5 and 20 Hz in addition to swing phase , first and second peak magnitude normalized by body weight, time of first peak, and DFA scaling exponent α for the left and right foot are used as features for ANN. The total accuracy is recorded to be 95%. Fourier transform coefficients served as inputs as stated in a review article [29] into ANN with one hidden layer and achieved also 95% accuracy in distinguishing pathological gait from normal one. Kohonen maps is also used for clustering locomotion kinetic characteristics in normal and Parkinson's disease based on the following features: Mean Coefficient of Variation, Mean Sum of Variation, Mean Max and Mean Standard deviation of the VGRF. A sensitivity and specificity of 94.44% and 88.23% respectively are being recorded [42]. On another study, applying Principal component analysis to Spatial-Temporal Image of Plantar pressure that includes both temporal and spatial information among the change of plantar pressure during heel to toe motion, yields a classification of accuracy of 91.73% by applying support vector machine using the weights on each principal components [56].

1.6 Falls risk assessment, prediction, and detection

Fall by definition is “an event whereby an individual comes to rest on the ground or another lower level with or without the loss of consciousness” [57]. A kind of fall is preceded by missteps which is defined near falls but if no sufficient recovery mechanisms are activated, a fall will result due to loss of balance [58]. Note that the mentioned is one type that reveal an etiology of fall. Most falls occur during whole-body movement like walking. It can be analyzed from two perspectives: kinematics to know the motion and position of different joints and/or kinetics by studying the force that cause the motion. Therefore, dynamic stability and its control mechanism during walking are crucial to understand falling. It is known that greater variability indicates greater instability. That’s why there is a need for accurate gait analysis that provide with specific risk factors for falls that improve diagnosis and better understand risk of falling [1]. Occasionally, Psychophysical, Biomechanical, Tribology, and Epidemiology of falls in the Elderly are not introduced in complete details. For occurrence, dementia-related gait changes could be used to diagnosis the risk of falling in dementia and pre-dementia stage [1]. Subjects with Alzheimer’s disease tend to walk in a slower speed and therefore support time increase and decrease in stride length [1]. Furthermore, elderly tend to move slower but this will not ensure the risk of fall because younger people could also move slowly. Though, elderly usually exhibit significantly faster horizontal heel contact velocity but shorter step length and slower transitional acceleration of the whole body center-of-mass (COM) than younger. This affect initiation of slip-induced falls [59]. That is why when heel contact occur, the heel sliding velocity should decrease to a certain level. The major cause of falling among elderly is reported when trying to avoid an obstacle [60]. The faster a step is executed

during perturbations increases the chance of preventing a fall from occurring and this clinically viewed from the parameter “foot contact time” among the step execution parameters (Initiation Phase, Preparation Phase, Swing phase, Foot off time, Foot contact time) extracted from GRF [61]. Study findings show an increase in mediolateral sway in narrow base stance in older faller individuals. Also, static two-point discrimination (TPD) seems to be weakened in elderly fallers. This could be used as an indicator of falling risk [62]. For aged individuals who fell more than once during 12 month exhibited linear association between double support phase besides to step length variability and increased risk of multiple falls [41, 63]. Multiple falls can be predicted from gait dysfunction in cognitive impaired older adults and is mediated largely by sensorimotor function and to a lesser extent by neurophysiological function [41]. One study demonstrates the deficit of co-existing sensory like poor vision and hearing form a key to increase risk of falling [64]. In another study, Lyapunov exponents directly quantify how the neuromuscular system responds to local perturbations and this should have a study to investigate if it has a relationship with a risk of fall [49]. In the other side, developing a model for detection of balance impairment and estimation of the falls risk in the elderly using Support Vector Machines (SVM) based on wavelet multiscale analysis of minimum foot clearance (MFC) as a gait variable [8]. Again, the postural perturbations combined with a cognitive task shows that older influenced more than young during quiet standing [65]. Therefore regaining postural stability is highly perturbed by a secondary task during obstacle clearance which increase the risk of falling because of the inability to recover from slips and trips during gait. This can be explained by the inability to effectively allocate attention to balance under multi-task conditions with poor executive function mainly in elderly [61, 66]. For illustration, when aged participants asked to count aloud backward from 50

associated with walking, this task was strongly linked with falls and this characterizes a new way to predict falls among elderly [67]. A measurement of standing balance termed “Functional Reach (FR) test” can predict falls in elderly people [30]. Furthermore, Berg Balance Test (BBS) and Timed Get Up and Go (TUG) can be used to assess balance and gait function, however they don’t indicate any significant statistical difference between elderly fallers and non-fallers. In contrast, adding cognitive load to the Voluntary can identify elderly individuals at risk of falls [68]. In order to discriminate fallers from non-fallers, fractal scaling index of gait is useful [7].

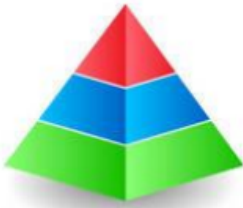
Given that there is still no worldwide consensus on the definition of falling, some research documented falling to be approximately one in three people over the age 65 [57]. Elderly are the most rapidly increasing proportion of the society [65]. Reported falls in older adults shows 40-60% of falls lead to injuries and this costs social and economic apprehensions [57]. For instance, it can cause considerable mortality, morbidity, reducing functioning and home nursing [69]. That’s why a fall with its psychological impact can increase the self-restrictions of activities and therefore a decrease in quality of life [68]. Table 1.1 explains the common fall risk factors [57].

	Intrinsic	Extrinsic
Non-modifiable	Age, Gender History of previous Falls Acute or Chronic medical problems (e.g. Parkinson’s, osteoporosis, cardiovascular disease) Neurological function	Environment outside of home (e.g. uneven paving, ice)

Modifiable	Gait, Balance, Mobility levels,	Poly-pharmacy
	Lower extremity joint function	Footwear
	Lower extremity muscle strength	Home Environment (e.g. loose rugs, steps)
	Cardiovascular status (e.g. blood pressure, heart rate and rhythm)	
	Visual Acuity	
	Self-efficacy, and Fear of Falling	

Table 1.1: Common falls risk factors

1.7 Research Motivation



- > **Approximately 36,000 older people are reported to be fatally injured from falls every year in the EU**
- > **1,443,000 fall-related injuries are admitted to hospital each year (40 x number of deaths)**
- > **2,314,000 older people attend emergency departments with fall-related injuries each year (65 x number of deaths)**

Figure 1.7. Falls injury pyramid

In this section, we will present the key motivation points of our research and can be summarized as follows:

- Falls are a leading cause of serious injury and death among elderly people over 65. For instance, the falls injury pyramid in European Union (EU) for those people is reported as in Fig. 1.7 [70].

The fatal falls reported over the years 2010-2012 by EU-member states to the WHO-office for the European Region is shown in Table 1.2. The mean age in France standardized incidence rate (IR) per 100.000 persons with age of 65 and older (IR 65+) is reported to be 45.85 [28].

	Fatal falls 65+	Pop 65+	IR 65+
Austria	704	1706551	41,23
Belgium	1107	1676350	66,06
Bulgaria	128	1414308	9,07
Croatia	910	762664	119,32
Cyprus	16	5676956	0,28
Czech Republic	733	1185077	61,88
Denmark	439	823617	53,30
Estonia	46	982505	4,72
Finland	971	3655800	26,55
France	5015	10936782	45,85
Germany	8681	11553329	75,14
Greece	274	5734847	4,78
Hungary	1522	1135797	133,97
Ireland	176	558561	31,57
Italy	2864	7816841	36,64
Latvia	79	817381	9,62
Lithuania	164	364934	45,03
Luxembourg	42	906153	4,67
Malta	28	526893	5,38
Netherlands	1602	3711225	43,17
Poland	2776	4445561	62,45
Portugal	243	1373418	17,72
Romania	556	2316382	24,02
Slovakia	202	771813	26,17
Slovenia	449	767308	58,52
Spain	1718	8445526	20,35
Sweden	822	1201149	68,46
United Kingdom	3578	8669589	41,27

Table 1.2: fatal falls in numbers

- **First** cause of accidental death, **third** cause of chronic disability, and the **fifth** most common cause of death [71- 72].

- In France, the yearly number of falls is approximately 2.7 million[73]

- One person in three over the age of 65 will fall on average once a year, and from the age of 80 this ratio rises to one in two. [73]

- Every year in France, nearly 400,000 seniors are an accidental fall.

- Nearly 12,000 people die.

- The number of fractures of the femoral neck in France each year is estimated to be 50,000 [74].

- 70% of all fatal falls occur at home [73].

- After a fall, the risk of falling again in the same year is multiplied by 20. fallers develop phobia of falling again

- The risk of falling increases with age. Each year, falls affect:

- 35% of those aged 65 to 79 people;

- 45% of people 80 to 89 years;

- 55% of people over 90 years.

- The costs of falls is

- 25 billion Euros each year in the EU
- \$19.2 billion in the US in 2006 [75].
- More than £4.6 million a day in UK [76]

1.8 Research Objective

As mentioned previously, human gait is considered complicated dynamical system and their analyses based on observable data contaminated by noise. Therefore, improper methods can lead to wrong outcomes. Fourier transform can be effectively applied to stationary signals and make little sense when applied to non-stationary [78]. Even wavelet has been applied widely to non-stationary signals, it is still has its limitations like the limited length of wavelet base function and therefor energy leakage, adjustable window, outcome with a fixed scale and others [78]. It is become more essential to use or to develop methods that can extract essential components. In fact, previous studies put the data under certain limitations for example by some filtering which usually force the gait data to be stable and linear. However, this is not the case. Most of the experimental data certainly gait data should be criticized to be non-stationary and nonlinear. This will avoid us from handling the data in artificial way by going into linear analysis of these nonlinear and non-stationary signals. Merely, methods of non-stationary can be employed to emphasize the real changes in the gait time series data signals.

CHAPTER 2

METHODOLOGY & TECHNIQUES

This chapter will introduce the main techniques being used to come up with the analysis throughout this work. This chapter starts with the database description being used. Then some data transformation techniques are introduced as a try to get more deep understanding of gait signals. Finally, some definitions are introduced as a basis for the upcoming chapters.

2.1 Gait Data Description

VGRF in Newton as a function of time are extracted from 8 sensors (Ultraflex Computer Dyno Graphy, Infotronic Inc.) underneath each of the right and left foot. They were captured from 29 patients with idiopathic PD (disease stage was 2–3 on the Hoehn and Yahr scale, mean age: 66.3 years; 63% men), and 18 healthy controls (mean age: 66.3 years; 55% men). Subjects provided written informed consent prior to performing the experiment.

Eight sensors were placed underneath each of the subject's feet to collect VGRF while each subject walked at his/her usual back and forth for two minutes at their self-selected pace level ground without any secondary task in a well-lit, obstacle free, 25-m long, 2-m wide corridor. the sensors location inside the insole as lying approximately at the following (X, Y) coordinates measured as a person is comfortably standing with both legs parallel to each other are shown in Fig.2.1. The origin (0, 0) is located between the legs and the person is facing towards the positive side of the Y axis. The sampling rate is 100 Hz. Fig.2.2 displays a sample of the data captured by

the array of the eight sensors in addition to their summation. It displays a sample of the data for both Normal and Parkinson gaits. This database has been drawn from physionet gait database [54].

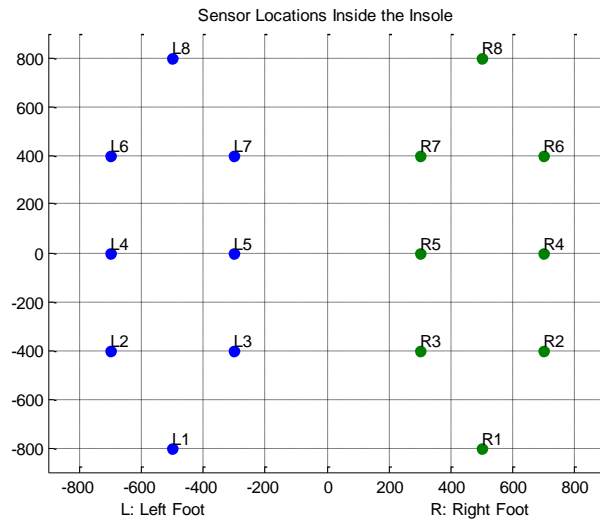


Figure 2.1: Sensor's position as distributed underneath both feet.

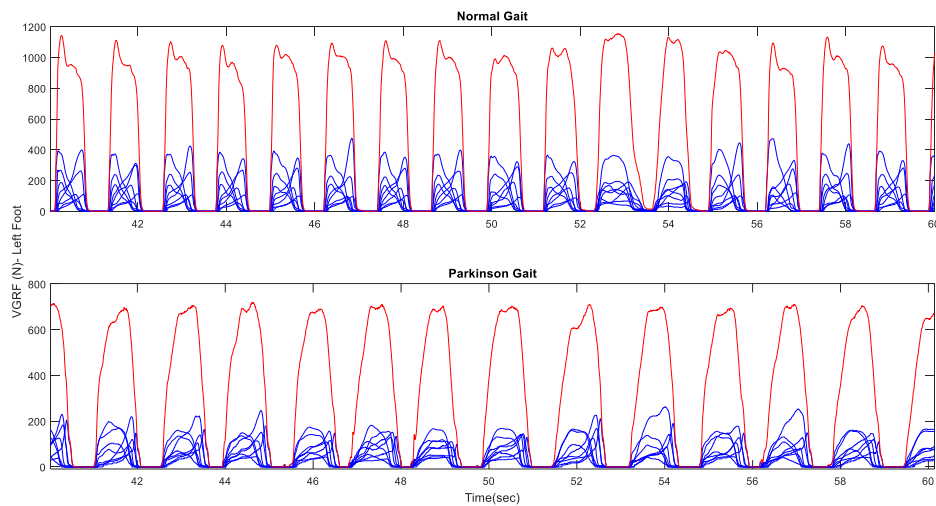


Figure 2.2: Sample of VGRF data captured by the eight sensors underneath the left foot. The red curve represents the resulting signal of their summation. The first row corresponds to normal gait and second row corresponds to Parkinson gait subject

2.2 Data Transformation Techniques

Signal is a physical quantity that we can measure such as gait VGRF. However, the latter is a composition of non-stationary signals that require a deep understanding of their instantaneous amplitude, phase and frequency. From this, one can model its stationary and non-stationary part and approximate the noise. In addition, one can practice such features for inter-subject classification of the VGRF signals such as between normal and pathological gait. Moreover, one could also concentrate in intra-subject classification like between usual gait and gait associated with cognitive tasks for the same subject.

2.2.1 Fourier Transform

A periodic signal has a property of $X(t) = X\left(\frac{2\pi t}{T}\right)$ where T is the period of the signal and 2π exist as indication of repetition of trigonometric functions. Even “ t ” here stands for time, it can also be generalized to cover spatial repetition. Fourier stated that such repetitive complex functions could be decomposed into an infinite series made up of cosine and sine terms then by equation (2.1) we can examine the frequency domain analysis [79].

$$X(t) = a_0 + \sum_{k=1}^{\frac{N-1}{2}, \frac{N}{2}} [a_k \cos(2\pi f_k t) + b_k \sin(2\pi f_k t)] + \varepsilon_t \quad (2.1)$$

Where $t=1, 2, \dots, N$

$$f_k = \frac{k}{N}, \quad k = 1 \dots \frac{N-1}{2} (N \rightarrow \text{odd}), \quad k = 1 \dots \frac{N}{2} (N \rightarrow \text{even})$$

ε_t is the residual and K stands for the K^{th} harmonic of the fundamental frequency ($1/N$) and N is the number of observations. Then coefficients a_k and b_k can be computed up to $k=N/2$ as in equation (2.2):

$$\begin{aligned}
 a_0 &= \bar{x} \\
 a_n &= \frac{2}{N} \sum_{t=1}^N X(t) \cos(2\pi f_k t) \quad k = 1, 2, \dots, M \\
 b_n &= \frac{2}{N} \sum_{t=1}^N X(t) \sin(2\pi f_k t) \quad k = 1, 2, \dots, M
 \end{aligned} \tag{2.2}$$

And M is maximum lag given by $0.25N$.

This is a good indication that degree of dependence and other computations are highly dependent on the sample size.

Then the amount of variance per interval of frequency is given by spectral density in equation (2.3):

$$I(k) = \frac{N}{2} [a_k^2 + b_k^2] \quad k = 1, 2, \dots, M \tag{2.3}$$

However it is better to have the power spectrum, a smoother diagram given by equation (2.4):

$$I(k) = 2[c_0 + 2 \sum_{j=1}^{N-1} \lambda_j c_j \cos(2\pi f_k j)] \tag{2.4}$$

$$c_j(t_k, t_i) = \text{Auto covariance function} = E[(X(t_k) - m_x(t_k))(X(t_i) - m_x(t_i))]$$

And m is mean function of process $X(t)$.

Lag window (λ_j) can be estimated using Tukey window as indicated in equation (2.5):

$$\lambda_j = \frac{1}{2} \left[1 + 2 \cos\left(\frac{2\pi}{M}\right) \right] \quad (2.5)$$

Certainly, this is not the only decomposition. Fourier transforms has its own limitations and her we can summarize some of them:

- Cannot not provide simultaneous time and frequency localization.
- The power spectrum derived from Fourier, there is a duplication of frequency coefficients.

Thus only $N/2$ points are unique. This is called the Nyquist sampling theorem

- Not very useful for analyzing time-variant, non-stationary signals.
- Not appropriate for representing discontinuities or sharp corners (i.e., requires a large number of Fourier components to represent discontinuities).
- An artificial effect is created by the finite sampling time T in which the value of the frequency coefficients “leaks” into adjacent coefficient positions. This means you get a reduced value of the wanted coefficient and contamination of adjacent coefficients.
- A sample time must be picked to ensure that all the frequencies in time signal resolved in the resulting bandwidth of the frequency coefficients. This is difficult certainly when the signal is not well understood beforehand. That is why filtering is done before Fourier transform to remove

unwanted frequencies otherwise signal aliasing or unwanted higher frequencies fold back into spectrum in unwanted places.

2.2.2 Time-Frequency Transforms

Fourier transform (FT) is used to examine the frequency content of the signal while short time Fourier transform (STFT), wavelet transform, Hilbert transform and many others provide the time-frequency representation of the signal [28]. Depending on the type of analysis and assumptions made, a transform is used. Table 2.1 shows a comparison between some different techniques used in processing VGRF signals.

	Fourier	STFT	Wavelet	HHT
Basis	A priori	A priori	A priori	Adaptive
Frequency	Convolution: global, uncertainty	Convolution: regional, uncertainty	Convolution: regional, uncertainty	Differentiation: local, certainty
Presentation	Energy-frequency	Energy-time-frequency	Energy-time-frequency	Energy-time-frequency
Nonlinear	No	No	No	Yes
Nonstationary	No	Yes	Yes	Yes
Based on theoretical	yes	yes	yes	No (Empirical)

Table 2.1: Comparison between various techniques used to analyze our VGRF signals

In order to comprehend the frequency content of the VGRF signals over time, both STFT and WT can serve a good foundation.

2.2.2.a Short Time Fourier Transform (STFT)

The STFT or Gabor transform, $G_s(w, t)$ is a Fourier-related transform used to determine the sinusoidal frequency and phase content of local sections of a signal as it changes over time. It is done by segmenting the signal into narrow time intervals (i.e., narrow enough to be considered stationary) and take the FT of each segment. Then each FT provides the spectral information of a separate time-slice of the signal and thus it provides simultaneous time and frequency information.

It is defined as in equation (2.6) of signal $s(t)$ [79]:

$$G_s(w, t) = \int s(u)g(u-t)e^{-iw_h u} du \quad (2.6)$$

where $s(t)$ is the signal of interest, $g(u)$ is the windowed function (e.g. a rectangular window) of size L , “ t ” stands for time and “ w_h ” is the digital harmonic frequency in radian defined by equation (2.7), and N is the total number of harmonics. Frequency and respectively [79].

$$w_h = \frac{2\pi h}{N}, \quad h = 0, 1, 2, \dots, N-1 \quad (2.7)$$

In this thesis the Gaussian window is being a topic of interest given by equation (2.8) since the signal shape is Gaussian. f_0 is the resolution frequency that specifies the spread of Gaussian window in both time and frequency:

$$g(u) = \frac{1}{\sqrt{2\pi}f_0} e^{-u^2 / 2f_0^2} \quad (2.8)$$

Since the Window should be narrow enough to ensure that the portion of the signal falling within the window is stationary, this do not offer good localization in the frequency domain. That is why wavelets in which a use of multiple window sizes compromises a good solution.

2.2.2.b Wavelet Transform (WT)

WT offers effective time-frequency representation of signals. It is based on a short duration wavelet of a specific center frequency. It is defined by $W_s(w,t)$ as in equation (2.9):

$$W_s(w,t) = \int s(u) \psi^* \left(\frac{u-t}{a} \right) \frac{du}{a} \quad (2.9)$$

“a” is the scale and $\psi^*(u)$ is the chosen wavelet function and is given in equation (2.10) as lognormal analogous to Gaussian in STFT [79]:

$$\psi^*(f) = e^{-(2\pi f_0 \log f)^2 / 2} \quad (2.10)$$

The * is the complex conjugate symbol. It is crucial to mention that time and frequency resolutions are must be paid attention in short time Fourier transform (STFT) and wavelet transform (WT). In addition, when comparing signals of the same type but from different groups like normal and pathological gait signals, those techniques hardly provide an insight to the main difference. Synchrosqueezing is raised up as a better resolution in both domains and will be explained later in this chapter.

2.2.2.c Hilbert-Haung Transformation

Hilbert-Haung transformation is an empirical algorithm that is convenient on nonstationary and nonlinear time series data. It is a combination of both Empirical Mode Decomposition (EMD) and Hilbert Spectral Analysis (HAS):

1) Empirical Mode Decomposition (EMD)

A self-adaptive method applied for non-stationary and nonlinear signal-processing, EMD is proposed by Haung et al [78]. Empirical unlike other transforms which relies on theory, EMD derived from observation or experiment in time domain. Mode stands for a particular form or variety. Decomposition because it generates a set of finite time series basic parts called Intrinsic Mode Functions (IMF) resulted from the separation of the original signal. Those IMFs include different frequency bands, with different frequency component, ranging from high to low. It's intrinsic because they naturally derived from the raw signal itself based upon the local time scale of the signal. That's why EMD is adaptive. The technique can be summarized as follows [80]:

- Identify all local extreme (maxima and minima) then interpolate between minima (maxima) ending up with upper and lower envelopes curve [$X_{\min}(t)$, $X_{\max}(t)$] that encompasses the whole data set.
- Subtract the mean of the two envelopes from the raw signal to obtain new function:

$$h_{11}(t) = X(t) - \frac{X_{\min}(t) + X_{\max}(t)}{2} \quad (2.9)$$

- Use the above sifting techniques frequently to minimize the mean to approach zero. The stopping criterion is given by:

$$SD_k = \frac{\sum_{t=0}^T |h_{k-1}(t) - h_k(t)|^2}{\sum_{t=0}^T h_{k-1}^2(t)} \quad \text{T is the whole time period} \quad (2.10)$$

- The number of extrema and zero crossing are equal or differ at most by one.
- The original signal $X(t)$ can be reconstructed using the following equation

$$X(t) = \sum_{j=1}^n c_j(t) + R_n(t) \quad (2.11)$$

This results on a set of IMFs with a certain frequency range and the last IMF is the residue $R_n(t)$. The IMFs are arranged from higher frequency components into lower one. The residue represents the trend (i.e. the time-varying mean) of the raw signal and which characterized by being monotonic or having one extreme i.e. not having periodic behavior.

The method can be summarized by the following flow chart as shown in Fig.2.3:

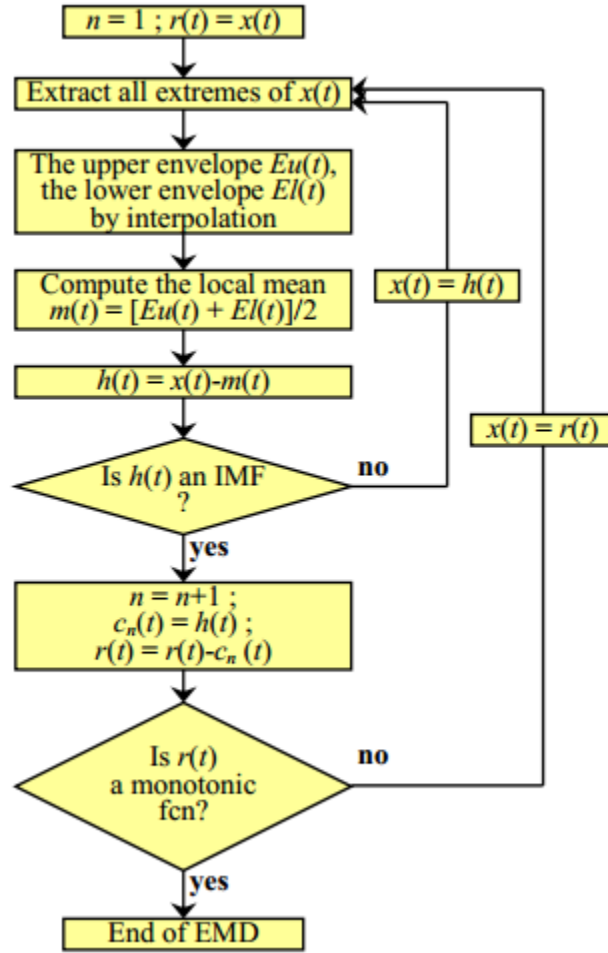


Figure 2.3. Flowchart of Empirical Mode Decomposition algorithm

2) Hilbert Spectral Analysis (HSA)

HAS is an energy-frequency-time representation which enables to obtain the time evolution of the instantaneous frequency of each IMF.

The Hilbert Transform $y(t)$ of the raw signal $x(t)$ is given by:

$$y(t) = \frac{1}{\pi} PV \int_{-\infty}^{+\infty} \frac{x(\tau)}{t - \tau} d\tau \quad (2.12)$$

Where PV is the Cauchy principle value.

The analytic signal associated to $x(t)$ which forms the complex trace is given by:

$$z(t) = x(t) + iy(t) = a(t)e^{-i\theta(t)} \quad (2.13)$$

“ i ” stands for a rotation of the complex number counterclockwise (CCW) by 90° .

The amplitude:

$$a(t) = \sqrt{x^2(t) + y^2(t)} \quad (2.14)$$

$e^{-i\theta(t)}$ is the complex number or the tip of phasor then the phase (radians/sec) can be derived as shown in equation (2.15):

$$\theta(t) = \tan^{-1} \left(\frac{y(t)}{x(t)} \right) = 2\pi f_0 t \quad (2.15)$$

Where f_0 corresponds to cycles/sec or Hertz. Take $f_0=3\text{Hz}$, then the point will rotate 3 times per second counterclockwise around the circle in the complex plane.

Therefore $Z(f)$ in frequency domain is single sided Fourier transform and therefore:

$$Z(f) = 0 \quad \text{for } f < 0 \quad (2.16)$$

$$Z(f) = Z(0) \quad \text{for } f = 0 \quad (2.17)$$

$$Z(f) = 2Z(f) \quad \text{for } f > 0 \quad (2.18)$$

$a(t)$ is the amplitude and $\theta(t)$ is the phase.

The instantaneous angle speed: $w(t) = \frac{d\theta(t)}{dt} \quad (2.19)$

The instantaneous frequency (IF): $w(t) = \frac{1}{2\pi} \frac{d\theta(t)}{dt} \quad (2.20)$

From equation (2.20), the local derivative of the phase defines the frequency resolution. IF is defined as the rate of change of the phase angle at time t of the analytic version of the signal with no need for long wave to characterize it.

It is worthy then to plot time-frequency graph where $a(t)$ and $w(t)$ are time-dependent. Then the original signal can be expressed in terms of a Fourier-like expansion as a function of instantaneous amplitude and frequency

$$x(t) = \text{real} \sum_{j=1}^n a_j(t) e^{i \int w_j(\tau) d\tau} \quad (2.21)$$

$$x(t) = \text{real} \sum_{j=1}^n a_j e^{i w_j t} \quad (2.22)$$

The Hilbert spectrum, $H(t, w)$ is thus obtained by the time-frequency representation of the amplitude representing a measure of energy contribution for each frequency and time. That's why Hilbert spectrum is useful for determining the frequencies covered by each IMF preserving the instants in which they occurred.

Formerly the marginal spectrum can be obtained with different point of views:

- Marginal time and this is when integrating the signal $H(t, w)$ with respect to frequency to obtain distribution in time domain i.e. marginal time

$$h(t) = \int_0^N H(t, w) dw \quad (2.23)$$

- Marginal frequency when integrating with respect to time to obtain frequency distribution and this is given by:

$$h(w) = \int_0^N H(w, t) dt \quad (2.24)$$

Where N is the total data length. This is useful in providing measure of the total amplitude/energy contribution from each frequency.

2.3 Synchrosqueezing of Time-Frequency Transform

As we mentioned, STFT and the WT form the fundamental approaches to simultaneously decompose a signal into time and frequency components. “synchrosqueezing transform” (SST) is an extension of the wavelet transform incorporating elements of EMD , however it has a theoretical foundation, and frequency reallocation techniques by combining all time-frequency (TF) coefficients corresponding to same instantaneous frequencies into one SST coefficient. SST is also an adaptive and invertible transform that improves the readability of a wavelet-based time-frequency map using frequency reassignment by condensing the spectrum along the frequency axis [81].

Starting from equations (2.6) and (2.9) the instantaneous frequency can be computed by equations (2.25) and (2.26) respectively:

$$v_G(w,t) = \frac{\partial}{\partial t} \arg[G_S(w,t)] = \text{Im}[G_S^{-1}(w,t) \frac{\partial G_S(w,t)}{\partial t}] \quad (2.25)$$

$$v_w(w,t) = \frac{\partial}{\partial t} \arg[W_S(w,t)] = \text{Im}[W_S^{-1}(w,t) \frac{\partial W_S(w,t)}{\partial t}] \quad (2.26)$$

Nowadays, it's become casual to get the synchrosqueezed STFT (V_s) and synchrosqueezed WT (T_s) as in equation (2.27) and (2.28):

$$V_s(w,t) = C_g^{-1} \int \delta(w - v_G(\varpi,t)) G_S(\varpi,t) d\varpi \quad (2.27)$$

where: $C_g = \pi g(0)$

$$T_s(w,t) = C_\psi^{-1} \int \delta(w - v_w(\varpi,t)) W_S(\varpi,t) d\varpi \quad (2.28)$$

where: $C_g = \pi g(0)$

Then it would be simple to show that the signal can be reconstructed by equation (2.29):

$$S^a(t) = \int_0^{\infty} V_s(w, t) d_w = \int_0^{\infty} T_s(w, t) d_w \quad (2.29)$$

Most importantly, it is possible to reconstruct the component's parameters using time frequency representation (TFR) values at the ridge points denoted as ridge reconstruction. The ridge reconstruction formulas are for STFT, WT, SSTFT, SWT are shown in equations (2.30), (2.31), (2.32) and (2.33) respectively:

$$v(t) = w_p(t) + \delta v_d(t), \quad A(t)e^{i\Phi(t)} = \frac{2G_s(w_p(t), t)}{\hat{g}(w_p(t) - v(t))}, \quad (2.30)$$

$$v(t) = w_p(t)e^{\delta \log v_d(t)}, \quad A(t)e^{i\Phi(t)} = \frac{2W_s(w_p(t), t)}{\hat{\psi}^*(w_p(t)/v(t))}, \quad (2.31)$$

$$v(t) = w_p(t), \quad \Phi(t) = \arg[V_s(w_p(t), t)], \quad (2.32)$$

$$v(t) = w_p(t), \quad \Phi(t) = \arg[T_s(w_p(t), t)], \quad (2.33)$$

To sum up, synchrosqueezing improves the “readability” of the TFR, providing a more visually appealing picture.

2.4 Modelling

Modelling of signals is used to represent the given signal with some model parameters. The objective of modelling can be used for signal compression, prediction of behavior of a time series from past values alone, reconstruction and understanding of the physical system. There are different model classes. We will consider here the Autoregressive moving average model (ARMA) in brief for its importance. The General equations are summarized as follows for autoregressive (AR) and moving average (MA) separately [84].

A) AR(p): $x_t = \rho_1 x_{t-1} + \rho_2 x_{t-2} + \dots + \rho_p x_{t-p} + e_t$

The autoregressive model states that there is a linear dependence of the output variable on its own previous values and on a stochastic term. The model is in the form of a stochastic difference equation. $\rho_1 \dots \rho_p$ are parameters of the model and e_t is white noise. The order (p) of an autoregression is the number of immediately preceding values in the series that are used to predict the value at the present time. So, the preceding model is a first-order autoregression, written as AR(1).

B) MA(q): $x_t = e_t + \theta_1 e_{t-1} + \theta_2 e_{t-2} + \dots + \theta_q e_{t-q}$

Moving-average (MA) model of order “q” is another time series analysis method. $\theta_1 \dots \theta_q$ are the parameters of the model. $e_t \dots e_{t-q}$ are white noise error terms. The model indicates a linear regression of the current value of series against current previous and current white noise error terms. The error terms are mutually independent and generated from the same distribution. For instance, the normal distribution with zero mean and fixed variance is used.

C) ARMA(p,q): $x_t = \rho_1 x_{t-1} + \rho_2 x_{t-2} + \dots + \rho_p x_{t-p} + e_t + \theta_1 e_{t-1} + \dots + \theta_q e_{t-q}$

Autoregressive–moving-average (ARMA) models is a combination of the previous two models. From equations above, the model main concern is the persistence, or autocorrelation, in a time series.

2.5 Feature Selection techniques : Receiver Operating Characteristic

In order to develop robust classifiers and learning models, a subset of features must be carefully selected. Receiver operating characteristic (ROC) curve compares sensitivity or true positive rate (TPR) against the fall-out (1-specificity) or false positive rate (FPR) to exemplify the performance of binary classifier. Therefore it can serve a direct evaluation of feature by plotting equation (2.25) versus (2.26) [82].

$$TPR = TP/(TP + FN) \quad (2.25)$$

$$FPR = FP/(FP + TN) \quad (2.26)$$

Where T refers to true whenever the prediction matches the actual situation. Therefore, TP is true positive, TN is true negative and FP is false positive. Thus, with 95% confidence interval, the area under the curve (AUC) will reflect the accuracy on how well a feature could well separate normal gait from Parkinson's gait. The following scores could be used to evaluate the accuracy:

0.9-1: Excellent

0.8-0.9: Good

0.7-0.8: Fair

0.6-0.7: Poor

0.5-0.6: Fail

If AUC=1 refers to a perfect discrimination and has a ROC curve that passes through the upper left corner i.e. 100% sensitivity and 100% specificity with no overlap in the two distributions.

Consequently, ROC curves are constructed by simply ranking the population according to their test result. This means that the area under the ROC curve does not reflect the shapes of the

underlying populations (i.e. normal or not normal) and it is non parametric. This means that the AUC is a useful parameter regardless of the distribution of the underlying populations. It also means that AUC can be used even when a test result does not give an accurate number – as long as one can rank the results and construct the curve.

2.6 Classification Techniques

In order to map every new observation into its own category a classifier is needed. The objective is to introduce a learning algorithm having the ability to classify two different groups based on certain chosen features. Therefore, the algorithm has the ability to draw certain decision boundary between both groups. This will give the capacity to predict new introduced subjects to which group they fall by observing on which side of the decision boundary they drop.

Various classifiers serve this goal such as logistic regression, Decision Tree, Naive Bayesian, boosting, Artificial Neural Network, K Nearest Neighbors, Support Vector Machine. A good classification system should have the following characteristics:

- Use all information available.
- Make few classification errors.
- Minimize the negative consequences of making classification errors.

2.6.1 logistic regression Classification

For instance logistic regression Classification is based on the choice of hypothesis function which is chosen to be nonlinear function [83]. If θ is the weight then it is given by equation:

$$h_{\theta}(x) = g(\theta^T x) = \frac{1}{1 + e^{-\theta^T x}} = P(y=1|x;\theta) \quad (2.27)$$

g is the sigmoid function and fitted as a threshold function:

$$g(z) = \frac{1}{1 + e^{-z}} = \begin{cases} 1 & \text{if } z \geq 0 \\ 0 & \text{if } z < 0 \end{cases} \quad (2.28)$$

The cost least mean square function in logistic regression to make $h(x)$ close to y is given by:

$$J(\theta) = \frac{1}{m} \sum_{i=1}^m [-y^{(i)} \log(h_{\theta}(x^{(i)})) - (1 - y^{(i)}) \log(1 - h_{\theta}(x^{(i)}))] \quad (2.29)$$

$(x^{(i)}, y^{(i)})$ is the i -th training example and m is the number of training examples. In order to optimize the cost function $J(\theta)$ with parameters θ , Newton's method serves the ability to minimize this function. The update rule for Newton's method is emphasized by equation (2.30):

$$\theta^{(t+1)} = \theta^{(t)} - H^{-1} \nabla_{\theta} J \quad (2.30)$$

The gradient and Hessian (H) matrix are given by:

$$\nabla_{\theta} J = \frac{1}{m} \sum_{i=1}^m (h_{\theta}(x^{(i)}) - y^{(i)}) x^{(i)} \quad (2.31)$$

The decision boundary is defined as the line:

$$P(y=1|x;\theta) = g(\theta^T x) = 0.5 \quad (2.32)$$

And this corresponds to

$$\theta^T x = 0 \quad (2.33)$$

2.6.2 Principle component analysis (PCA)

PCA is an orthogonal transformation to convert a set of observations of possibly correlated variables into a set of values of linearly uncorrelated variables called principal components. The first principal component has the largest possible variance, and each succeeding component in turn has the highest variance possible under the constraint that it is orthogonal to the preceding components. The resulting vectors are an uncorrelated orthogonal basis set. The principal components are orthogonal because they are the eigenvectors of the covariance matrix, which is symmetric. PCA is sensitive to the relative scaling of the original variables [83].

Given the centered data $\{x_1 \dots x_m\}$, then the principal vectors are computed by equations (2.34) representing 1st PCA vector and (2.35) represents k^{th} PCA vector:

$$\mathbf{w}_1 = \arg \max_{\|\mathbf{w}\|=1} \frac{1}{m} \sum_{i=1}^m \{(\mathbf{w}^T \mathbf{x}_i)^2\} \quad (2.34)$$

We maximize the variance of projection of \mathbf{x} .

$$\mathbf{w}_k = \arg \max_{\|\mathbf{w}\|=1} \frac{1}{m} \sum_{i=1}^m \{[\mathbf{w}^T (\mathbf{x}_i - \sum_{j=1}^{k-1} \mathbf{w}_j \mathbf{w}_j^T \mathbf{x}_i)]^2\} \quad (2.35)$$

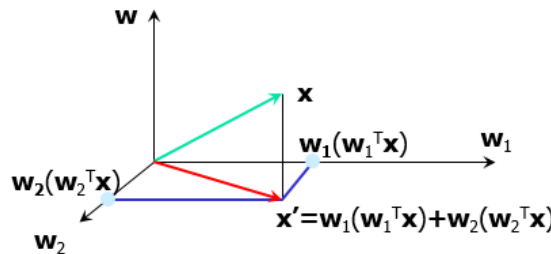


Figure 2.5. Maximizing the variance of the projection in the residual subspace

2.6.3 Discriminant analysis

Discriminant analysis (both for discrimination and classification) is a statistical technique to organize and optimize:

- the description of differences among objects that belong to different groups or classes, and
- the assignment of objects of unknown class to existing classes.

Discriminant analysis (DA) is based on Bayes' Rule and likelihood that yields a posterior probability as in equation (2.36) [83]:

$$p(c_i/x) = \frac{p_i f(x/c_i)}{\sum_{j=1}^i p_j f(x/c_j)} = \frac{p_i (2\pi)^{-p/2} |\Sigma_i|^{-1/2} \exp(-0.5 z_k^2)}{\sum_{j=1}^i p_j (2\pi)^{-p/2} |\Sigma_j|^{-1/2} \exp(-0.5 z_j^2)} \quad (2.36)$$

$$z_k^2 = (x - \mu_k)' \Sigma_k^{-1} (x - \mu_k) \quad (2.37)$$

z_k^2 is the squared Mahalanobis distance from the data vector x to the k th group mean. $p_i = P(c_i)$, the probability of a subject to be in group c_i . $i = \{\text{Normal, Parkinson}\}$. $f(x / \pi_i)$ is the conditional probability density function. Then classifying an observed subject's gait to whether a subject have a balanced or unbalanced gait, given the hypothesize is true, by which $p_i f(x / c_i)$ is highest.

If the covariance matrix determinants are equal then the decision boundary is a line:

$$\begin{aligned}
p(\mathbf{x}|c=1) &= \frac{1}{\sqrt{(2\pi)^m |\Sigma|}} \exp\left(-\frac{1}{2}(\mathbf{x}-\boldsymbol{\mu}_1)^T \Sigma^{-1}(\mathbf{x}-\boldsymbol{\mu}_1)\right) \\
P(c=1) &= q_1 \\
\log p(\mathbf{x}|c=1)P(c=1) &= -\frac{1}{2}(\mathbf{x}-\boldsymbol{\mu}_1)^T \Sigma^{-1}(\mathbf{x}-\boldsymbol{\mu}_1) + \log q_1 - \frac{m}{2} \log 2\pi - \frac{1}{2} \log |\Sigma| \\
&= -\frac{1}{2} \mathbf{x}^T \Sigma^{-1} \mathbf{x} + \boldsymbol{\mu}_1^T \Sigma^{-1} \mathbf{x} - \frac{1}{2} \boldsymbol{\mu}_1^T \Sigma^{-1} \boldsymbol{\mu}_1 + \log q_1 + \dots \\
\log p(\mathbf{x}|c=2)P(c=2) &= -\frac{1}{2} \mathbf{x}^T \Sigma^{-1} \mathbf{x} + \boldsymbol{\mu}_2^T \Sigma^{-1} \mathbf{x} - \frac{1}{2} \boldsymbol{\mu}_2^T \Sigma^{-1} \boldsymbol{\mu}_2 + \log q_2 + \dots \\
\log \frac{p(\mathbf{x}|c=1)P(c=1)}{p(\mathbf{x}|c=2)P(c=2)} &= \boldsymbol{\mu}_1^T \Sigma^{-1} \mathbf{x} - \boldsymbol{\mu}_2^T \Sigma^{-1} \mathbf{x} - \frac{1}{2} \boldsymbol{\mu}_1^T \Sigma^{-1} \boldsymbol{\mu}_1 + \frac{1}{2} \boldsymbol{\mu}_2^T \Sigma^{-1} \boldsymbol{\mu}_2 + \log q_1 - \log q_2 \\
&= \mathbf{w}^T \mathbf{x} + w_0
\end{aligned} \tag{2.38}$$

If the covariance matrix determinants are not equal then the decision boundary is quadratic function:

$$\begin{aligned}
p(\mathbf{x}|c=1) &= \frac{1}{\sqrt{(2\pi)^m |\Sigma_1|}} \exp\left(-\frac{1}{2}(\mathbf{x}-\boldsymbol{\mu}_1)^T \Sigma_1^{-1}(\mathbf{x}-\boldsymbol{\mu}_1)\right) \\
P(c=1) &= q_1 \\
\log p(\mathbf{x}|c=1)P(c=1) &= -\frac{1}{2}(\mathbf{x}-\boldsymbol{\mu}_1)^T \Sigma_1^{-1}(\mathbf{x}-\boldsymbol{\mu}_1) + \log q_1 - \frac{1}{2} \log (2\pi)^m |\Sigma_1| \\
&= -\frac{1}{2} \mathbf{x}^T \Sigma_1^{-1} \mathbf{x} + \boldsymbol{\mu}_1^T \Sigma_1^{-1} \mathbf{x} - \frac{1}{2} \boldsymbol{\mu}_1^T \Sigma_1^{-1} \boldsymbol{\mu}_1 + \log q_1 - \frac{1}{2} \log (2\pi)^m |\Sigma_1| \\
\log p(\mathbf{x}|c=2)P(c=2) &= -\frac{1}{2} \mathbf{x}^T \Sigma_2^{-1} \mathbf{x} + \boldsymbol{\mu}_2^T \Sigma_2^{-1} \mathbf{x} - \frac{1}{2} \boldsymbol{\mu}_2^T \Sigma_2^{-1} \boldsymbol{\mu}_2 + \log q_2 - \frac{1}{2} \log (2\pi)^m |\Sigma_2| \\
\log \frac{p(\mathbf{x}|c=1)P(c=1)}{p(\mathbf{x}|c=2)P(c=2)} &= \mathbf{x}^T W \mathbf{x} + \mathbf{w}^T \mathbf{x} + w_0
\end{aligned} \tag{2.39}$$

Then the decision boundary fall when the ratio $\frac{p(\mathbf{x}|c=1)P(c=1)}{p(\mathbf{x}|c=2)P(c=2)}$ is equal one. If the ratio is greater than one then the subject drops into the first class; otherwise the subject's gait fall under the second class.

Comparing DA with PCA yields that DA has X and Y variables, whereas in PCA there is only one set of variables. In addition, DA has predetermined groups. However, both use the concept of creating new variables that are linear combinations of the original ones.

2.6.4 *k-Nearest Neighbors Algorithm (K-NN)*

K-NN is a non-parametric method used for classification and regression. The input consists of the k closest training examples in the feature space. The output depends on whether k-NN is used for classification or regression [83].

K-NN classification divides data into a test set and a training set. For each row of the test set, the K nearest (in Euclidean distance) training set objects are found, and the classification is determined by majority vote with ties broken at random. If there are ties for the K^{th} nearest vector, all candidates are included in the vote. In order to measure the distance Euclidean:

$$\|x - x'\|^2 = \sum_j (x_j - x_j^i)^2 \quad (2.40)$$

Fig.2.6 shows a flowchart that summarizes the algorithm of K- nearest neighbors.

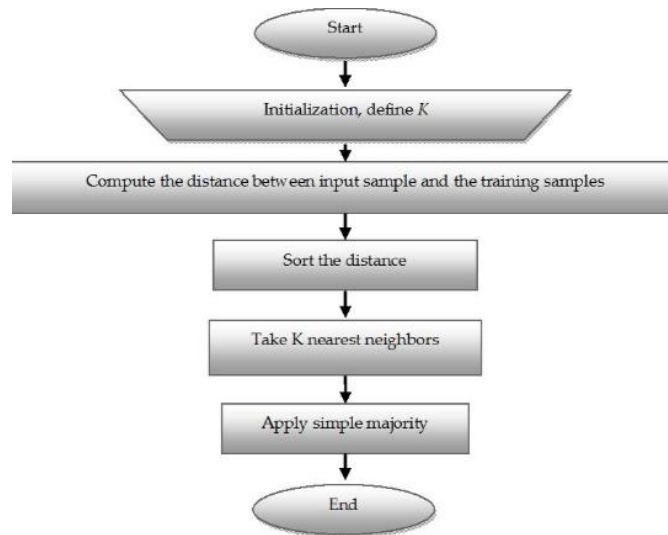


Figure 2.6. Flowchart for the K-NN

2.7 General Definitions

- The mean is given by: $\bar{x} = \frac{1}{m} \sum_{i=1}^m \mathbf{x}_i$

- Standard deviation: $\sigma = \sqrt{\frac{1}{N} \sum_{i=1}^N (x_i - \bar{x})^2}$

- Covariance matrix : $\Sigma = \frac{1}{m} \sum_{i=1}^m (\mathbf{x}_i - \bar{\mathbf{x}})(\mathbf{x}_i - \bar{\mathbf{x}})^T$

- Autocorrelation with lag K :

- Skewness (Absence of symmetry, Extreme values in one side of a distribution:

$$\text{skew}(X) = E\left[\frac{(X - \bar{x})}{\sigma}\right]^3$$

- Kurtosis: Peakedness of a distribution: $\text{kurt}(X) = E\left[\frac{(X - \bar{x})}{\sigma}\right]^4$

- A signal is said to be stationary (time-invariant spectra) if the local statistics do not change with time over the entire duration of the signal. That is why the probability density function does not depend on the definition of the time origin. Thus, a periodic signal is a stationary signal, but a transient signal that occurs locally in a long time domain is not stationary and therefore is said to be time-varying spectra. As to bond our definition, throughout this wok, we will limit the definition of stationarity to the change in the frequency content of the signal over time. If a DC-frequency is obtained then the signal is said to be stationary. Otherwise non-stationarity of signal is assumed. The only way to examine the later signals is by time varying spectrum. Fig.2.7 highlights this idea where time varying characteristics of the VGRF signal is shown.

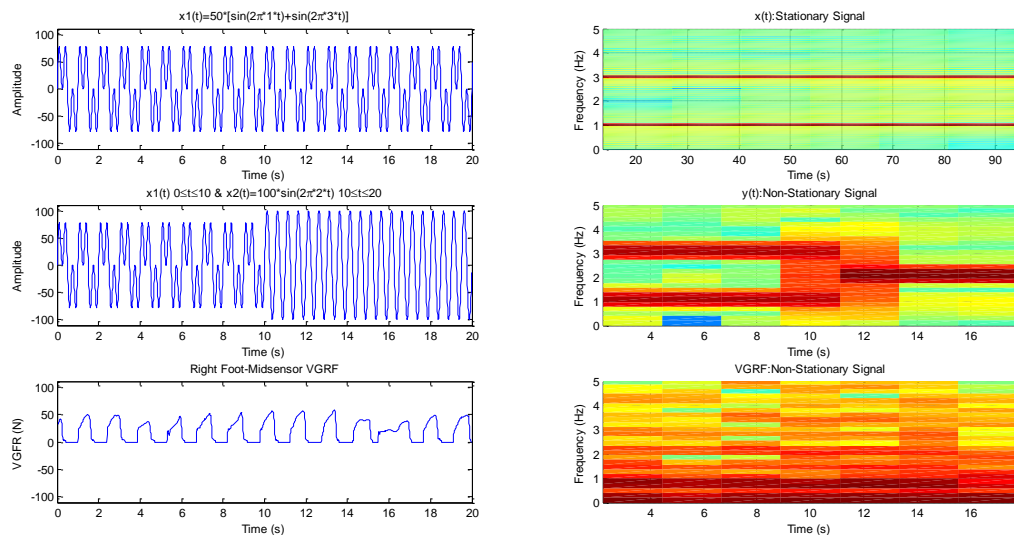


Figure 2.7: the first row plot is for stationary signal and the rest corresponds to non-stationary signal

Fig.2.7 shows how the VGRF signal varying in its nature (amplitude, frequency, phase), that is why we can set it as a transient signal which is a class of non-stationary signals.

Different methods are adopted for nonstationary data processing and here are some: Evolutionary spectrum, Spectrogram, Wigner-Ville distribution, Wavelets analysis, Empirical orthogonal function expansion (EOF), Smoothed moving average, Trend least-squares estimation and many others.

CHAPTER 3

ANALYSIS & CLASSIFICATION OF VGRF SIGNALS

In this chapter, the analysis and manipulations of the GRF data will be carried out to give an insight about the VGRF signals themselves. This would help in extracting significant features and specific information that help in predicting or even preventing falls in elderly. First we have proved the best sensors among other sensors that best can be used for classification purposes. We have also treated the total VGRF signals issued from the array of sensors as various studies in the literature commit to use it.

Pressure distribution underneath the foot has been a topic of interest for assessing falls in elderly and certain pathology like Parkinson's disease. In this chapter, we performed spatial and time signal analysis over VGRF signals. This was done to classify gaits between balanced and unbalanced. The synchronization of consecutive gait steps in elderly subjects in both normal and Parkinson was analyzed. This helped us in building a classifier that work well in the classification of both groups.

3.1 Filtering

While standing at rest, the VGRF is the only one existing .However at the time of heel-strike that separates the swing phase from the stance phase in addition to the toe-off, the vertical force is no longer vertical, it tilts over to produce shear force. When the foot hits the ground as termed heel strike, the VGRF associated with tangential forces slanted from GRF vector component parallel to the ground acting backwards. It is formed by an exchanging of frictional

forces with ground that leads to a brake impulse and therefore the body slow down. This prevent foot sliding forward along the ground. Fig. 3.1 shows the horizontal component affecting the vertical ground reaction force contaminated by noise. However, the dynamic characteristics of gait reaction forces are usually exploited by filtering as shown in Fig.3.2. Filtering at 25 Hz is useful for certain data while it is not applicable for another subjects as in Fig.3.2. Given that the foot will act also as a shock absorber as to disperse the force of the body during landing. The GRF vector is illustrated by a black arrow on Fig.3.1 during contact, midstance and propulsive phase.

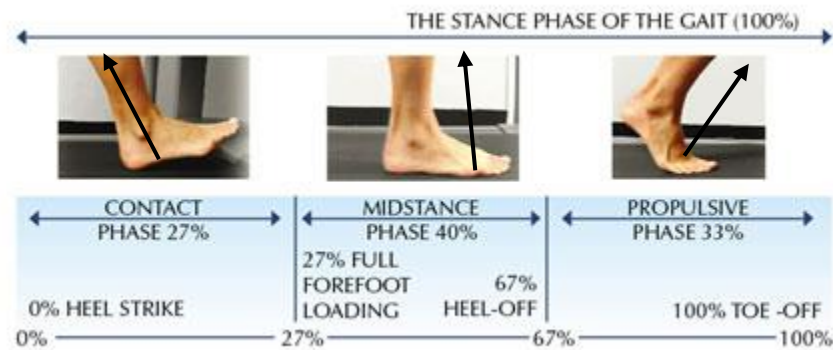


Figure 3.1: Vertical GRF vector during Gait Cycle

Likewise, during toe-off there will be an appearance of propulsive impulse to stimulate motion due to tilting of the force over forwards. This helps accelerating the body.

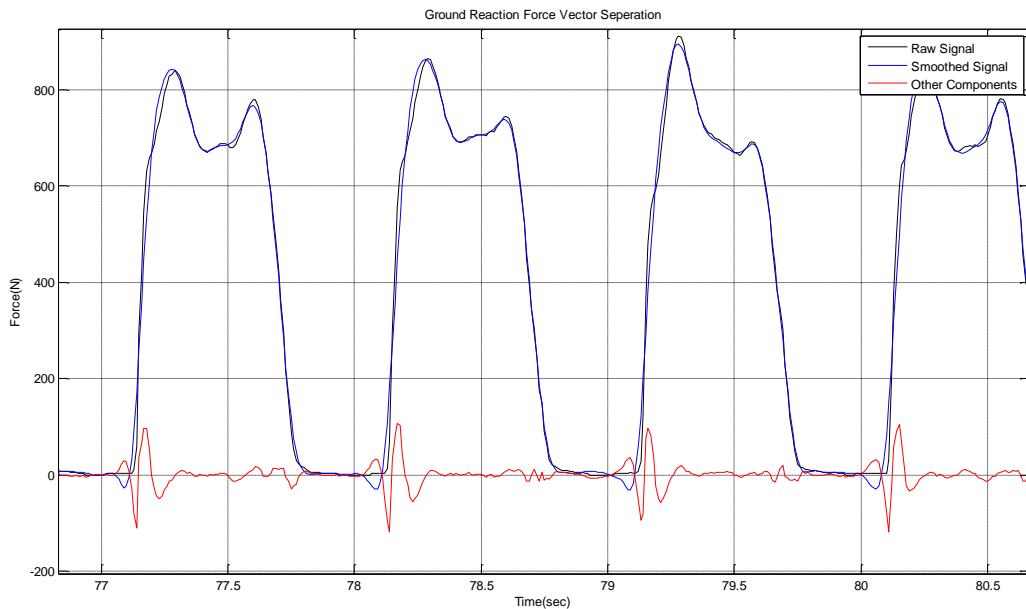


Figure 3.2: Ground Reaction Force filtering by second order Butterworth filter of 25 Hz shows a vital part being attenuated colored in red

Knowing that concavity upward horizontal and normal forces indicate brake impulse which is followed by deceleration motion while concavity downward signifies propulsive impulse followed by acceleration motion. This specifies an important coefficient to consider which is named static friction. Static friction is defined as the ratio of the magnitude of the horizontal frictional force to the normal force. This coefficient could yield when slippage could occur. Knowing that, part of this noise reflects the speed horizontal speed of the foot during the touchdown of the heel with the ground.

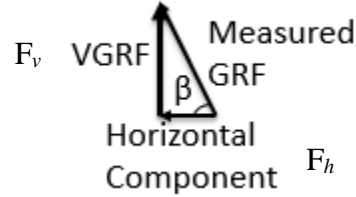


Figure 3.3: During Heel strike, the measured VGRF consist of horizontal frictional component

Using Fig.3.3 and by Pythagoras theorem the measured ground reaction force is given by equation (3.1):

$$F_m^2 = F_v^2 + F_h^2 \quad (3.1)$$

Then $\tan \beta = \frac{F_v}{F_m}$ (3.2)

Where

F_m : The measured ground reaction force

F_v : The vertical component of ground reaction force, load

F_h : The horizontal frictional component exerted by each surface on the other.

β : The angle indicating the direction of the measured GRF

This horizontal friction is considered as non-fundamental force but is a result from intermolecular and interatomic kinetic dry friction between ground and foot which make it complicate to be calculated and considered as highly stochastic. This energy that examined as frictional forces by subject is lost as heat. An empirical law termed as Coulomb's Law of Friction can approximate this model by equation (3.3):

$$F_h \leq \mu F_v \quad (3.3)$$

Where, μ is the dimensionless coefficient of friction. It can be defined from equation (3.3) as the ratio of the force of friction between foot and ground and the pressing normal force.

To sum up, and by newton's law the force is given by: $F=ma$ where "m" is the mass of the parts contributed to this force, and "a" is the acceleration. Since a frictional backward force exist, this suggest definitely the existence of backward acceleration as a braking action on the body, slowing it down.

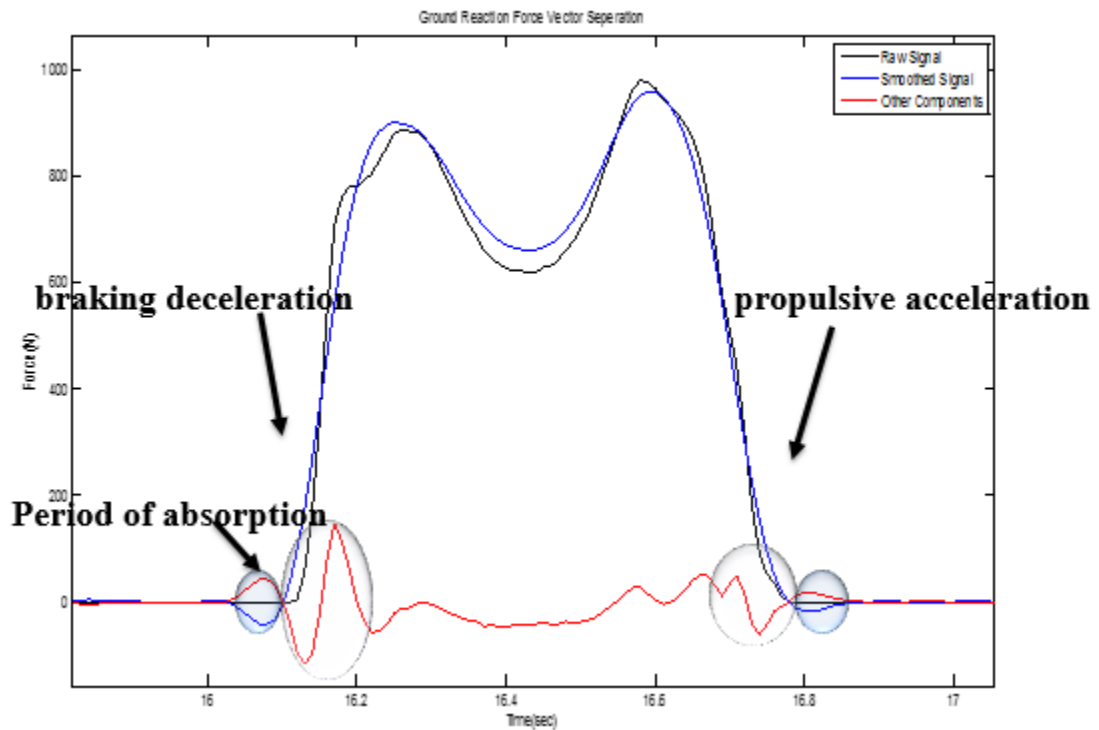


Figure 3.4: loading response and the push-off are circled.

From Fig.3.4, at instant just prior to the collision of the heel with ground i.e. as it start to touches the ground the normal force is in negative due to the fact that a forward directed force termed as “claw back” due to initial parameters [37] and in addition the skeletal system act as a shock absorber. At those moments slippage is occurring and shown by the small red peak and this indicate the existence of force with direction of motion. However, this pronation activate information record by the lower central nervous system through sensory neurons that registered in central nervous system which in turns activate the muscles contraction to prevent the forefoot from slapping down and therefore generate forces and moments at synovial joints to invoke the movement regulated by rigid links. Fig.3.4 can be used for illustration. The last exert ground reaction force which followed by a decreasing in magnitude of the horizontal component as shown in Fig.3.3 to serve a friction in the opposite direction of motion preventing the subject from slipping and therefore falling. As a result, at the period of absorption shown in Fig.3.4 indicates that the horizontal and frictional force are equal in magnitude but in opposite directions where still there is no movement. This can be verified by newton’s third law that states that for every action i.e. force there is an equal and opposite reaction i.e. counter force.

As a summary, in this thesis instead of using a fixed filtering bandwidth of frequencies over all gait VGRF signals ($x[n]$), we have developed an adaptive filter using the EMD technique as shown in Fig.3.5.

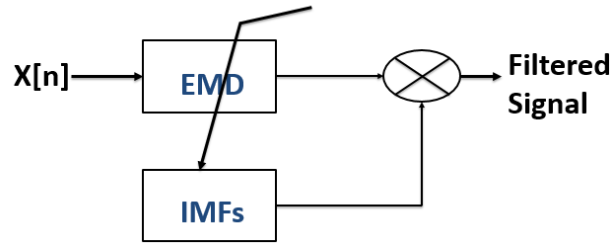


Figure 3.5: Adaptive filter

Then we choose to remove certain intrinsic mode functions (example is shown in Table 3.1) according to their weighted energy and preferred number of intrinsic mode function.

Channel	Zero Crossings	Extrema Counts	Mean Freq. [Hz]	Power (%)
IMF_h1	7050	4056	29.09068	0.045846
IMF_h2	2506	1676	10.34326	0.354629
IMF_h3	736	472	3.04068	9.128521
IMF_h4	494	316	2.042248	4.668593
IMF_h5	229	114	0.948923	84.29544
IMF_h6	158	86	0.655995	1.052419
IMF_h7	75	40	0.313557	0.241007
IMF_h8	35	18	0.148527	0.089646
IMF_h9	18	10	0.078389	0.041991
IMF_h10	10	6	0.045383	0.008957
IMF_h11	2	4	0.012377	0.031212
IMF_h12	3	1	0.016503	0.041738
IMF_residual	0	1	0.004126	

Table 3.1: Intrinsic mode function characteristics

An example of EMD applied to a data from a control subject is shown in Fig.3.6. The first subplot represents the raw signal. Fig. 3.6 illustrates the idea that the first IMF captures the largest frequency components. The second IMF has a lower oscillation and so on to reach a trend with the lowest component as shown in the last row of Fig.3.6. Therefore EMD acts as an adaptive filter to extract the components present in the signal. It's worthy therefore to mention that the first IMF extracts most of noise present in signal.

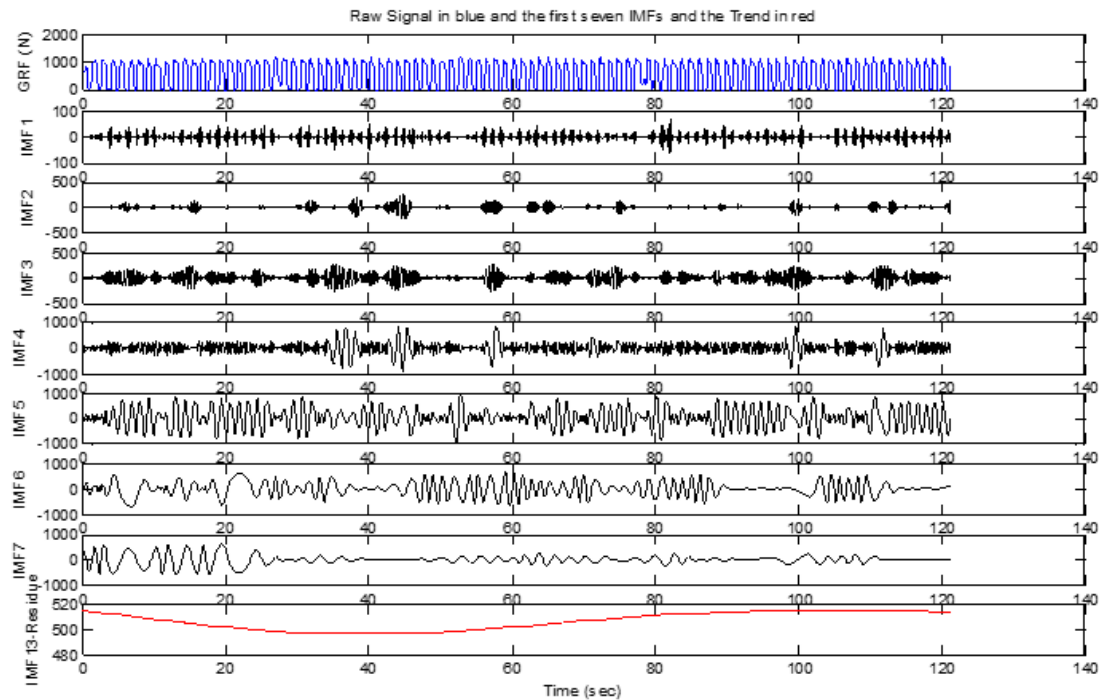


Figure 3.6. The first raw is the original signal. Seven IMFs plus the trend are plotted

As a result, it is better to filter the signal at a mean frequency of 29.09 Hz instead of filtering it by 25 Hz second order Butterworth filter and losing crucial part of the signal. This filtering could

be at 28 Hz on another gait if it represents the mean frequency of the highest oscillations. This is because we have assumed in this case that noise exist in the IMF1. Fig.3.5 therefore indicates that EMD is applied to the signal then a choice of the number of intrinsic mode functions that must be removed from signal must be made. This would remove same number of oscillations between different gait subjects but not necessary the same frequency content.

The foot- ground contact part of the VGRF time series signal are then extracted forming steps. Some steps are being eliminated when their statistical properties form outlier in the vast of other segmented step signal, mainly this is done by computing the mean and standard deviation. For instance the black segment of VGRF shown in Fig.3.7 forms an outlier. Those are so called turning points.

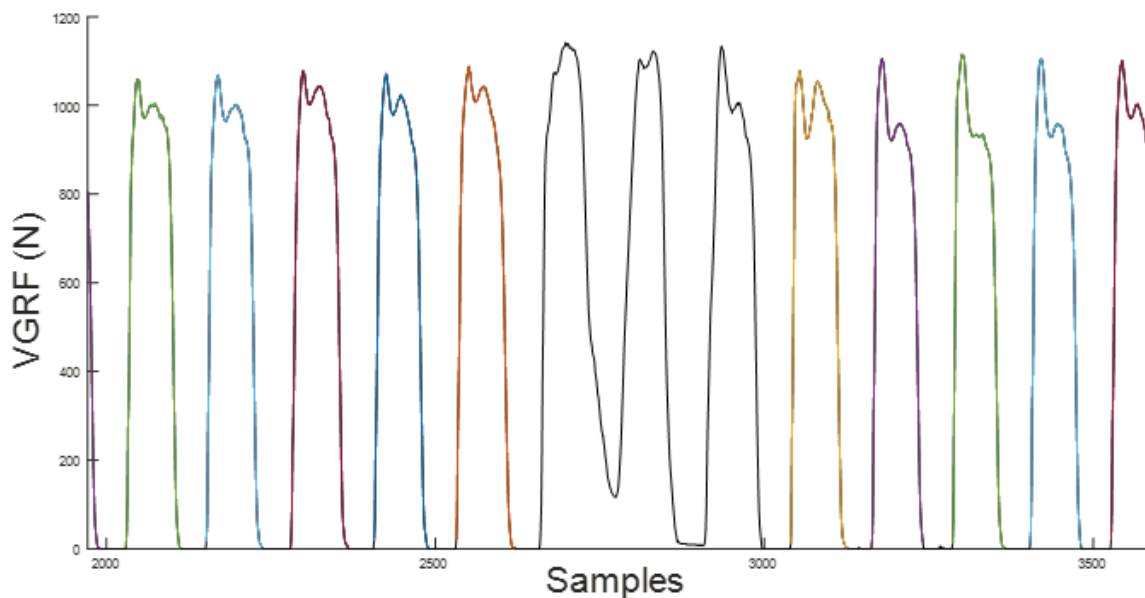


Figure 3.7: Segments colored in black are being omitted

3.1.1 *Synchrosqueezing Characterize Non-Stationary Signals*

Synchrosqueezing of time-frequency representation is being used to spot its power in non-stationary signal analysis and classification. It is has been used to when signal components are not well separated in STFT, WT and empirical mode decomposition (EMD). It also gives a more readability of the frequency spectrum. In order to have more concentrated time –frequency representation, the algorithm of synchrosqueezing of STFT or WT will be convenient to be used by joining all coefficients having same instantaneous frequency into one coefficient [2]. Keeping in mind it is nonlinear transformation of time- frequency (TF) method. It is an alternative to empirical mode decomposition (EMD) that fits the analysis of a time-varying spectrum. From the modulus of TF representation, one can evaluate the instantaneous frequency. This technique helped in developing an accurate detection of outliers within such time series signal like when subjects encounter turning points during walking. This is needed also to track the instantaneous frequency with respect to time to have better understanding of the signal [45].

In order to show the power of synchrosqueezing on analyzing non-stationary signal, we will consider the signal generated using equation (3.4):

$$\begin{aligned} x(t) &= A_1 \cos(w_1 t + \vartheta_1) \dots 0 \leq t \leq T \\ &+ A_2 \cos(w_1 t + \vartheta_1) \dots 0 \leq t \leq t_1 \\ &+ A_3 \cos(w_2 t + \vartheta_2) \dots t_1 \leq t \leq T \end{aligned} \quad (3.4)$$

$x(t)$ as shown in equation (3.4) is stationary either in $0 \leq t \leq t_1$ or $t_1 \leq t \leq T$. The spectral is fixed with respect to time within those two intervals. However this is not true when considering the whole interval $0 \leq t \leq T$. In this later whole interval, the signal is made up of stationary component ($A_1 \cos(w_1 t + \vartheta_1)$) and non-stationary part ($A_2 \cos(w_1 t + \vartheta_1) + A_3 \cos(w_2 t + \vartheta_2)$).

Time-frequency representation is powerful for non-stationary analysis [45], however, they don't infer enough knowledge for the correct analysis when the non-stationary signal is made up of multiple closed frequencies. For illustration and simplicity, assume the amplitudes are $A_1 = A_2 = A_3 = 1$ and the phases are assumed to be $\vartheta_1 = \vartheta_2 = \vartheta_3 = 0$. The angular frequencies are given as $w_1 = 2\pi$, $w_2 = 2\pi \times 1.3$ and $w_3 = 2\pi \times 1.4$.

Performing STFT and synchrosqueezed STFT on $x(t)$ yields Fig.3.8 and Fig.3.9 respectively. One can investigate the main difference in the two time-frequency representation of the signal. The STFT vaguely provides the frequency content of the signal and do not show the two representations of the signal.

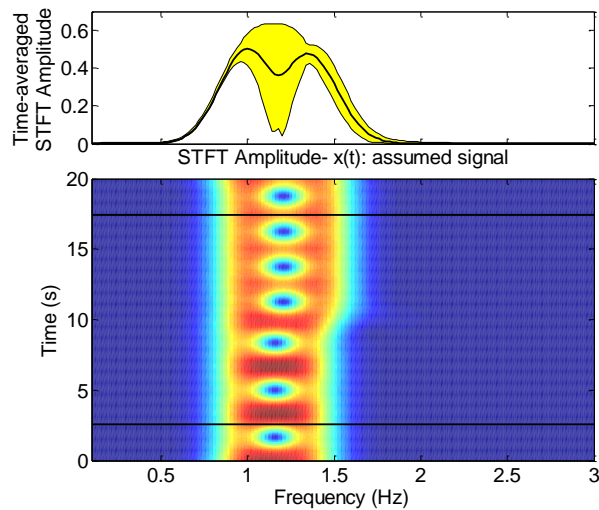


Figure 3.8. STFT and its time averaged applied on the assumed signal $x(t)$

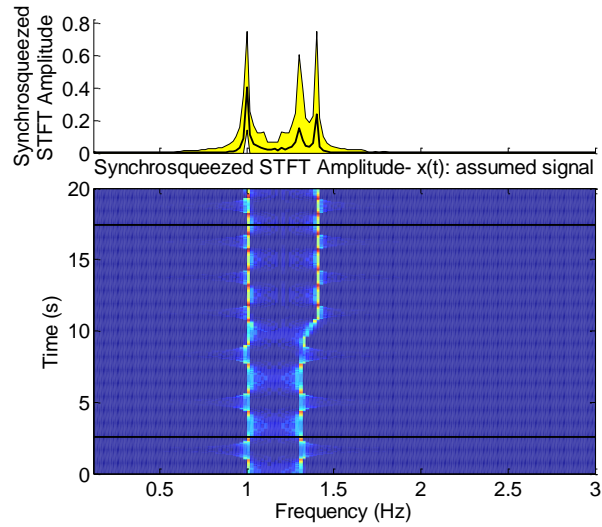


Figure 3.9. Synchronsqueezed STFT and its time averaged applied on the assumed signal $x(t)$

Performing synchronsqueezing on the STFT of Fig.3.8 leads to Fig.3.9 that detects the three components of the signal and suggest its capability in emphasizing the point of change in frequency. It is also clear that such frequencies do not appear in the spectrogram clearly while the three peaks are well recognized in synchronsqueezed STFT. VGRF is assumed to be governed by equation (3.8), then one can detrend the DC-frequency component ($VGRF_{st}$) and the remaining match with the frequency content of non-stationary part ($VGRF_{nst}$) in addition to noise ($\varepsilon(t)$). The late can be reduced by using the appropriate filtering techniques.

$$VGRF = VGRF_{st} + VGRF_{nst} + \varepsilon(t) \quad (3.8)$$

This suggests the power of synchronsqueezing in non-stationary signal analysis and would be helpful in separating the active and impact peaks in VGRF, differentiate the effect of heel-strike, mid-stance and propulsion on gait and many others as mentioned by figuring out the outliers in the signal

3.1.2 Turning Points Filtering

The divergence of instantaneous frequency marked as turning points when subject reaches the end of the walking line and then the subject is asked to turn come back. Those must be treated separately for comparison between normal and Parkinson. They are outliers in a typical study. Knowing that turning while walking is highly associated to falls in elderly [53].

Fig.3.10 indicates ellipses at certain instant of times. When recording the signals, subjects were asked to walk at their own pace for two minutes. Those ellipses are obtained when the subject reaches an end point and then asked / required to turn around. Such turning points as shown in the figure will alter the frequency content of the signals and therefore the analysis. The frequency at those instants scatters from 0.6 to 0.9 Hz. That's why it is become important to reconstruct those part. Otherwise, different segments of the signal must be treated separately.

The divergence in the frequency content from its rigid form introduces instantaneous change in frequency content. In order to relate this phenomena to the real experiment, those are obtained at turning points in the experiment as the subjects are asked to move without any secondary task in a well-lit 25-m long corridor. Such change suggest either to consider those events as outliers or they should be investigated separately in cases of classification between normal and pathological gait.

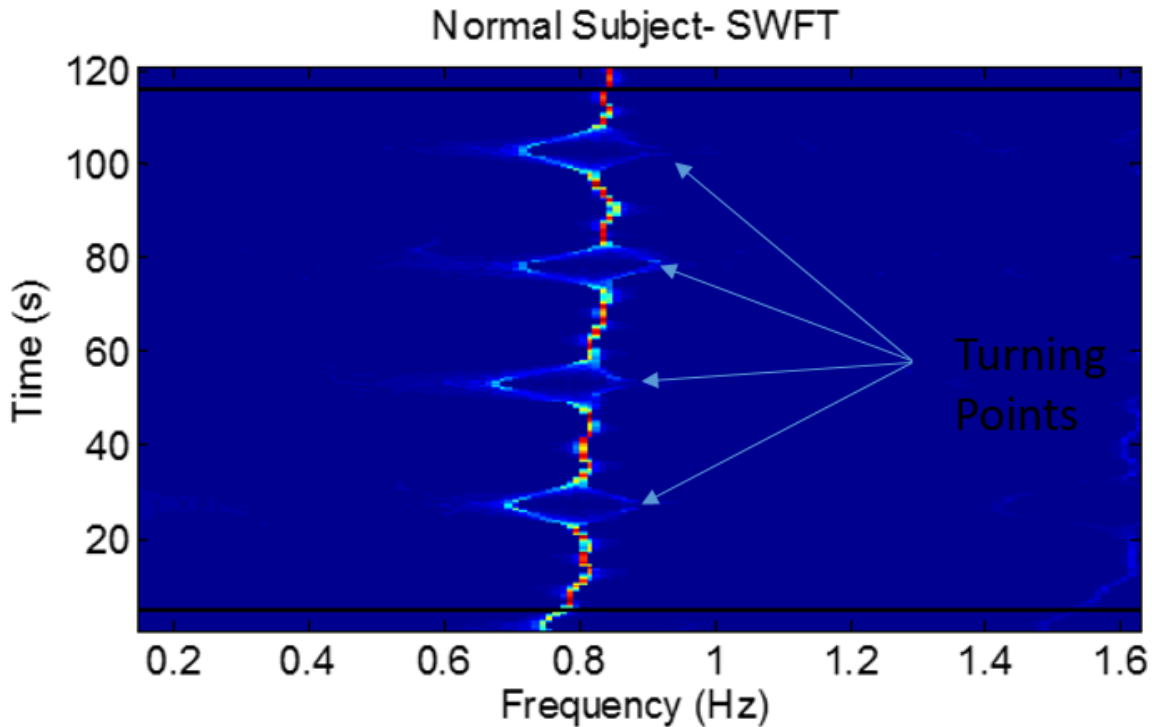


Figure 3.10: synchrosqueezed short time Fourier transform

3.1.3 Effect of Dual Task on Gait : Instances where Normalization Fails

Dual task induced a significant increase sway parameters variability in both control and Parkinson subjects [55]. In this part, two sets of measurements for VGRF derived from six elderly normal control subjects and six elderly patients with Parkinson are used due to database limitations. Participants then walked and performed a second task: serial 7 subtractions. The effect of dual task gait training is pointed out by comparing gait properties before and after training. It improves balance and gait abilities of chronic stroke patients [37]. Furthermore, another study shows the rhythmic walk is not affected by cognitive tasks in healthy subjects and have an

influence on pathological gaits [85]. In addition, during specific dual task the gait speed decreased ($p < .001$) and swing time variability increased ($p < .001$) [43].

To sum up, a bunch of literature directly pointed out some features that would be affected as a result of adding cognitive task during walking. However, a need for deep analysis of main properties (like instantaneous frequency) of gait changes while performing a dual task as this part will focus on. In addition, VGRF consist of close frequency components contaminated by noise. Such signals are time varying frequency and amplitude. However, major stationary component is dominating the VGRF signals that masks the detection of such non-stationary components that would give the most relevant difference between two signals.

Fig.3.11 shows two main important phenomena. A shift in the frequency and this is explained by change in the speed of subjects performing a certain task while walking. The second fact is a change in the amplitude in the time averaged synchrosqueezed STFT while performing dual task. This is due to divergence of the power from certain frequency component into other frequencies. Therefore, it would be beneficial to extract the instantaneous frequencies and track their variation.

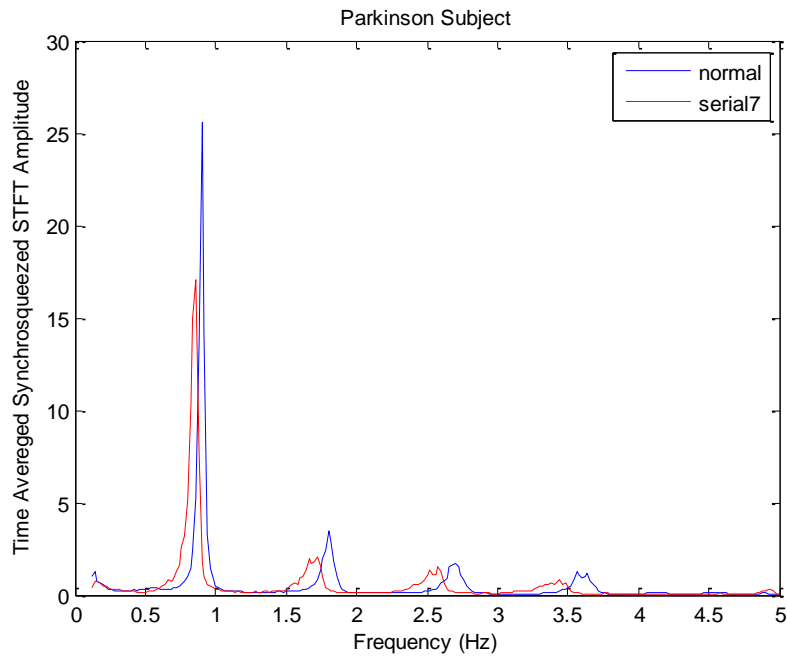


Figure 3.11: Time Averaged Synchrosqueezed STFT

In order to summarize the ability of synchrosqueezing in revealing valuable info about the gait, Fig.3.12 is obtained for the total ground reaction force so we can generalize the following differences:

- Fluctuation in the instantaneous frequency as a function of time
- Some components disappear
- A shift in the frequency content is obtained
- The power is relatively different

As a result, one important recommendation is pointed out: dual task while walking affect the gait in a tremendous way in all subjects whether normal or Parkinson. The shift in the value of

the frequencies is due of the voluntary or automatic movement during dual task. This is revealed by hypokinetic. Hypokinetic disorders usually appeared in Parkinson subjects' gait.

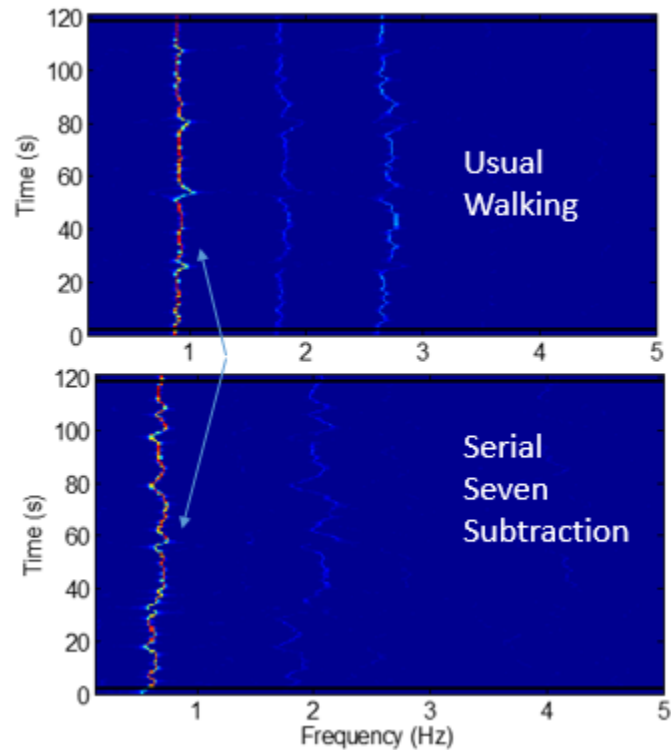


Figure 3.12: Synchrosqueezed STFT for total VGR signal extracted from the gait of Parkinson subject on both walking conditions

That is why filtering and normalization must be given specific attention. While we perform gait pathological assessment, it is hard to normalize signals from cognitive tasks or even when it comes to physiological or other situations. Therefore, significant content of the signal will be altered. That is why the adaptive filtering model best fit in such cases. Keeping in mind it is always to go over the frequency content of the signal. In addition, normalizing VGRF from parameters like cognitive tasks for comparison purposes among subjects became problematic. In order to overcome this debate, we focused mostly on this thesis on inter subject – VGRF comparison. This

is done by comparing VGRF from right and left foot of the same subject in addition to comparing two consecutive steps with each other from the same foot.

3.2 Treating the Total VGRF

A new method for analyzing human gait is based on Hilbert Haung Transform (HHT) which is doing well in non-stationary and nonlinear analysis. The proposal is based on the Hilbert spectrum of raw signal to show relation between gait pressure and frequency. Results indicate an inversely proportional relationship. Usual human gait analysis like Fourier transform is conducted to get the different spectral components of the signal. However, to detect the occurrence of fall or walking abnormality, a need for a more advanced analysis to take into account the instantaneous and therefore quick lateral changes in the raw gait signal observed over small time windows. Such instantaneous features like frequency, magnitude, and phase are observed from the complex trace / analytic signal given by Hilbert transform. The ground reaction force is observed and the results shows variation of the first IMF by getting the number of zero crossing and standard deviation as a good indicators to distinguish normal subjects from those who are patients with idiopathic PD.

3.2.1 Indications from Hilbert spectrum applied to the raw signal

Fig.3.13 shows the Hilbert spectrum of the original VGRF. The U-shaped pattern characterizes all Hilbert spectrum plots of subjects in time frequency evolution as shown in the considered example in Fig.3.13 for a normal subject. If the instant just after heel contact with the ground is taken, indicated by a middle dotted black line in Fig.3.13, VGRF exerted by the subject starts to increase.

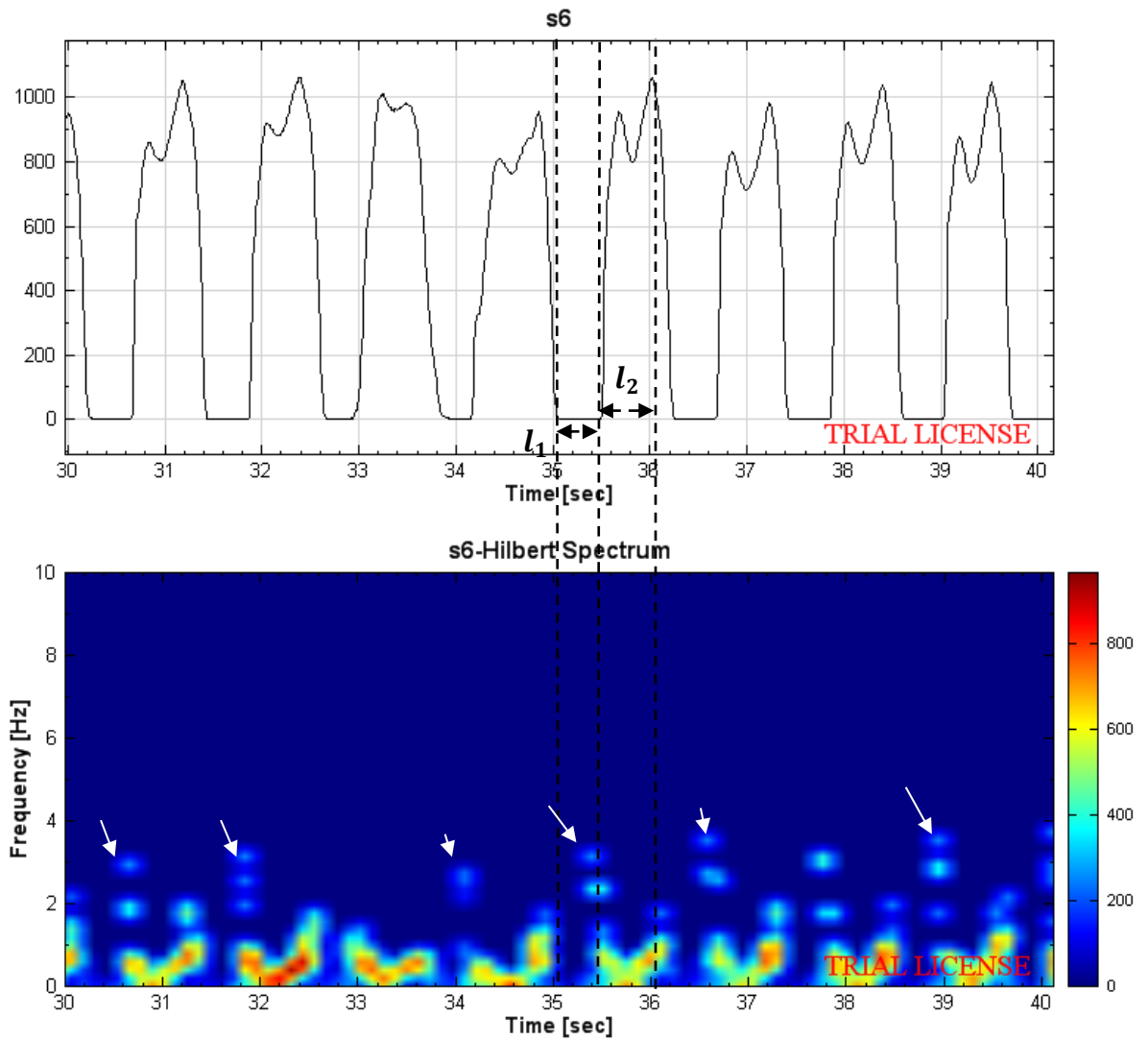


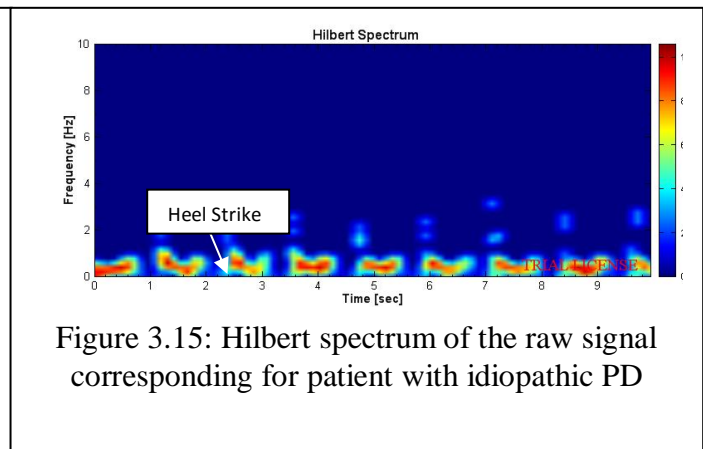
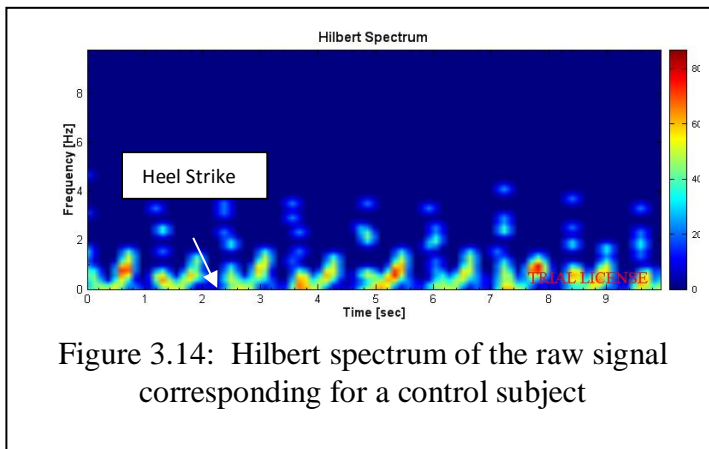
Figure 3.13: Hilbert spectrum of the VGRF for a normal subject.

The frequency as shown in Hilbert spectrum is at high and starts to decrease as the foot becomes plantar with ground. From the color bar, the amplitude of frequency starts from minimum and starts gradually increasing as inferred by time interval l_1 . When the foot is in plantar position with ground, the force is at maximum while the frequency is at minimum, however, its magnitude is at maximum suggesting the long time and this can be

inferred [12]. As the force decreases during the toe-off, the frequency starts to increase. As a result the maximum frequencies exist at the heel strike and toe-off during gait. In addition, this suggests that the frequency opposes the change which produces it as a trying to retain the body in balance and therefore of not falling [13]. Hilbert Spectrum of both normal and Parkinson subject indicate difference in frequency pattern distribution [13] and this is clearly shown at different mean frequencies represented by IMFs

3.2.2 Normal and Parkinson

The Hilbert spectrum of gait signals in Fig.3.14 and Fig.3.15 corresponds for normal and patient with idiopathic Parkinson disease respectively. The GRF is at minimum as shown in Fig.3.14 by arrow at moment of heel-strike.



This indicates that the frequency of the signal is high at heel-strike and at the toe-off and also suggests that the frequency opposes the change which produces it as a trying to retain the body in balance and not falling. Fig.3.14 and 3.15 also show the control

subjects have higher frequency at instants of heel-strike and toe-off than those in the patient. Thus, the information in the first IMFs extracted from ensemble empirical mode decomposition (EEMD) important for analysis.

3.2.3 IMF General property

Plotting the number of zero crossing versus average instantaneous frequency for each IMF including all subjects shows the same linear relationship and is given by equation (3.10) after a linear fitting is done as shown in Fig.3.16 where IMF2 is deliberated.

$$\text{Mean Frequency}=0.0041(\text{zero crossing} + 1) \quad (3.10)$$

As a result using both features couldn't affect classification performance but can computationally expensive. Accordingly, either Mean frequency or zero crossing could be used.

A set of intrinsic mode functions are generated using the sum of the 8 sensor outputs of the left foot. 18 control subjects and patients with idiopathic PD are considered. The counting number of IMFs is shown in table 3.2.

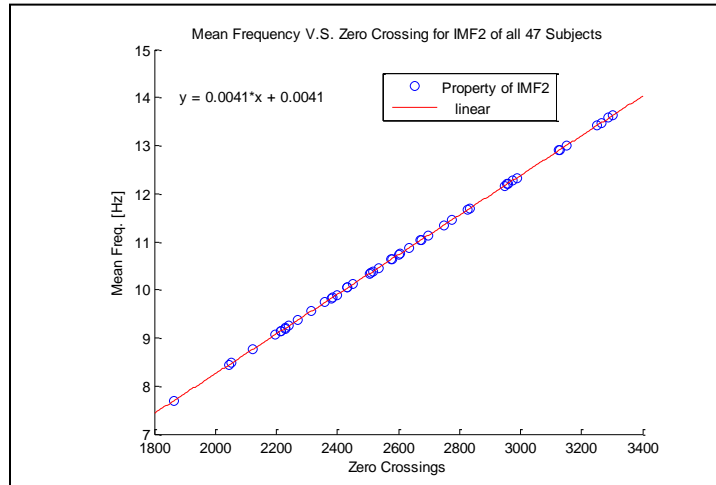


Figure 3.16: Mean frequency V.S. Zero Crossing for IMF2 of all 47 subjects.

# of IMFs	12 IMFs	13 IMFs	14 IMFs	15 IMFs
Control (%)	16.66	<u>72.22</u>	11.11	0
Patients (%)	35.7143	<u>25</u>	32.1429	7.1429

Table 3.2: The percentage of certain number of IMFs present in raw signal

From Table 3.2, there is a clear indication 72% from control subject have 13 IMFs while 25% of Patients are recorded to have 13 IMFs. This suggests that a certain frequency band is either added or omitted from the signal. Later in this document, this will indicate that frequency is related to pressure evolution and therefore the elderly is either having a certain frequency band more than usual to control and balance his/her walking, and this could be voluntary. A less IMF indicates that elderly is walking on his usual and a decrease of reaction time and this suggests a more body shiver and the patient is subjected to the risk of falling.

Again, the weakness of EMD in our case can be summarized as follows: for the closed envelopes that formed using cubic spline and at a height away from zero, there will be a combination of frequencies rather than a clean IMF signal. This is called mode mixing.

3.2.4 Zero Crossing effect of each IMF on training accuracy

In each step, one of the IMFs features are omitted and then its effect on the training accuracy can be formed. Table 3.3 presents the result. For instance, in row 1 where none of the IMFs is gone is able to classify 95.7% of the examples in the training set correctly. In row 7, the IMF6 is excluded and the training accuracy decreased to 76.6%. As the table indicates, excluding IMF5 and IMF13 from the training set has no effect in the training accuracy. Knowing that IMF5 is recorded to have the highest energy percentage compared to the total energy of the original signal in all subjects, except for Residue as shown in Table 3.4. IMF13 forms the trend of the signal and all subject therefore have the same mean instantaneous frequency for IMF13. All other IMFs will affect the training accuracy specifically IMF3, IMF11 and IMF6 were the most important one since they encounter low training accuracy in their absence.

Table 3.3. Omitted IMF effect on training accuracy

i-th Omitted	IMF	Training Accuracy	i-th Omitted	IMF	Training Accuracy
None is omitted		95.744681= 2 out 47 subjects classified incorrectly	7		91.489362
1		93.617021	8		91.489362
2		93.617021	9		93.617021
3		89.361702	10		91.489362
4		91.489362	11		89.361702
5		95.744681	12		91.489362
6		76.595745	13		95.744681

Table 3.3. Energy percentage compared to the total energy of the original signal, except for Residue

	Normal		Parkinson	
	Mean	Stdv	Mean	Stdv
IMF_h1	0.075	0.05	0.061	0.058
IMF_h2	0.442	0.212	0.246	0.193
IMF_h3	9.723	4.493	5.872	3.899
IMF_h4	6.451	3.771	10.05	9.051
IMF_h5	80.03	6.201	81.93	10.47
IMF_h6	2.704	2.18	1.345	1.923
IMF_h7	0.252	0.122	0.18	0.126
IMF_h8	0.099	0.046	0.088	0.058
IMF_h9	0.067	0.03	0.059	0.051
IMF_h10	0.048	0.034	0.058	0.065
IMF_h11	0.065	0.154	0.063	0.082
IMF_h12	0.044	0.07	0.051	0.112

3.3 Frequency Content Analysis

The aim of this section is to investigate more on the main fundamental frequency content of gait VGRF. In addition, a comparison between normal and Parkinson subjects in terms of their frequency is developed.

3.3.1 System's Frequency Nonlinearity

A linear system in frequency is achieved when the net amplitude frequency (A_{freq}) of the summed signal (total VGRF) is equal to the sum of the amplitude frequencies produced by each sensor's signal. More clearly this is emphasized in equation (3.9) where "i" is the sensor number:

$$A_{freq}(\sum VGRF_i) = \sum A_{freq}(VGRF_i) \quad (3.9)$$

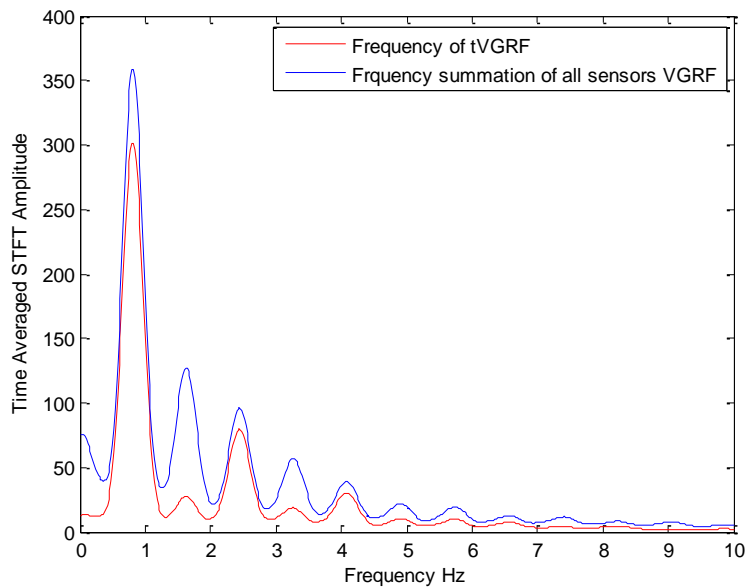


Figure 3.17: The power of frequency content present in tVGRF and the summed amplitude is different from the summation of frequencies for sensor's VGRF.

However, this is not the case on gait VGRF. Fig.3.17 emphasizes clearly the difference between the frequency content of the total VGRF (tVGRF) and the summation of frequencies of the array of 8 sensor's VGRF. The most fact is that the second peak becomes of lower amplitude compared to the third peak in tVGRF. This suggests the Heterodyne phenomena around ~ 1.63 Hz. In addition, the even harmonics are most likely to be affected.

3.3.2 Frequency content

Up to our knowledge, the marginal level of frequency in the gait VGRF is noted to be less than 20 Hz [42]. Consequently, our focus will not exceed the 20 Hz for the reason that STFT confirms no valuable power frequency content revealed for frequency above 15 Hz. Fig.3.18 displays up to 5Hz for graph clarity in addition that concentrated power frequency content is located at this region.

First, all sensors contain the same frequency content with a relatively small different amplitudes as shown in Fig.3.19 within the same person, this is found in all subjects and can be explained as a tend to maintain coherence in gait at least during experimenting for small duration. This also quantifies that participants are walking on free obstacle level ground!

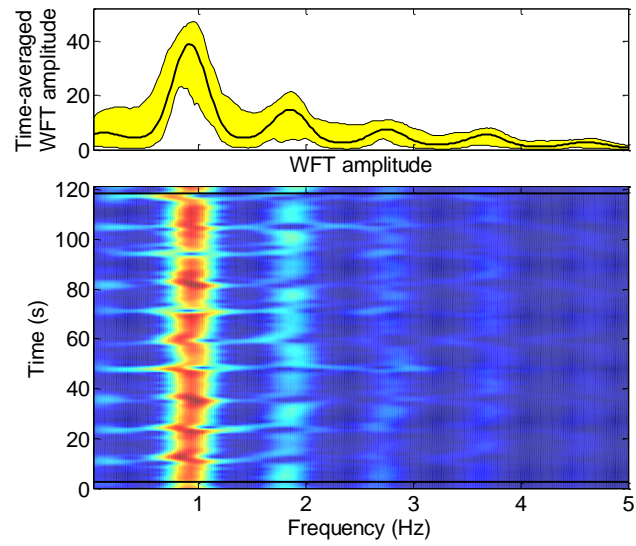


Figure 3.18: STFT plot and upper plot is time averaged STFT

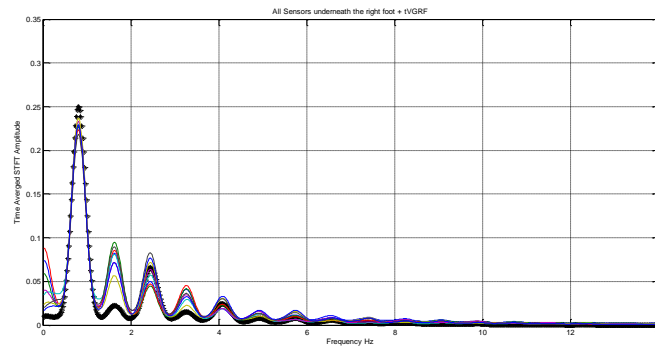


Figure 3.19: Amplitude of time averaged STFT amplitude for all 8 sensor underneath right foot for a normal subject. The strikes corresponds to frequency tVGRF.

Again, the main major frequency content is at a lower values. That's why WT is better used to tell more about the principal frequency components of gait VGRF. The first three peaks revealed a 94 % power from the whole spectrum. That's why they are considered.

Table 3.4 demonstrate the first three fundamental peaks that cover the most power of the frequency content. The first peak is in the range of $\sim 0.5658 - 1.1182$ Hz for almost 98 % of subjects. It is approximately 2.0276 Hz for the second peak on average and 2.7108 Hz for the third peak.

TABLE 3.4: FREQUENCY CONTENT

Peak #	Normal (mean \pm std)		Parkinson (mean \pm std)	
	Frequency range (Hz)	Peak value	Frequency range(Hz)	Peak value
1 st	0.9154 ± 0.0676	~ 0.22	0.8985 ± 0.1109	~ 0.24
2 nd	1.8347 ± 0.1292	~ 0.09 8	2.1473 ± 0.7278	~ 0.07 3
3 rd	2.9458 ± 0.8859	~ 0.05 9	2.5650 ± 0.7220	~ 0.04 5

3.3.3 Difference between Normal and Parkinson

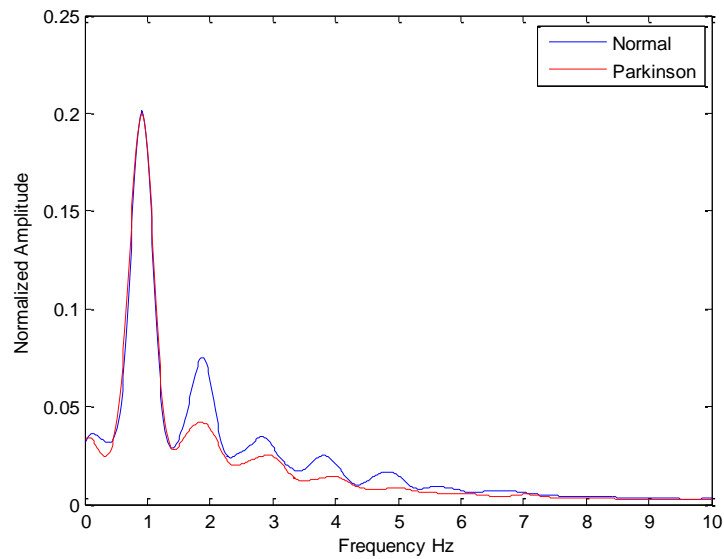


Figure 3.20: Amplitude of time averaged short time Fourier transform - Gaussian

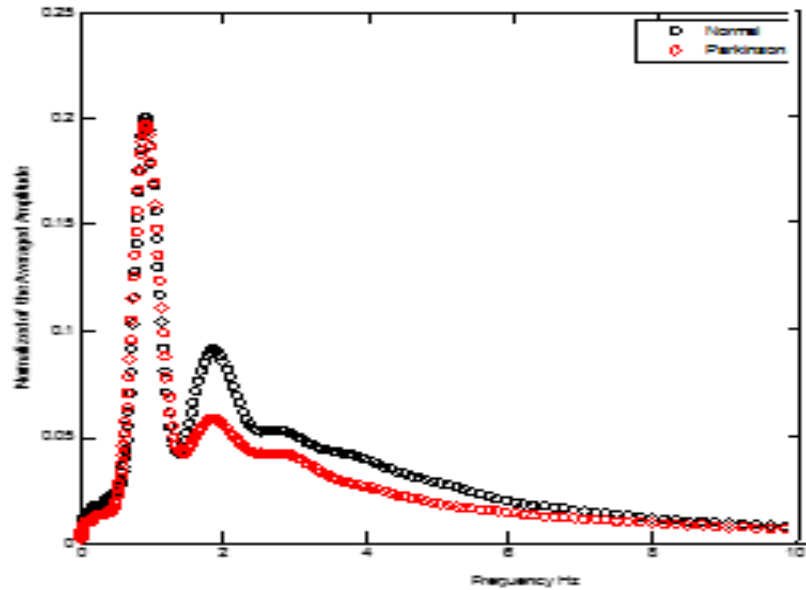


Figure 3.21: Amplitude of time averaged wavelet transform – Lognorm

The first peak covers the most important part of active part of the VGRF signal as shown in Fig.3.20. One research demonstrate at a cutoff frequency of 3 Hz leads to imperfect separation of both active and impact peaks [86]. While it is not that such frequencies don't exist in Parkinson subjects as frequency tends to increase (i.e. the more they correspond to the impact peak), but the peaks and the valleys tend to be much more muted. That justifies the damping oscillations of the decomposed impact curve [86], on other words the result of spectral decomposition of VGRF. The lack of such peaks can be related to the stiffness or rigidity of limbs and consequently the postural instability that most Parkinson subjects will encounter. Nonetheless, Parkinson's restricted step length reduces their walking speed and number of steps per minute [87]. In order to discriminate the low frequencies (that usually forms the identity / main characteristics of the signal)

- τ is the time shift or lag between signals ; $0 \leq \tau \leq N - 1$
- “ C_{LR} ” :the covariance sequence given as the mean-removed cross-correlation sequence

$$C_{LR}(\tau) = R_{LR}(\tau) - \mu_L \mu_R$$

$$K_{LR}(\tau) = E\{L_t R_{t-\tau}\}$$

- μ is the mean and E is the expectation and K is cross-correlation and therefore cross-covariance can be computed using (4.3):

$$C[L_i R_j]_{\tau} = \frac{1}{N-1} \sum_{t=1}^N L_i(t) R_j(t - \tau) - \bar{L}_i \bar{R}_j \quad (3.12)$$

$$0 \leq \tau \leq N - 1 \quad i, j \in [1 \quad 8]$$

Each covariance matrix allows us to characterize the direction of the greatest variance in our data. This is so called principal component analysis (PCA) used to reduce the dimensionality of the data by selecting directions along which our data has the largest variance. Finding such eigenvectors have the property of not rotating when multiplied by the covariance matrix. Then eigenvectors (e) having largest eigenvalues (λ) corresponds to our principal components that will give a new dimensions of our data.

$$M_c(\tau).e = \lambda.e \quad (3.13)$$

The eigenvalues are obtained by solving equation (3.14). Fig.3.22 shows eigenvalues of the 8 principal components for normal subject.

$$[\det(M_c(\tau) - \lambda.e) = 0] \quad \text{at a given } \tau \quad (3.14)$$

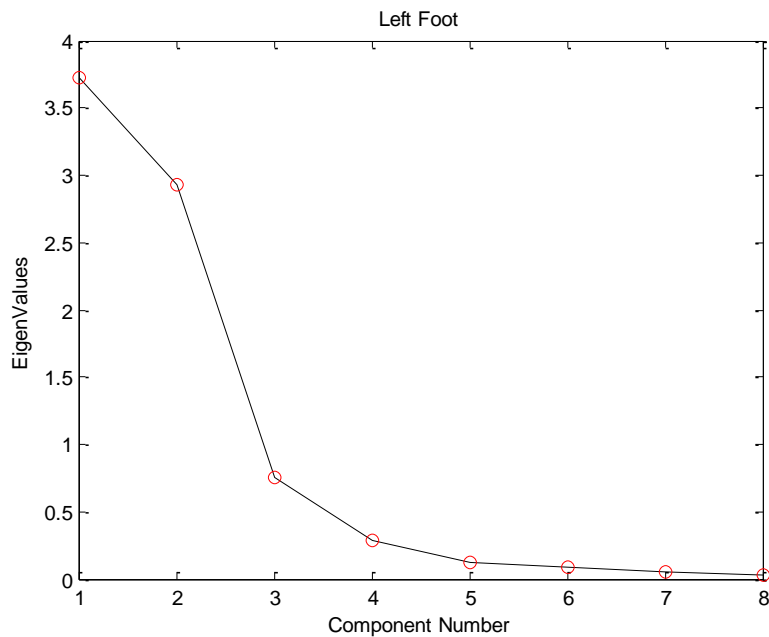


Figure 3.22: Eigenvalue versus its component number for Left foot sensors in a normal subject

The first principal component has variance (eigenvalue) 6.6677. The first three principal components accounts for 84.46 % of the total variance. The first four counts for 94%. This is a good indicator that most of the data structure can be captured in three or four underlying dimensions. The remaining principal components account for a very small proportion of the variability and are probably unimportant.

The same analysis is performed to obtain the eigenvalues for all 16 sensors. Then the maximum eigenvalues is plotted against different time lags as shown in Fig.3.23. The smooth decrease that forms the trend forms a non-stationarity relation among sensor's data.

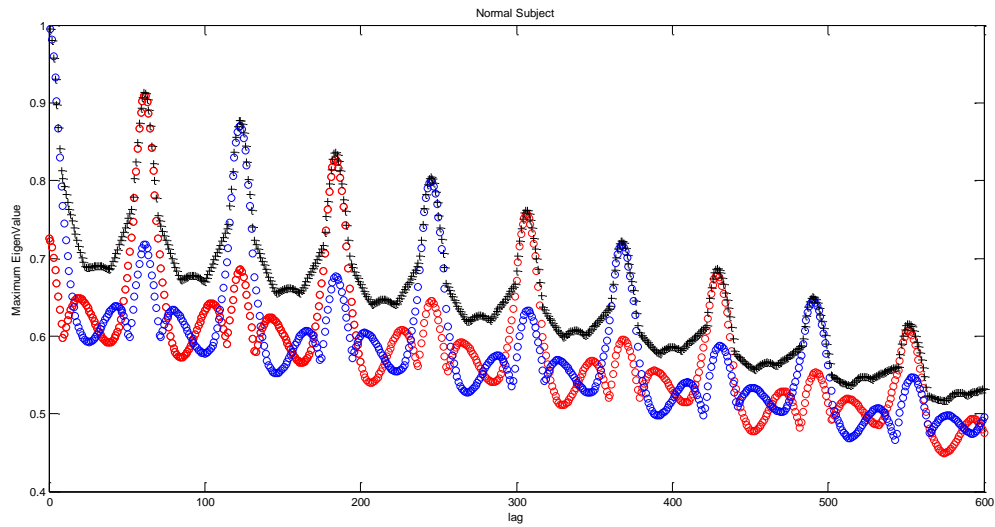


Figure 3.23: Maximum Eigenvalues being computed at different time lags for left sensor to right foot sensors (Red), left sensor to Left foot sensors (Blue), and black indicates when computed for all sensors as one matrix.

However, a seasonality that described by the repeated patterns are observed after certain period lags around 60 points (100 Hz sampling frequency). Knowing that when the covariance didn't attain zero value, this specify that the randomness situation no longer available. In consequence, the VGRF signal are a mixture of stationary and non-stationarity sources. They are stationary from macroscopic point of view but microscopically they are non-stationary. The latter is of lower power component as Fig.3.23 illustrates.

3.5 Sensor Selection

However, still many studies consider the sensor location to measure the Ground reaction force either at both toe and heel or usually by analyzing the total force from sensors underneath each foot [13]. Though, a need to investigate more exploration of choosing the correct position of a sensor or set of sensors in the insole becomes crucial. This is for the reason that some features

are used for classification and better work when they are extracted from sensors data at a given location. Then features being used widely in the literature are passed into a KNN classifier.

ROC curve is then used to evaluate each feature for all sensors. This could contribute to other research conducting in the goal of anticipating the risk of falling among people and especially among elderly [14].

3.5.1 Features Used

In this part, simple features were extracted after the data being pre-processed. Then their performance was tested. The features used here are used from literature, we found 23 features. In this section the 11 most relevant features were retained. A list of the commonly wide used features are shown below [1], [13], [15], and [37]:

- Mean: Signal averaging
- Median: numerical value separating the higher half of a data from the lower half.
- standard deviation: measures the amount of variation or dispersion from the average
- range: the difference between the maximum and minimum values
- Interquartile range: robust estimate for the spread of the data being equal to the difference between the upper and lower quartiles $IQR = Q3 - Q1$.
- 95% percentiles of the distribution of the signal. A percentile (or a centile) is a measure used in statistics indicating the value below which a given percentage of observations in a group of observations fall.
- Skewness: measure of lack of symmetry

- Kurtosis: measure of whether the data are peaked or flat relative to a normal distribution.
- Power of the signal
- Mean power frequency
- Magnitude of peak frequency

3.5.2 Testing: Features Evaluation by ROC

As too many statistical features could be extracted and evaluated in time domain analysis and frequency domain, in this section one feature is used to demonstrate the evaluation. However this is done for all features among all sensors for the 47 subjects. For instance the skewness is chosen since it has been used widely in various studies related to VGRF [13] and has demonstrated its capability in distinguishing normal and Parkinson's disease person.

Once again when $AUC = 1$, this refers to a perfect discrimination and has a ROC curve that passes through the upper left corner i.e. 100% sensitivity and 100% specificity with no overlap in the two distributions. Fig.3.24 shows a plot of the ROC curve for skewness feature tested over sensor 5 in the right foot among normal and Parkinson. Each point on the ROC curve represents the sensitivity and specificity pair corresponding to a particular decision threshold. The diagonal line dividing the ROC space is also called line of no-discrimination in which a point on this line corresponds to a completely guess. When points are above the diagonal, this indicates a good classification results and on the other

side points below this line indicate a poor predictors. Therefore the distance from the random guess line is the best indicator of how much predictive power a method has.

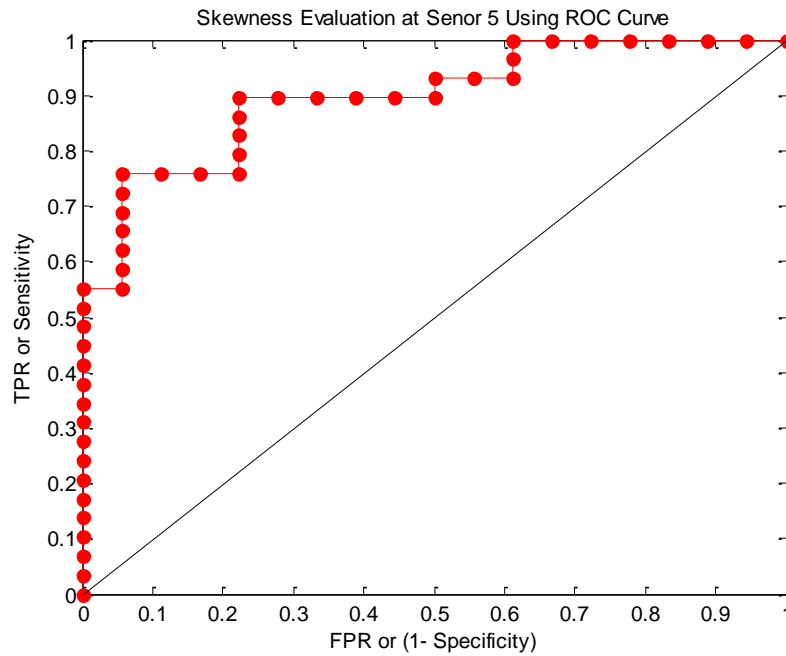


Figure 3.24: Skewness ability in discrimination between Normal and Parkinson Gait using ROC curve.

The evaluation of skewness shows the following:

ACC	85.1064
MCC	0.6822
Sensitivity	0.8966
Specificity	0.7778
Area Under Curve	0.902

Using the above listed data, 0.9 as area under the curve indicates an excellent performance of skewness in discriminating normal from Parkinson using VGRF from sensor 5.

The results of ROC evaluation among all the 47 subjects are shown in Table 3.5 for each sensor.

Table 3.5. ROC evaluation of skewness among all sensors.

Sensor # in Foot	ROC-AUC	
	Left Foot	Right Foot
1	0.645594	0.655172
2	0.609195	0.637931
3	0.609195	0.613027
4	0.701149	0.676245
5	0.904215	0.842912
6	0.787356	0.764368
7	0.850575	0.808429
8	0.62069	0.703065
VGRF corresponds to summation of the 8 sensors	0.605364	0.611111

Analyzing Table 3.5 indicates that unlike other studies similar to [13] that consider total summation of force signals from all sensors as the most important, however, its clearly shown that sensor 5 is the most important sensor (AUC = 0.9) to consider in building acquisition system to acquire data for analyses. Fig 3.25 shows the ROC curve of the total ground reaction force from sensors of the right foot. The sensitivity is recorded to be 0.6552

while the specificity is 0.5556. This yield $AUC = 0.5460$ which refers a fail level of accuracy in classification.

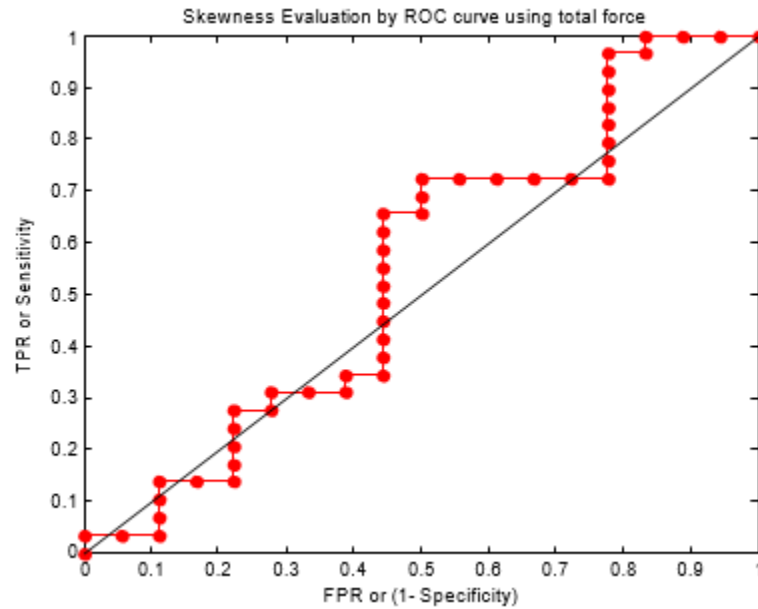


Figure 3.25. Skewness is extracted from the total force from sensors located under the right foot and its performance in binary classification is evaluated using ROC curve

This conclusion is generalized as the same procedure is applied over the rest of the features chosen in this study. If expanding data is needed, then adding sensor 7 and 6 corresponds as main sensors also to be considered for classification as shown in Fig.3.26.

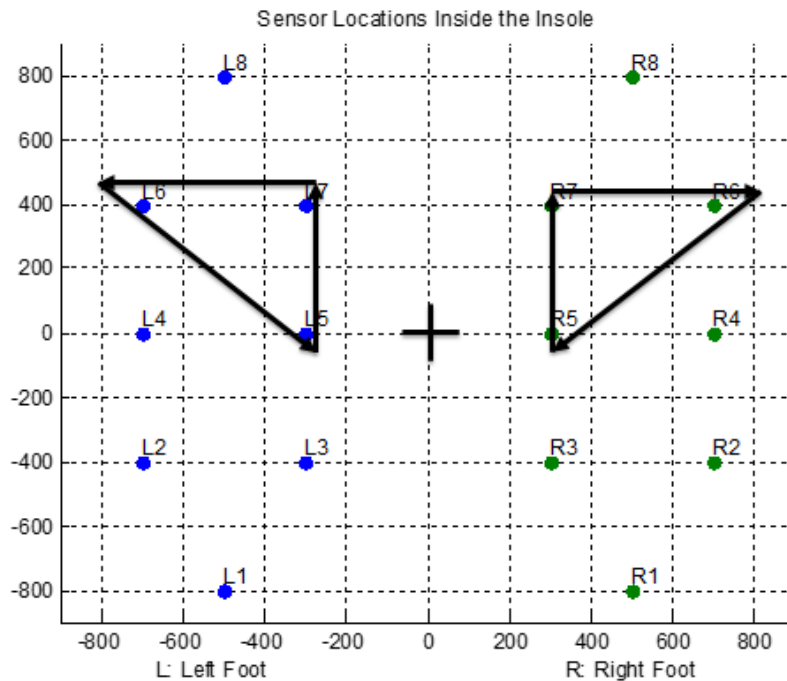


Figure 3.26: The most important locations to acquire data for Gait analysis.

Not to add, the average of the strides of the 2 classes corresponding to the 120 seconds of walking is also considered. As a result, each series of strides are represented by their average. Next, 3 features were extracted: the amplitude of the first peak, that is, the peak that corresponds to the heel contact (in case of total force), time to the first peak, stride time. The ROC evaluation also infers a better accuracy for sensor 5 compared to other sensors.

3.5.3 Verification

In order to verify results, the features are passed through a chosen classifier, k-nearest neighbors (KNN) in this case. As mentioned, KNN is not used to test its power in

classification, but to test the power of sensor 5 in a given classifier. Ten subjects from each class are chosen as training and the rest are tested by the classifier.

In this study, this is done in two ways. First, select one sensor among all subjects and then choose two features randomly and iterate between them. The feature chosen will have a high score from ROC evaluation and then feed them to KNN-classifier one example is shown in Fig.3.27. In a second case of study, fix the feature and iterate a number of sensors among the KNN classifier. The results of KNN classifier indicate an accuracy of around 83% on average in most cases where sensor five exist. Other sensor shows a relatively smaller value. While the total force when used shows an accuracy of around 15% smaller than sensor five.

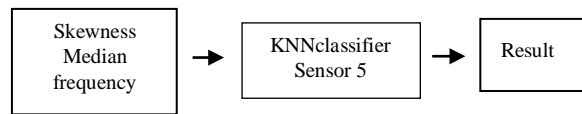


Figure 3.27. Skewness and Median Frequency are extracted from signals of sensor 5 in mid-foot.

3.5.4 A simple feature of the mid-sensor

The mean and the standard deviation of the segments of each step is computed and then they are plotted versus each other for mid-sensor signals. Fig.3.28 clearly shows that those statistics vary from one step into another. In our case the mean and standard deviation are highly correlated. Furthermore, such a change in the mean that ranges from 32 to 77

and a standard deviation that ranges from 70 to 135 is a clear indicator that the signal is non-stationary.

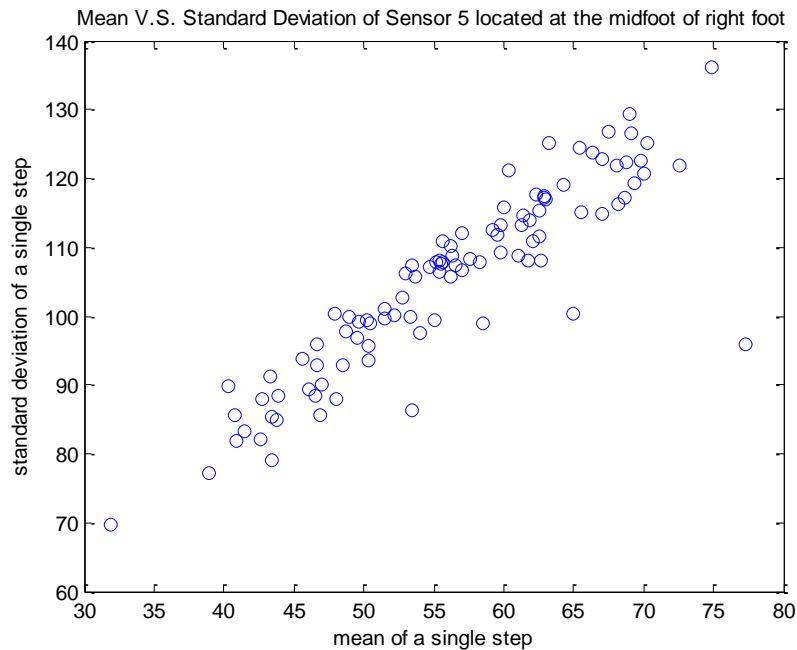


Figure 3.28: Standard deviation versus mean for an abnormal subject upon midsensor located in the right foot.

3.6 Classification Methodology

Vertical Ground Reaction Forces (VGRF) are reflection of the net forces exerted by human body on ground while walking. In this section, instead of summing VGRFs collected from various sensors underneath the foot as others do, they are treated separately. Therefore, the equivalent force will be on Center of Pressure (COP), i.e. at the centroid of the distributed load.

Starting from arguments that most falls in older adults are a result of variability in gait pattern, this study focuses on kinetic parameters: VGRFs and COP. As mentioned, VGRFs reflect

the resultant of forces encountered by external (gravitational) and internal (muscle) forces in addition to the feet-ground interaction forces (spring-damper model). Likewise, focusing on VGRFs decreases the effect of environmental interferences like friction on the wellful gait. The speed and age are also used in this analysis. This analysis constitutes setting up a nonlinear decision boundary between balanced and unbalanced gaits through two related hypothesized lemmas. Then the unbalanced gaits are excluded from the next step of the analysis. These unbalanced gaits are certainly considered abnormal due to their high gait variability measured by their load of distribution and speed times age. The remaining balanced gaits that include both normal and Parkinson subjects are taken into another classifier using a simple correlation feature. In fact, this would be very beneficial during real time implementation that will end up with a portable device. This analysis is helpful in evaluation of a rehabilitation program. It may turn out dropping injuries by enhancing fall prevention on the elderly in particular those affected by Parkinson.

3.7 Observations and methods

3.7.1 Center of pressure path

Center of pressure (COP) is a kinetic parameter that represents VGRF's point of application. Therefore, it can be used to track the transfer of weight to asses balance. The instantaneous location of COP was deliberated as a weighted average of the measured VGRF values for each sensor by means of equations (3.13) and (3.14):

$$X_{cop} = \frac{\sum_i^n VGRF_i X_i}{\sum_i^n VGRF_i} \quad (3.13)$$

$$Y_{cop} = \frac{\sum_i^n VGRF_i Y_i}{\sum_i^n VGRF_i} \quad (3.14)$$

(X_{cop}, Y_{cop}) are coordinates corresponding to the instantaneous place of the center of pressure. (X_i, Y_i) represents the location of sensor (i). $VGRF_i$ is the force obtained from sensor (i) and n is the total number of sensors.

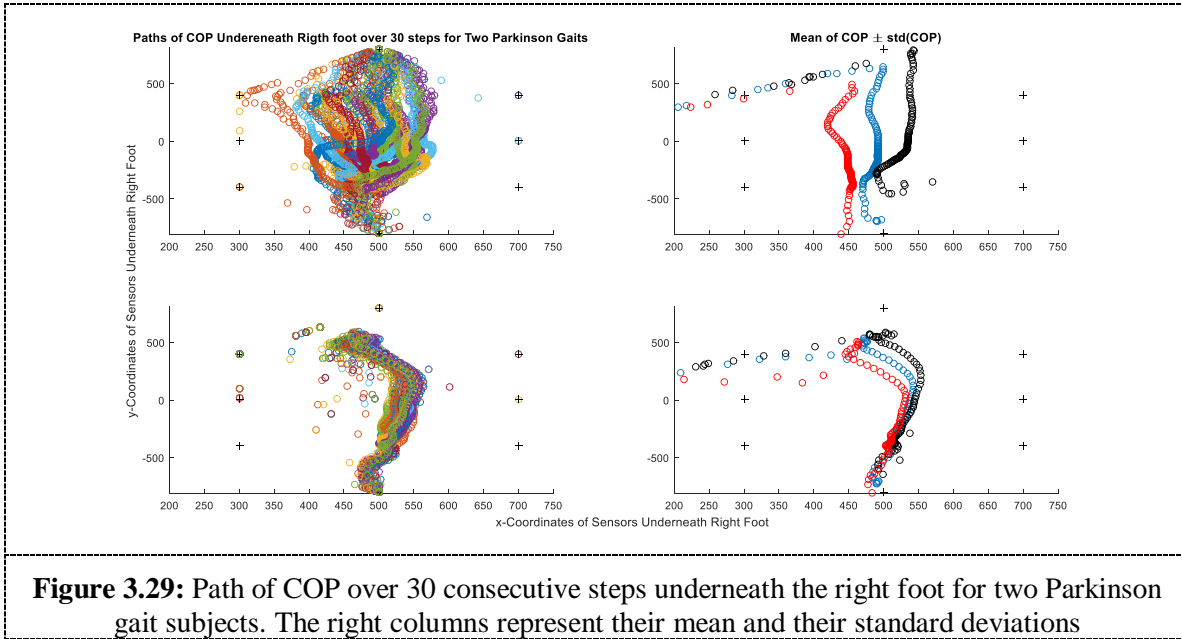
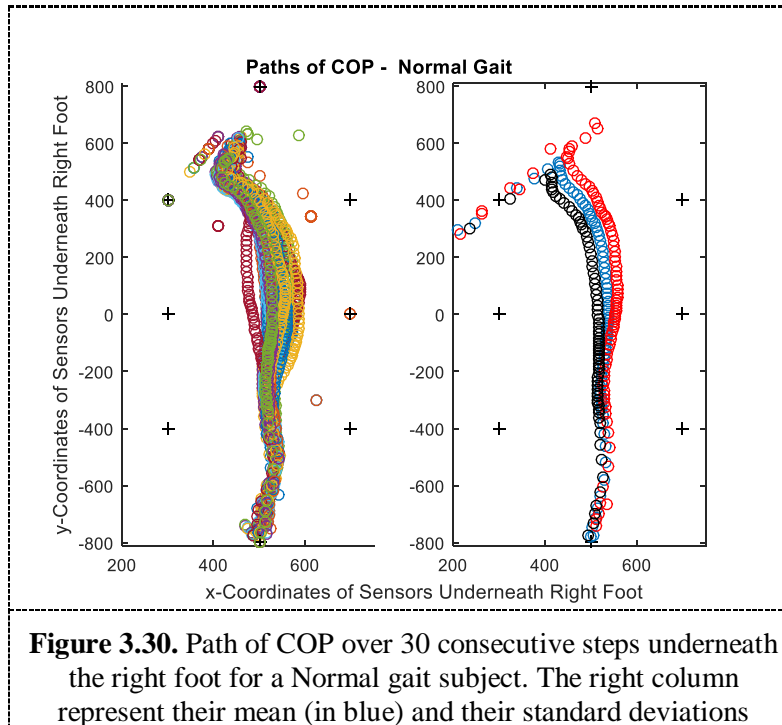


Fig. 3.29 signify the path of COP underneath the right foot for two Parkinson gait subjects. Getting the mean of the different paths of COP over the x and y-coordinates followed by their standard deviation shows a variation in the mean of 49.5576 and 54.1533 over the x and y-coordinates respectively for the first subject (first row). While the mean on the second subject varies in the range of 25.6551 and 46.6175 for x and y-coordinates respectively. Working out the ensemble variation and then their standard deviation over the x-coordinate is recorded to be 69.4985 on the first subject higher than the second subject of 53.4931. This shows the path of COP in the first subject deviates highly compared to

the second subject. This difference is not observed over the normal group subjects. Fig.3.30 is an illustration.



Formulating whatsoever is declared forms a good indicator that certain Parkinson subjects have the ability to synchronize their steps for diverse reasons (rehabilitation, short time experimentation (2 min), medication, level of pathology...). Such gait variability in the same group would lead comprehensive assortment of statistical discrepancy making it challenging to find fairly common properties between subjects. Taking 18 normal and 18 Parkinson subjects yields a mean of 58 ± 15 and 61 ± 15 (mean \pm std) respectively. Testing the null hypothesis that the pairwise difference between normal subjects and Parkinson

subjects has a mean equal to zero shows ($h=0$, $p=0.7$). This directs t-test not to reject the null hypothesis with 5% significance level. This is one of the real facts that the difference between the two groups will be masked as a subset of one group share same properties of the other group.

3.7.2 Load Distribution

The above observations in the gait variability within the same group of subjects and their overlapping in their characteristics, guide to have more or less rules in advance to perform any statistical interpretation of signals. This is because external factors could mask the real datum of signal being premeditated. The following two hypothesized lemmas:

Lemma 1: The axis of body balance is highly related to distribution of loads by subjects during switching of the feet. This axis appears clearly when walking in a straight line and passes through center of gravity. This center changes location in case of imbalance due to a certain disease.

Lemma1 outline Lemma2:

Lemma 2: The movement of feet is uniform when walking due to the distribution of loads between the feet. Therefore, imbalance is due to irregular distribution of loads between the feet. In a simpler way, pressure distribution between feet differs when a subject is affected with disease like Parkinson. This is more obvious in diseased subjects where their metabolic system is affected.

Setting up Lemma2 articulate the following hypothesis:

Hypothesis: Normal Gait must be balanced. However, balanced gait doesn't indicate normal gait subject.

The stemmed hypothesis points out that if a healthy gait subject is considered, then this subject must have a balanced bearing between feet. While if the subject is affected by a disease like Parkinson this disease replicated on his gait. It may appear as unbalanced gait, however this is not always the case. Parkinson subjects could be placed into rehabilitation program or get beforehand some medication prior to the experiment. This would mark the gait performance during the experiment and it would appear as balanced way of walking. That's why and before undertaking any statistical analysis, it's really become an essential task to differentiate Parkinson subjects as having balanced and imbalanced gait. Again, normal subjects are definitely considered to have balanced gaits. In this manner, Parkinson subjects are split to end up with a subset that for sure comprise Parkinson syndrome and the rest are driven into supplemental examination. In fact, reducing the dataset would be very beneficial as all statistical parameter will not be deviated and affected by parameters of subjects that we are guaranteed to partake irregular posture.

Since a classification is required on a first step, it is more than enough to train a classifier that draws a boundary for balanced gaits. It is mainly affected by the bunch of normal gait subjects as we have a conditional hypothesis.

The flowchart of the tracked technique is illustrated in Fig.3.31.

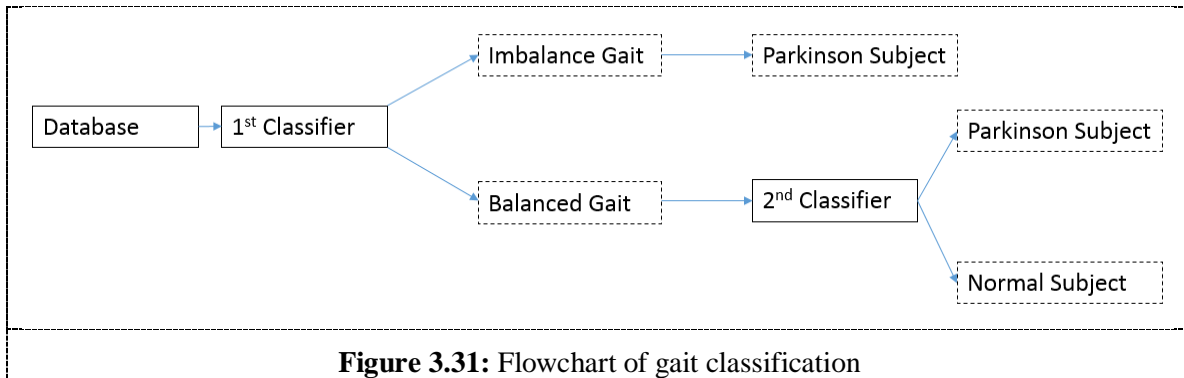


Fig.3.32 emphasize the load distribution for a four gait subjects. Two from each group are presented. Comparing the distribution of loads between right and left foot shows that normal subjects admits a comprehensible scattering between feet. This result is inspected in some Parkinson subjects (left bottom diagram) while others have a totally different patterns of distribution between feet (right end map).

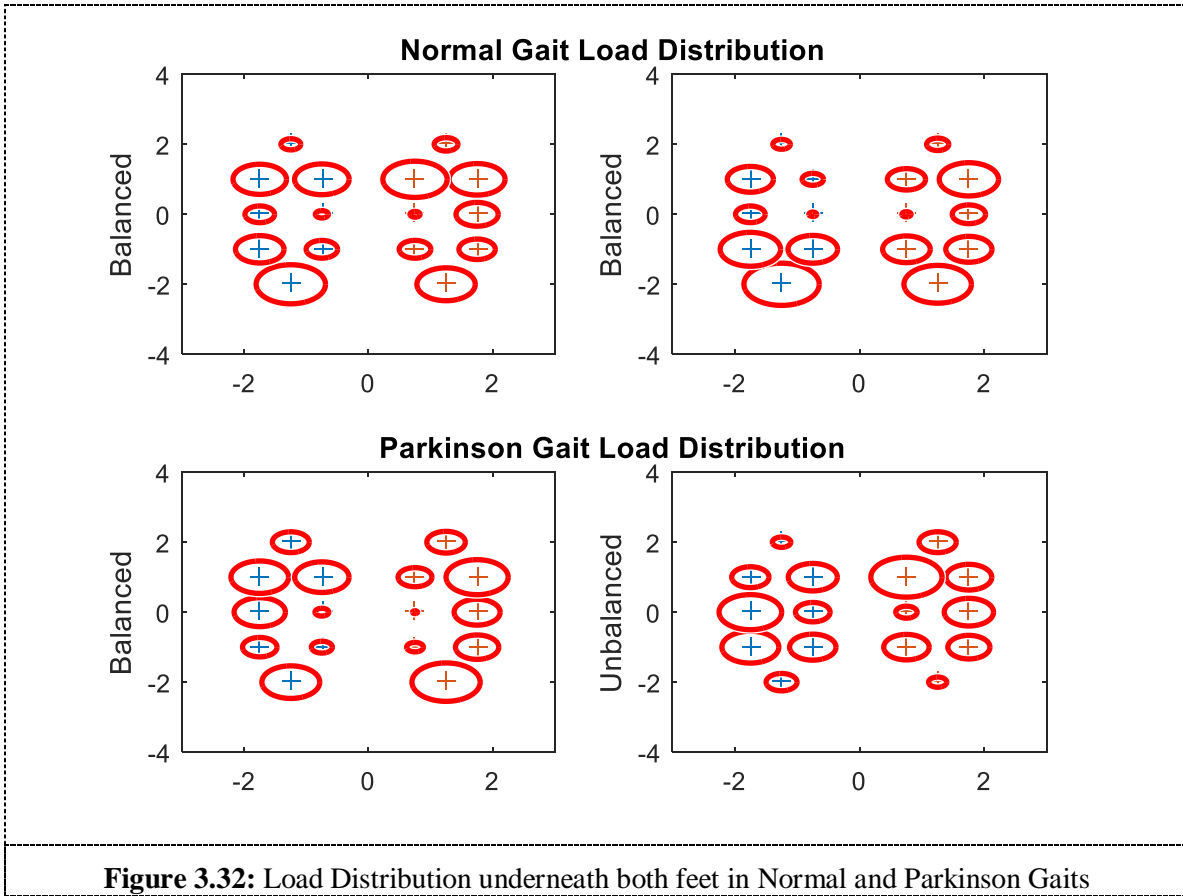


Figure 3.32: Load Distribution underneath both feet in Normal and Parkinson Gaits

The Euclidean distance to each sensor weighted by its consistent energy is then computed by equation (3.15):

$$\Gamma_i = E_i \sqrt{x_i^2 + y_i^2} \quad (3.15)$$

Γ_i is the load distribution at sensor (i), E is the equivalent averaged energy normalized to other total sensors energy, x_i and y_i are the coordinates of sensor (i). Then testing variation on Γ_i obtained from right whether it corresponds to variation on left foot or not is implemented by Pearson correlation coefficient (r) as in equation (3.16).

$$r = \frac{1}{n-1} \sum \frac{(\Gamma_{Li} - \overline{\Gamma_L})(\Gamma_{Ri} - \overline{\Gamma_R})}{s_L s_R} \quad (3.16)$$

3.7.3 Speed and age

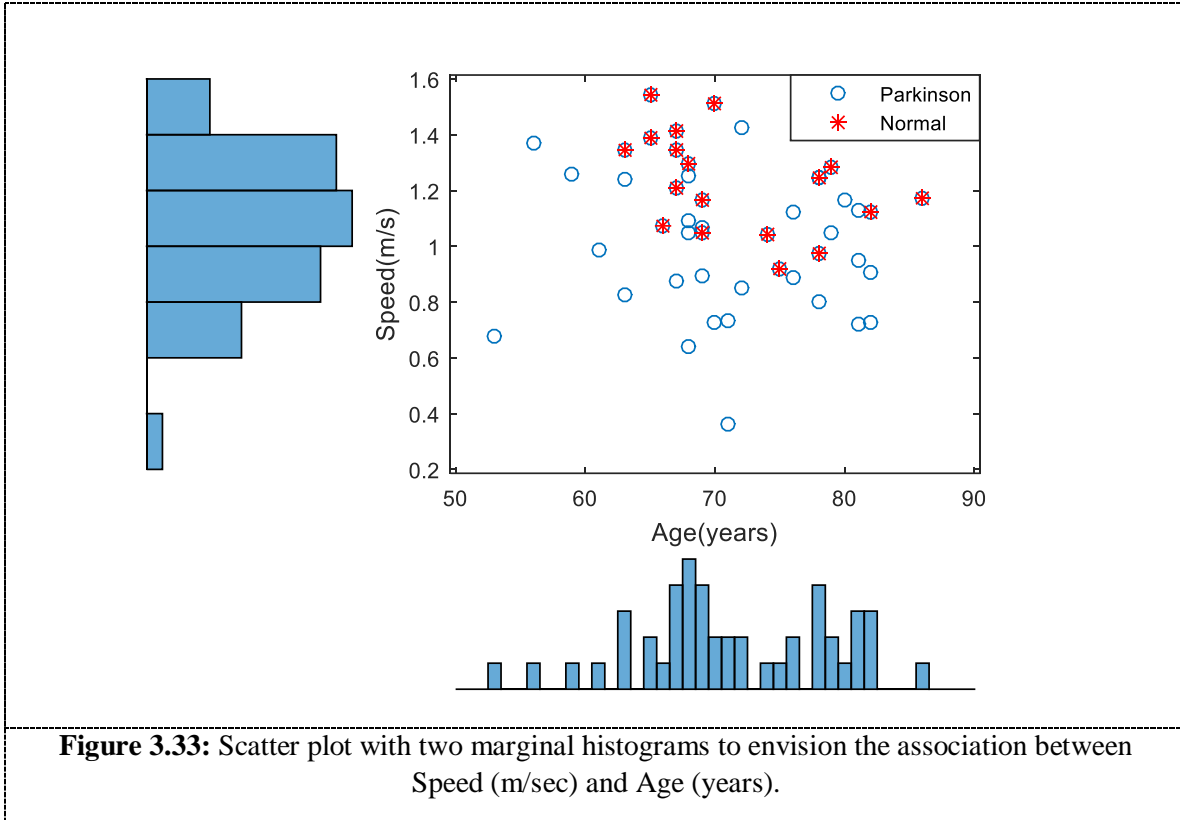


Fig.3.33 designate no significant correlation between speed and age in both normal ($r = -0.4513$) and Parkinson group ($r = -0.1064$) with a significant difference between the two groups. Based on reference [53], Age \times Speed forms an important parameter in the corresponding study. For case in point, having 18 normal and 18 Parkinson subjects yields a difference in speed [54] as shown in the box plot of Fig.3.34.

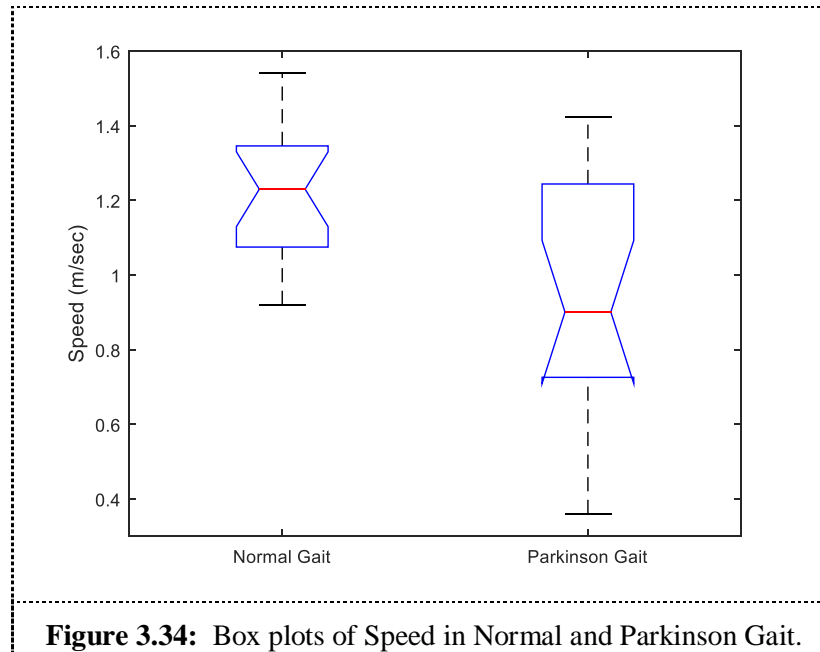
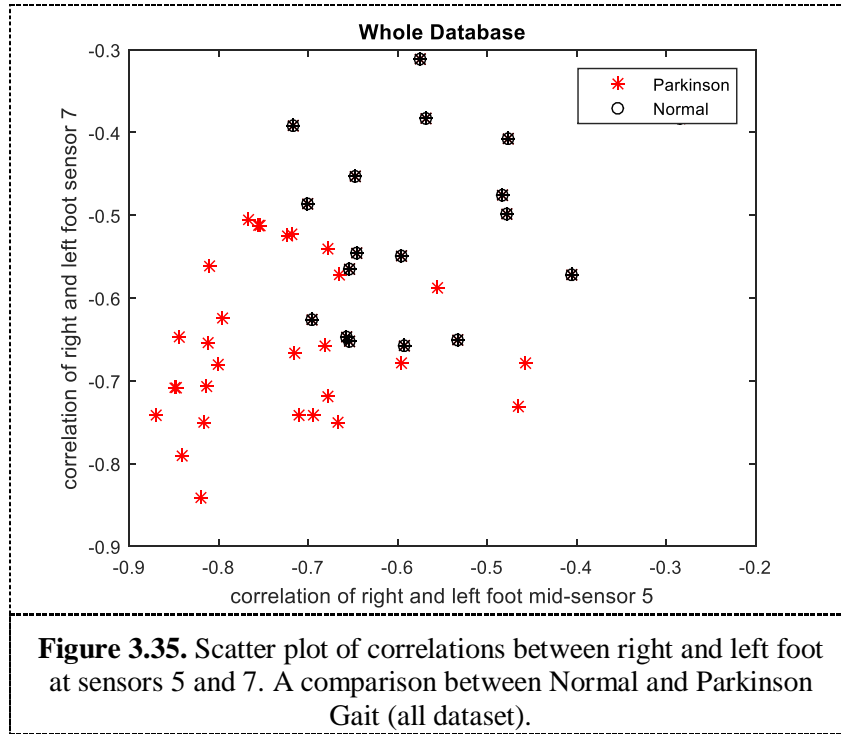


Figure 3.34: Box plots of Speed in Normal and Parkinson Gait.

The difference between the medians of the normal and Parkinson gait is around 0.33 m/sec. The medians are different with a confidence of 95% and this is indicated by notches in the box plot as they don't overlap.

3.7.4 Correlation

Some noticeable features are obtained in a previous work [28, 29]. For instance finding the correlation between the VGRF obtained from the sensor located in the inner sole of both right and left foot in addition to the correlation for the sensor just above this sensor (i.e. sensors 5 and 7 as allocated in Fig.1.1) yields the scatter plot shown in Fig.3.35.



The correlation between right and left foot sensors is computed using the Pearson correlation as in equation (3.17):

$$corr = \frac{n(\sum rl) - (\sum r)(\sum l)}{\sqrt{[n\sum r^2 - (\sum r)^2][n\sum l^2 - (\sum l)^2]}} \quad (3.17)$$

The number of sample is designated by n, r and l represent right and left foot VGRF. Fig.3.33 designates that VGRF in Parkinson gait has a high correlation and therefore the foot stay in contact with ground until the other foot turn out to be flat with ground. The negative sign is due to a decrease in VGRF (lifting ground to swing phase) in one foot and the increase in the other foot (striking ground to a stance phase). The correlation is relatively lower in normal subjects.

3.8 Investigation and results

Thirteen subjects from each normal and Parkinson groups are randomly. That is to say 26 out of 47 subjects are considered for training and the rest are used for testing. As mentioned above, $\text{Age} \times \text{Speed}$ in addition to load distribution between right and left foot could be used as prominent features in first classifier. Such features form a boundary between balanced and unbalanced gaits. Their scatter plot is exposed in Fig.3.36.

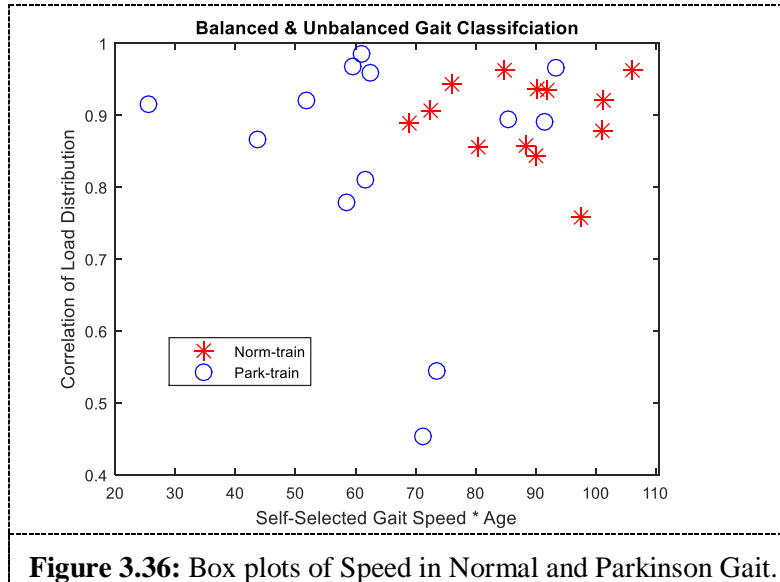


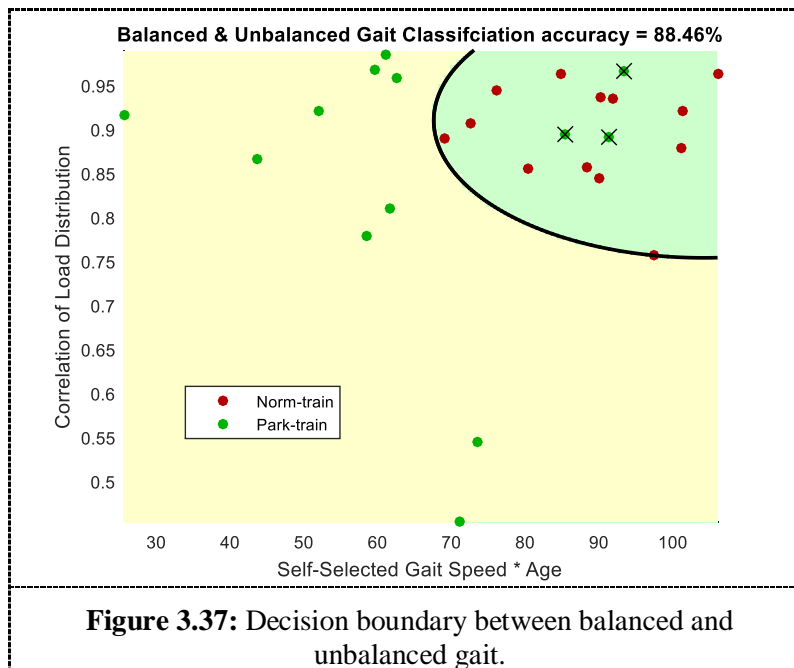
Figure 3.36: Box plots of Speed in Normal and Parkinson Gait.

The normal gait can be used to build the kernel of balanced gait while unbalanced are assumed to have unusual gait. In this case unbalanced corresponds for Parkinson gait according to the hypothesis. Since the covariance in the two groups is varying, then it is better to use some quadratic function rather than using a linear one. This boundary must have a closed-form solution

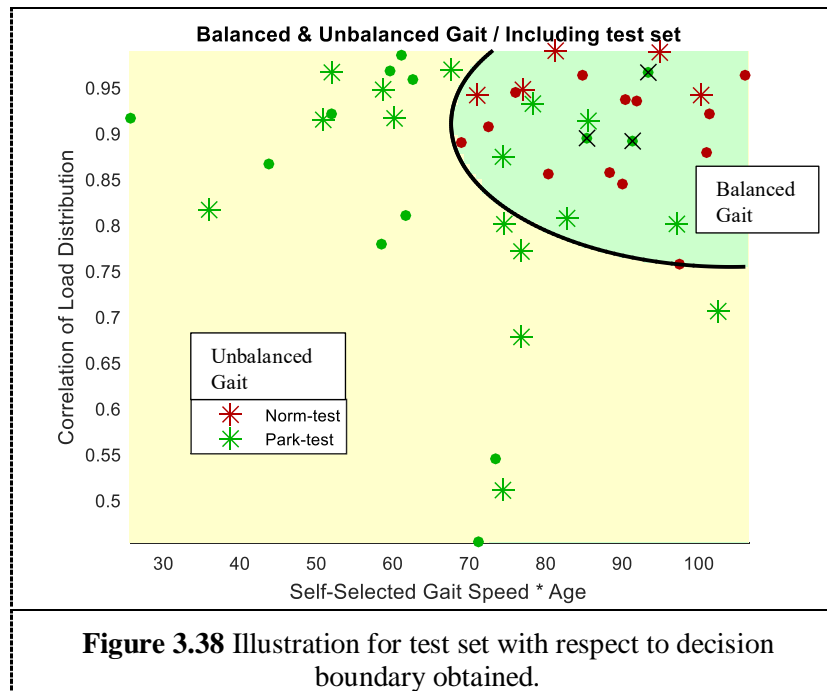
and have no hyper parameters to tune. That's why quadratic discriminant analysis are best fit for our situation for classification and discrimination.

Therefore, we stick to the fact that normal and Parkinson groups have a heterogeneous variance-covariance matrices: $\Sigma_{\text{normal}} \neq \Sigma_{\text{Parkinson}}$

This is also clear from the scatter in Fig.3.36. The decision boundary formed between balanced and unbalanced gait is presented in Fig.3.37 where the log of the ratio of equation (2.39) is equal to zero.



A testing dataset will serve as new observations and verified on the assembled clusters to evaluate this method in classification. The testing part will serve a trustworthy and unbiased estimate of classification error.



The assessment of the classifier can be summarized using Fig.3.38 by adding the test set to the scatter of Fig.3.37. It is better analyzed using the matching matrix on Table 3.6

Table 3.6: Balanced vs. Unbalanced Gait- Subjects

		Prediction	
		Balanced	unbalanced
Subjects	Normal	18	0
	Parkinson	8	21

As indicated in Table 3.6, all normal subjects have balanced gait while Parkinson subjects could have balanced or unbalanced gait. The latter could be a result of tactically improving their gait stability certainly during the experiment. In order to be more generous, Parkinson subjects near the boundary and tending to be normal will be considered for the second classifier. Therefore 10 out of 29 Parkinson subjects will be considered to have balanced gait. For the moment, a cluster of subjects having common properties and characteristic of walking denoted as balanced gait is formed. It is made up of both normal and Parkinson gaits. Subsequently, the overlapping between normal and Parkinson gaits diminish after the first classifier being used. Now, the load distributions between the two feet are similar.

In this part, the 10 obtained balanced Parkinson gait and 10 randomly chosen normal gait will be taken into consideration. Five from each group will be used as training and the rest for testing. Only the correlation out of many features is being tested to show the power of the previous methodology in simplifying investigation and discrimination of Parkinson and normal subjects. For simplicity the linear discriminant analysis as presented in equation 8 will be used given that the variance in both group is approximately similar and this is exposed in Fig.3.39.

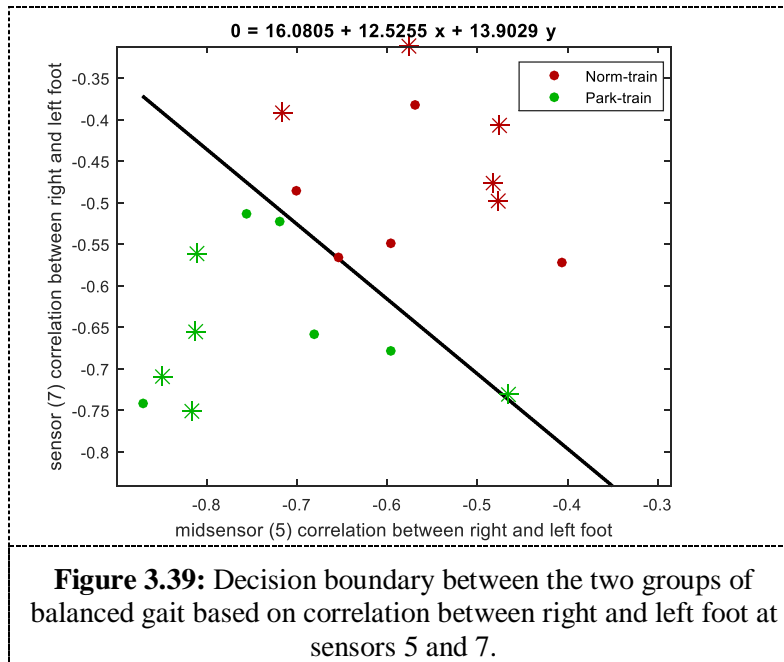


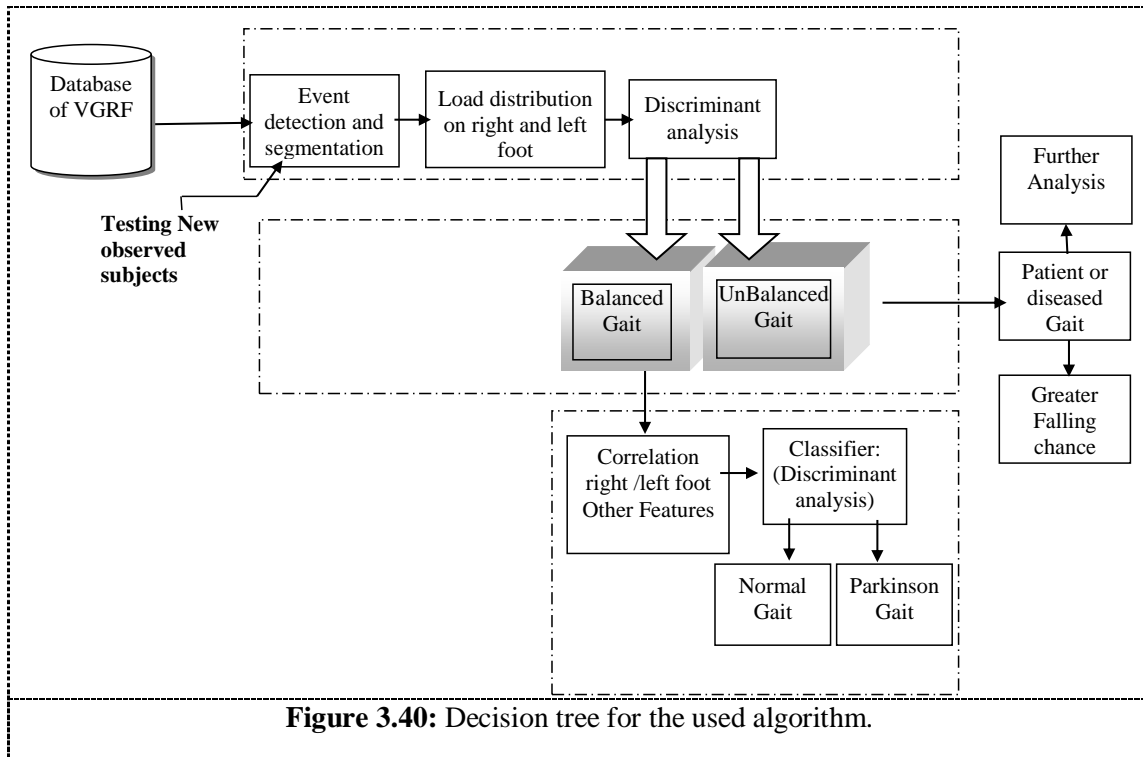
Fig.3.39 entitles a true classification of 90% with a 100% accuracy. A more featured result will be obtained in case of nonlinear decision boundary. The overall classification is beyond 95%.

3.9 Discussion and future work

The goal of this chapter is to shape preferences for gait analysis captivating into account the parameter that could affect our statistical analysis. In this chapter we highlighted the removing of turning points in the signal by synchrosqueezing. In addition, certain parameters like cognitive tasks could affect the content of gait signals and difficult then to be normalized. That is why we moved from intra-subject into inter-subject comparison to come up with relevant features. We highlighted the importance of the mid sensor in classification. This chapter also focused on the COP path difference in both right and left foot which led us to set a hypothesis that is verified by the load distribution. In order to avoid ourselves from examining certain thresholds, discriminant

analysis is used for discrimination and classification. Certain parameters like speed and age are used. The obtained results indicate that there is a great variety between Parkinson gait subjects and the result leads to take only the balanced gaits out of them. Then a new dataset is formed of balanced gaits made up of both normal and Parkinson gait. The overlapping is no longer exist and this is verified by a correlation feature of VGRF, in precise those obtained on the midfoot. This designates that normal subjects don't focus too much on the mid of the foot while switching the foot-ground contact in the course of walking. Nonetheless, this is not obtained for the case of Parkinson gait in which double support is a major feature in their postural stability. This agrees with other research that point out patients tend to decrease their double support as a designate preparation to transfer weight properly while stepping [89].

The decision tree is then formed as shown in Fig.3.40:



Following this method of analysis forms a good approach before handling the signal themselves directly like in [28, 29]. In this manner the results are better and easily achieved rather than using cutting-edge algorithms like BFT, BPANN, k-NN, SVM with Ln kernel, SVM with Polykernel and SVM with Rbf kernel that yields a classification rate of 66.43%, 89.97%, 87.00%, 88.47%, 86.80% and 87.53% respectively [90], in addition to various other techniques like Self-Organizing Map [21].

Based on Fig.3.28 (second row) and Fig.3.29, both normal and Parkinson subjects share same property in terms of synchronizing their steps, it is remarked that curvatures of COP's Paths are different. In Parkinson, the radius of curvature is observed to be smaller than the normal subject. A geometry point of view would be useful in differentiating Parkinson and normal subject.

Using the load distributions figures, they could form a gait signature for each subject which is recorded to be unique to each person. Fig.3.41 illustrates this point. To increase the resolution of the signature more sensors must be add underneath each foot.

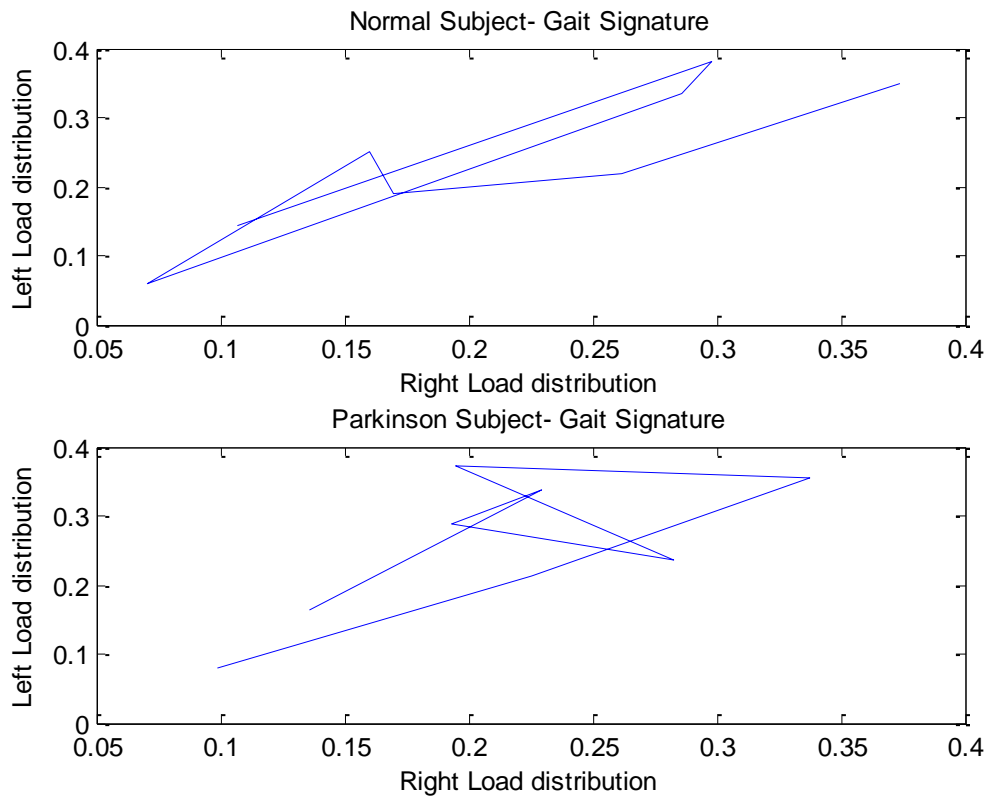


Figure 3.41: Gait Signature.

CHAPTER 4

MODELLING OF VGRF

Calibration and validation form an important strategy in signal modelling. In this chapter we used historical recordings of gait observed during experiment. Such past VGRF signals will be used to forecast of how such gait signals will look like in the near future.

4.1 INTRODUCTION

First the term failure should be defined. It is defined as nonperformance of something due, required, or expected. Then the reliability (when failure would occur), resiliency (how much algorithm through such features can recover from failure), and vulnerability (the effect of failure) in coming out with the correct predictions. Such uncertainties in the analysis outcomes are due to the fact that the gait is totally affected by many other factors like the mode of the person, tiredness, age, height, dual task

VGRF are modelled exponentially in terms of predefined loading height [16]. However, modelling VGRF mathematically in which parameters are updated based on historical values is introduced as an alternative method. This would help in avoiding in estimating new parameters. It has been tested and validated. The first half samples of observations are used for parameter estimation and the other half are used for validation. Markov Model is being updated to better fit the ground reaction force signals. An estimate of one step signal a head is conducted and the percentage of error is computed. It was found that the model better estimate the normal gait and

hard to fit different posture segments of Parkinson gait. The ultimate goal is to have a healthy and safe walk to prevent falls among elderly both with normal and patient gait by means of predicting one step ahead. Thus, if the real time measured signal don't follow the path of the estimated data, this could form an indicator of certain perturbation in gait and would serve as an alert.

This model doesn't cover in one equation both distinctive phases of gait: stance and swing. In fact, a switch control system is proposed that switches between the two phases of gait that corresponds to the real practiced segment during walking. This chapter focuses on the stance phase.

4.2 Analysis and Motivation

VGRF signal is used as part of kinetic analysis as a vertical net summation of all forces during walking observed over time.

Assumption: VGRF denoted X_t is made up of deterministic (future data predicted from past values) denoted D_t and stochastic (future data can be predicted in statistical probabilistic terms) denoted S_t . This is given in equation (4.1).

$$X_t = D_t + S_t \quad (4.1)$$

In this part, we will apply modelling techniques on a chosen sensor signal that is located under the heel of the left foot. Then we will generalize the model to all other sensors and try to figure out their relation. Fig.4.1 shows a sample of this signal:

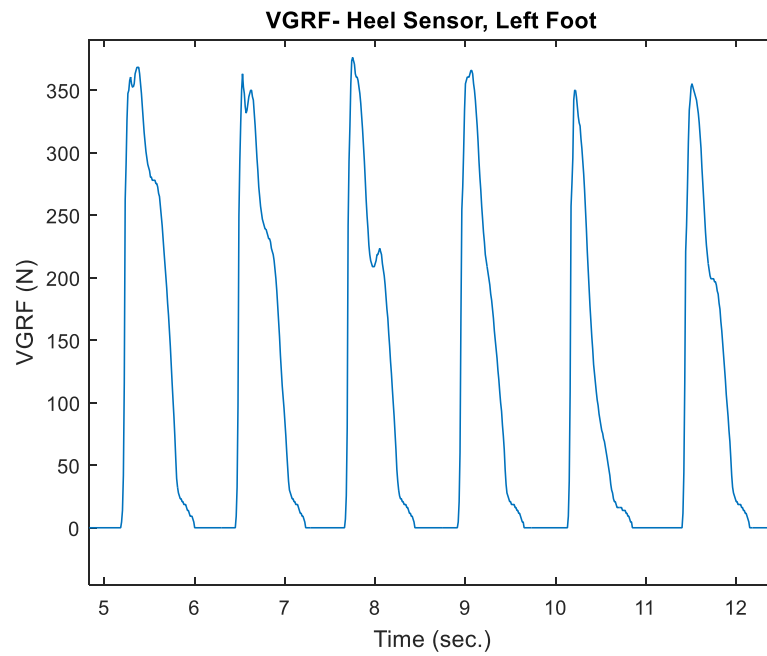


Figure 4.1: Sample of VGRF

Fig.4.1 indicated some repetitive and cyclic behavior and therefore correlate with each other. Correlogram describes the signal inertia and shows the persistence in the same state from one heel strike into another. It is given by equation (4.2):

$$\rho_j = \frac{\text{cov}(Y_t, Y_{t-j})}{\sqrt{\text{Var}(Y_t)\text{Var}(Y_{t-j})}} \quad (4.2)$$

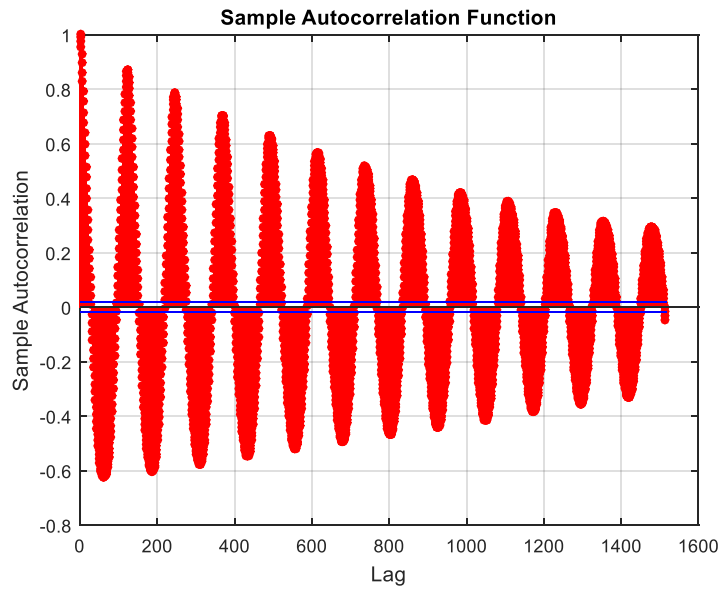


Figure 4.2: Correlogram of VGRF

The correlogram in Fig.4.2 dies down in a sinusoidal format indicating an attendance of periodicity within the heel VGRF signal. Most of the correlations are statistically significant falling outside the 95% confidence interval.

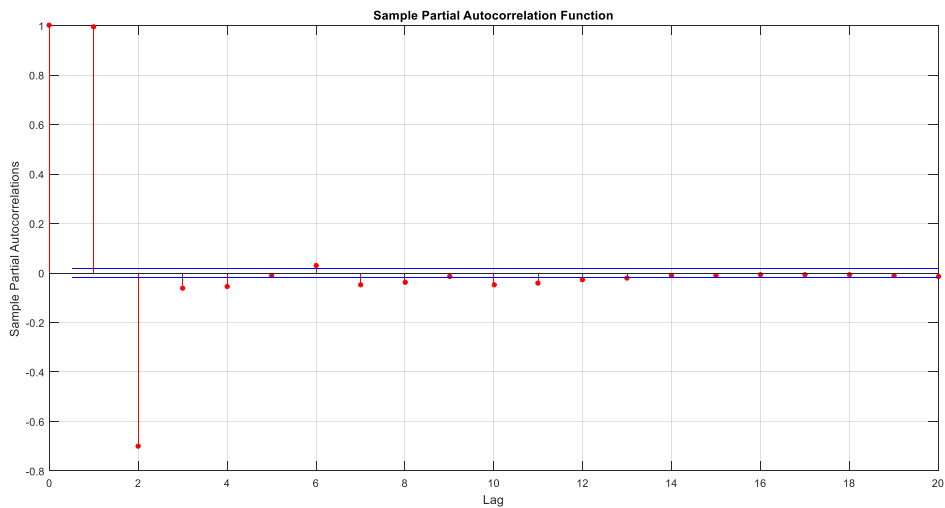


Figure 4.3: PACF of VGRF

The partial autocorrelation function (PACF) shown in Fig.4.3 which seeks the correlation between two values in series excluding their linear dependence on other values in the whole series. It specifies significant values at lag=1 and lag=2 associated with a slow decay in the ACF. This designate an autoregressive process AR (2) of order two.

4.3 VGRF Analysis for Normal Subject

The autocorrelation function (ACF) of VGRF for a normal subject gait articulates a slow decay as revealed from Fig.4.4. This indicates a long memory [92]. In addition, plotting the partial autocorrelation function (PACF) demonstrates the non-stationarity phenomena of the signal. This non-stationarity is of integration order 2 because the PACF value at lag two recorded to be one in absolute value. This proposes the existence of stochastic trend of order 2.

However, this range of dependence is not fixed throughout the different steps of the same signal. It would be interesting to investigate more on its range of variation.

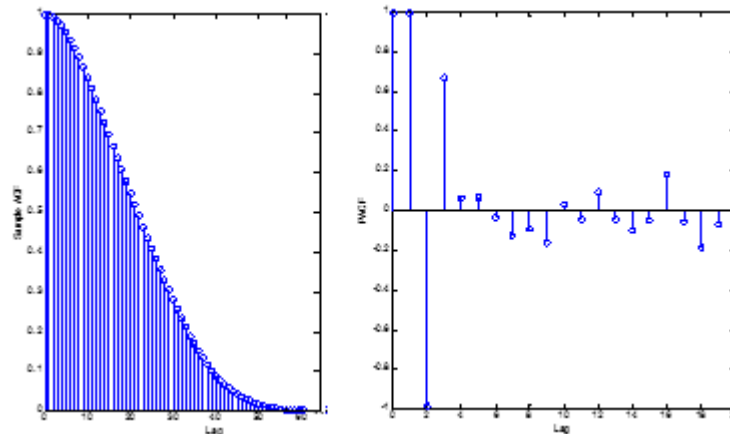


Figure 4.4: Sample and Partial Autocorrelation for a Normal subject.

4.4 VGRF Analysis for Parkinson Subject

Strong autocorrelation exposed in the ACF for Parkinson subjects don't die quickly over long range of observations compared to normal subjects. This is a good indicator of the non-stationarity of the signals in general. In particular, ACF recognized a longer memory in the gait signals of Parkinson subjects given the autocorrelation value in its minimum around 60 time lag as shown in Fig.4.5. Whereas it is documented to be in the range of 50 lag corresponding to normal gait as obtained in Fig.4.4. The PACF also indicates the non-stationarity of integration order 2.

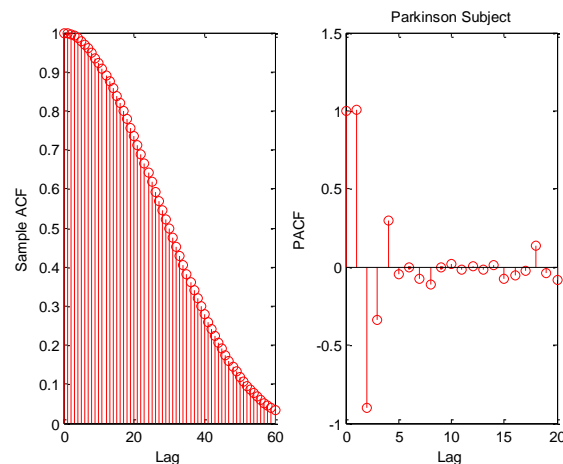


Figure 4.5: Sample and Partial Autocorrelation for a Parkinson subject.

Knowing that performing the difference transformation over the original data signals two consecutive times, no longer memory is then will be available as shown in Fig.4.6. However the non-stationarity of integration of order 1 will be available at the first difference.

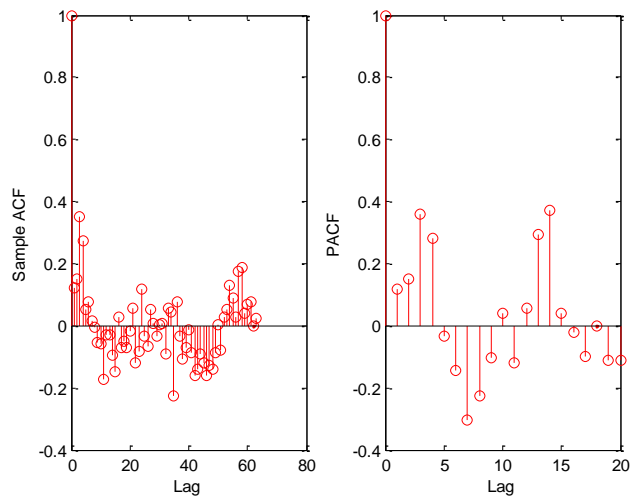


Figure 4.6. Sample and Partial Autocorrelation for VGRF signal differenced two times.

Fig.4.7 indicates the power spectrum after removing the mean to see the other fluctuations in signal:

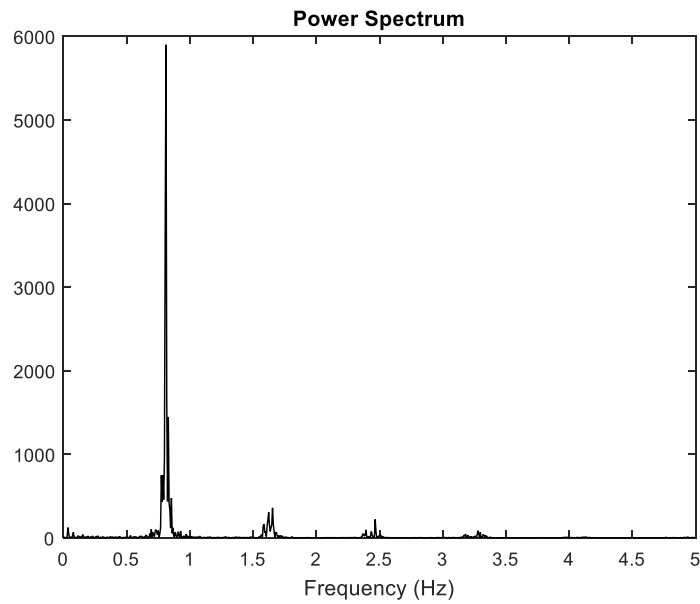


Figure 4.7: Sample and Partial Autocorrelation for VGRF signal differenced two times.

The power spectrum indicates a periodicity around 0.81 Hz then around 1.66 Hz and so on. This approve results indicated by the correlogram by dividing sampling frequency (100 Hz) by the time lag of the peaks. Therefore a regularity in the heel strike pattern during walking is registered mainly every 1.23 seconds. However, there is a need to test for significance of periodicity.

4.5 Modelling Insight into One Stride

In this section, the mid sensor is taken into consideration [16]. Fig.4.8 and Fig.4.9 display an interesting linear relationship between y_{t-1} and y_t . Knowing that the degree of linearity decreases as the time lag (τ) to the future values increases ($y_{t+\tau}$). In addition, the slope of the regressor starts to diverge from one in both increasing and decreasing phases of the foot step, where the slope from the “heel strike” to the moment where the foot becomes flat starts to decrease and the slope for “foot flat to toe off” starts to increase. This leads to elliptical shape in the whole data.

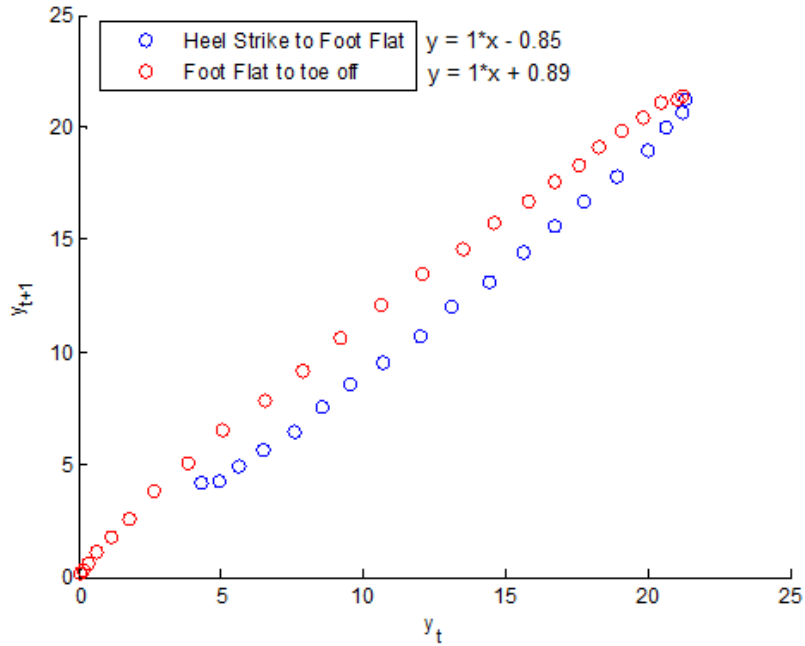


Figure 4.8: Linearity in the plot of current values versus past values in VGRF's data for midsensor on a single step. In this case the difference is one time lag. Given ($y = y_t$) and ($x = y_{t-1}$) in equations.

In this model, a deterministic trend can be obtained as a function of time. The model is given by the simplest first order autoregressive (AR (p=1)) model as in equation (4.8) where the future value is regressed on the current value:

$$y_t = \beta y_{t-1} + \alpha + \varepsilon_t \quad (4.8)$$

Where $0 \leq y_t \leq y_{max}$ and y_{max} is the maximum value that can be reached. It is related to the weight [86] in addition to the way a person walks (step starts by heel contact, toe contact or shuffling). This can be easily determined from a previous step and forms a parameter to the model. The slope is shown to be ($\beta = 1$) for both increasing and decreasing phases of the step. However,

the intercept α can be obtained either from a trained previous step or from the first few values i.e. local model is obtained as recent observations are used. The error term is important and forms the residual and its model is purely indeterministic as to be handled later. From Fig.4.6 the model for both phases are given as in equation (4.9):

$$\begin{cases} y_t = 1y_{t-1} - 0.85 + \varepsilon_{1t} \\ y_t = 1y_{t-1} + 0.89 + \varepsilon_{2t} \end{cases} \quad 0 \leq y_t \leq 22 \quad (4.9)$$

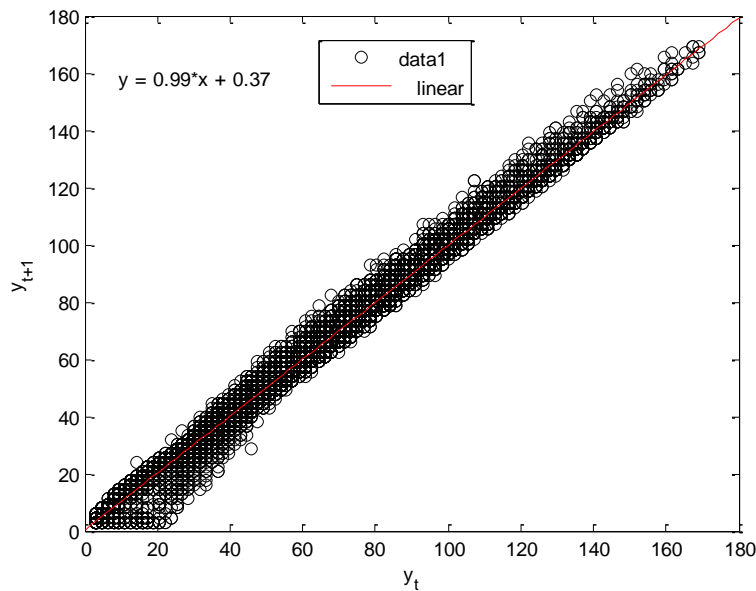


Figure 4.9: Linearity in the plot of current values versus past values in VGRF’s data for midsensor given the 2 min signal.

4.6 Periodizing VGRF Signals

On-off controller simply drives the acquisition of VGRF during walking from fully closed to fully open depending on the location of the foot. In other words, when the foot hits the ground entering the stance phase then VGRFs signal do exist. The acquired data will be saved into an

array with preliminary fixed size ending up with a matrix of stance phases. Its size is controlled by the preliminary defined stance interval depending on the sampling rate. This would eliminate any difference in the stride interval between subjects stemmed from their difference in height, weight, gender and so on. The signal then have fixed time periods (i.e. the time from one heel strike into the successive heel strike is fixed). That's why the VGRF signals are divided as shown in Fig.4.10.

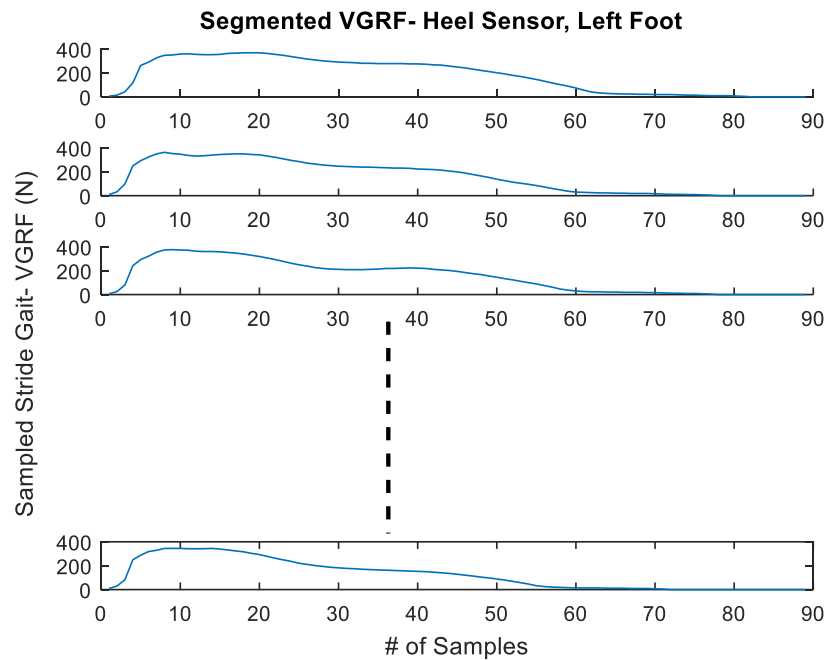


Figure 4.10: Step Isolation of VGRF stance phases at the heel. They are saved over 89 samples equivalent to 0.89 seconds.

The matrix of stance phases are reshaped into 1D array vector for analysis. Such fixing of sampling points interval for stance phase of the gait would definitely change frequency content analysis. Certainly, they will exist at different harmonics of the saved interval as shown in Fig.4.11:

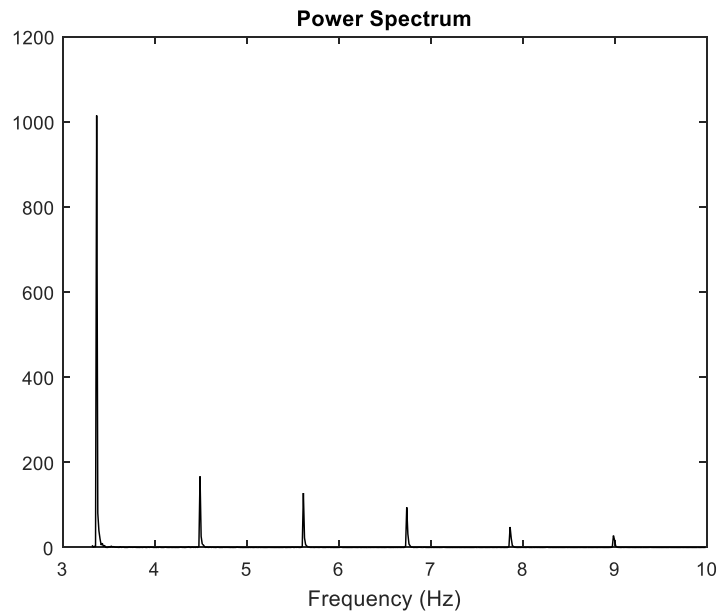


Figure 4.11. Power Spectrum of the new generated signal.

The Autocorrelation Function (ACF) of the altered signal indicates a very slow decay over lags and thus the signal becomes more non-stationary. This is inherited from the periodicity being added to the signal. Fig.4.12 is an illustration of the ACF.

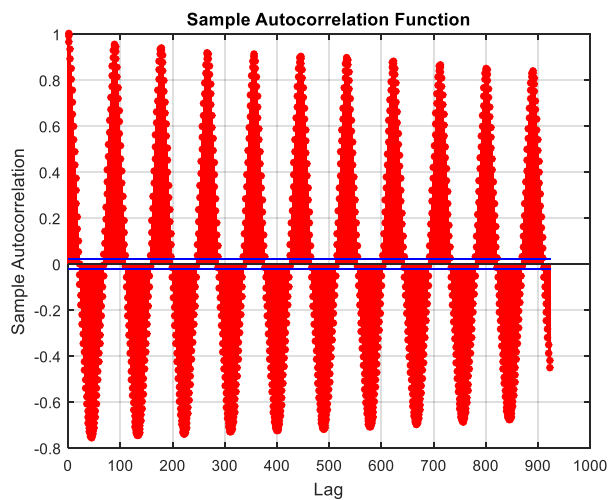


Figure 4.12: Sample Autocorrelation Function

Differencing the new signal by two consecutive times as an intention to remove periodicities signifies the interval chosen by implementing Partial Autocorrelation Function (PACF) as shown in Fig.4.13. It agree with the predefined interval of 89 lags:

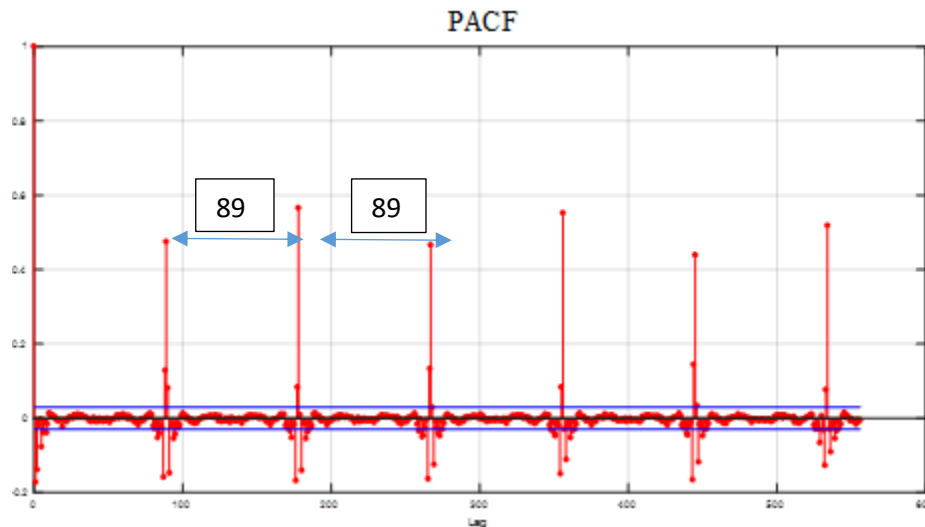


Figure 4.13: Partial Autocorrelation Function

4.7 Time series Comparison

Fig.4.14 indicates that the extracted stance phases from a normal subject VGRFs gait delivered by the heel sensor at the left foot preserves some fixed magnitude. This similarly remark them to be below the sample 20 and therefore below the 0.2 sec. while the Parkinson subject admits some variations certainly in the amplitude of various steps, this can be observed from the peaks in Fig.4.15. Furthermore the peaks are within the samples of 20 and above. Such a difference give an intuition of two important different properties: the change in the VGRF amplitude from one step into another admitted by Parkinson gait, and a change in time interval to reach maximum amplitude as an evidence to a change in the slope and those the stance phases are longer in Parkinson gait.

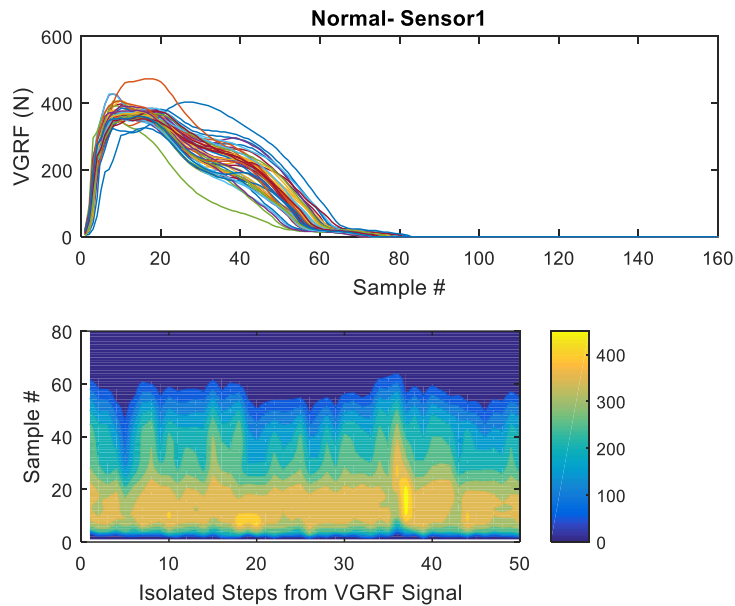


Figure 4.14: Stance phases being isolated from VGRF extracted from the heel sensor underneath the left foot of a normal gait subject and their contour plot

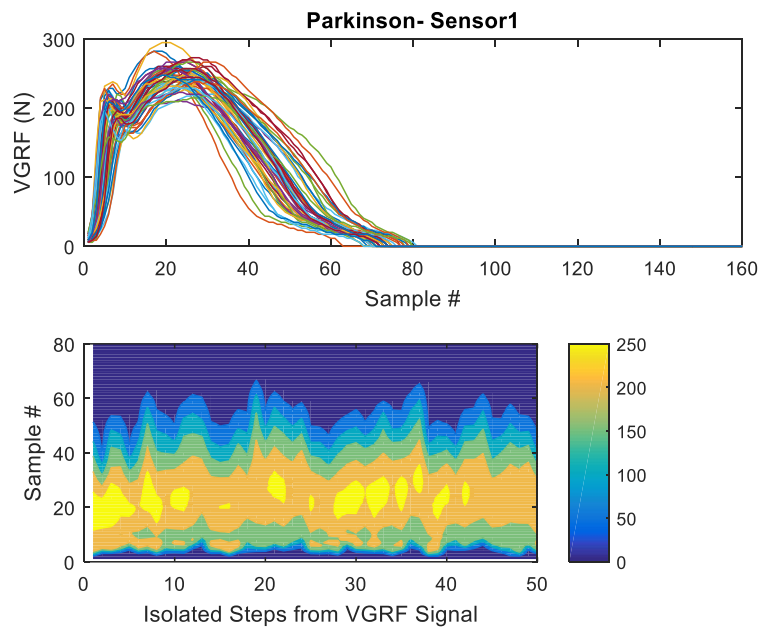


Figure 4.15: Stance phases being isolated from VGRF extracted from the heel sensor underneath the left foot of a Parkinson gait subject and their contour plot

4.8 Periodogram Comparison

Now fixing the size to 160 samples by zero- padding the step signals as to have a size of 160. 160 is chosen as a guarantee that neither of subjects will have stance interval beyond the 1.6 sec during walking after an investigation is done over all the database. This definitely will create an artificial fundamental frequency of $f_f = 0.625$ Hz in its periodogram indicating that the cyclic existence of the impulse starting of the gait stance phase. Furthermore a harmonics periodic of the fundamental will also be created ($2 f_f, 3 f_f, 4 f_f \dots$). To enhance the outcomes of the comparison, each step extracted from VGRF is normalized by Euclidean norm of the same step signal. This is given in equation (4.10).

$$\|x\|_2 = \sqrt{\sum_{n=0}^{N-1} \|x[n]\|^2} \quad (4.10)$$

Excluding the first harmonic, the amplitude of the power spectrum in Normal subjects is higher than a Parkinson subject as indicated in Fig.4.16, this is a good indicator that slope of VGRF measured at a certain sensor during the moments of contacting the ground is steeper than the one known by a Parkinson.

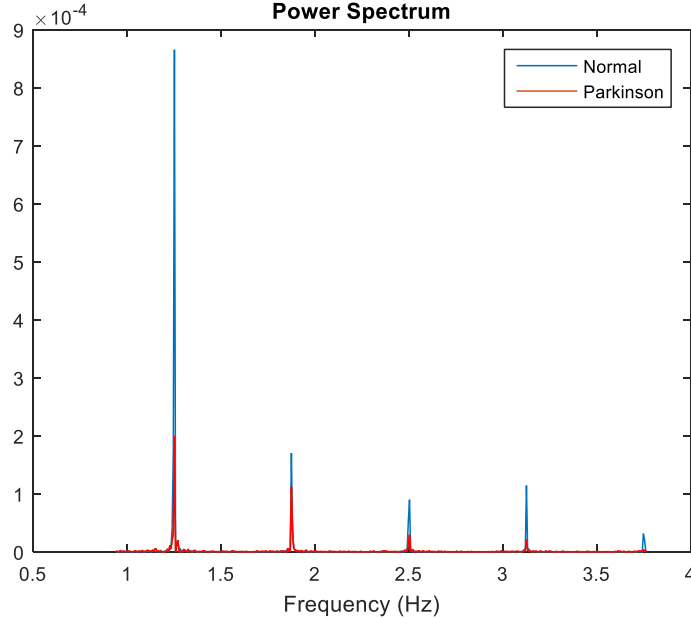


Figure 4.16: Power Spectrum for both altered signals of Normal and Parkinson gait subject

4.9 Hypothesis

Hypothesis: One stance VGRFs gait is directly affected by the very neighbor steps and up to a certain interval (i.e. number of steps).

The above hypothesis doesn't indicate whether one step affect the whole style of walking but definitely get capture some characteristics of the previous step and affect the step gait a head. The accumulation of errors between two steps that are far away from each other contribute also in gait variability. This means that certain parameters are needed to be adjusted continuously while generating the upcoming signals. To realize this hypothesis in practice, a model will be chosen then the parameters are fit into equation to achieve the minimum error between actual and simulated data. Then, modelling vertical ground reaction force signals based on historical data can reproduce and forecast the gait signals for a short period of time.

4.10 First order Markov model

A. Stationary

Suppose the future step values to be predicted are generated by the following 1st order Markov Model that is stationary with respect to mean, variance in addition to auto-correlation of first lag, this is indicated by equation (4.11).

$$X_{j+1} = \mu_x + \rho_1 (X_j - \mu_x) + t_{j+1} \sigma_x \sqrt{1 - \rho_1^2} \quad (4.11)$$

Where t_{j+1} stands for the standard normal variable ($\sim N(0, 1)$) which is a series generated randomly with zero mean and unity variance. μ_x , σ_x and ρ_1 are the mean, standard deviation and first lag autocorrelation respectively.

B. Non-Stationary

The same model will be generalized for nonstationary process as indicated in equation (4.12).

$$X_{i,j+1} = \mu_{j+1} + \rho_j \frac{\sigma_{j+1}}{\sigma_j} (X_{ij} - \mu_j) + t_{i,j+1} \sigma_{j+1} \sqrt{1 - \rho_j^2} \quad (4.12)$$

Where i is the number of stance phase of gait step, ρ_j is serial correlation between the j th moment of a stance phase and $j+1^{\text{th}}$ moment of the same stance phase. Once again the standard variable series is given by $t_{i,j+1} \sim N(0, 1)$.

As we proved previously, VGRF signals are non-stationary certainly in the variance and in the mean.

4.11 First order Markov model of VGRF with non-stationarity

The initial guess of parameter values in gait VGRF are taken to be zero and this makes sense in the real gait that every stance phase is followed by a swing phase where there is no contact with the ground and therefore the VGRF measured must be zero.

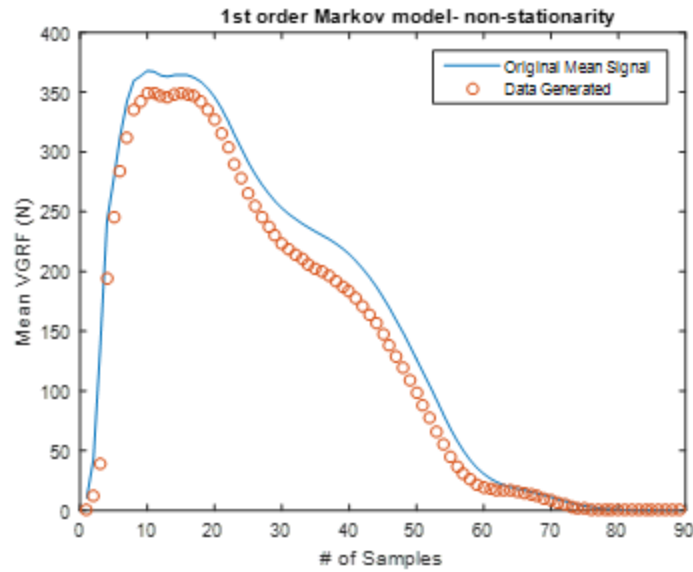


Figure 4.17: Data generated by markov-Model V.S. Raw Experimental Data

The coefficient of multiple determination (R-square) is a good choice for testing the model as the outcome of the square of the correlation between actual values and predicted values, would indicate a proportion of variance that is accounted by the model. This can be articulated in equation (4.13).

$$R^2 = \frac{\sum_{i=1}^n w_i(\hat{y}_i - \bar{y})^2}{\sum_{i=1}^n w_i(y_i - \bar{y})^2} \quad (4.13)$$

Where \hat{y}_i is the fitted values and \bar{y} represents the mean. Finding R^2 for the model in Fig.4.17 for a normal gait subject yields a value of 0.9143 and this means that the fit explains 91.43% of the total variation in the data about the average.

4.12 Modified First order Markov model of VGRF with non-stationarity

The first step in modifying the model, is by changing the cross-correlation between moments of consecutive steps into autocorrelation of the previous step moments only. Then as the above model is restricted to certain random values and falls under a standard normal distribution, it can best be adjusted by replacing it with the error term ending up with equation (4.14).

$$X_{i,j+1} = \mu_{j+1} + \rho_j \frac{\sigma_{j+1}}{\sigma_j} (X_{ij} - \mu_j) + (1 - R^2)\sigma_{j+1}\sqrt{1 - \rho_j^2} \quad (4.14)$$

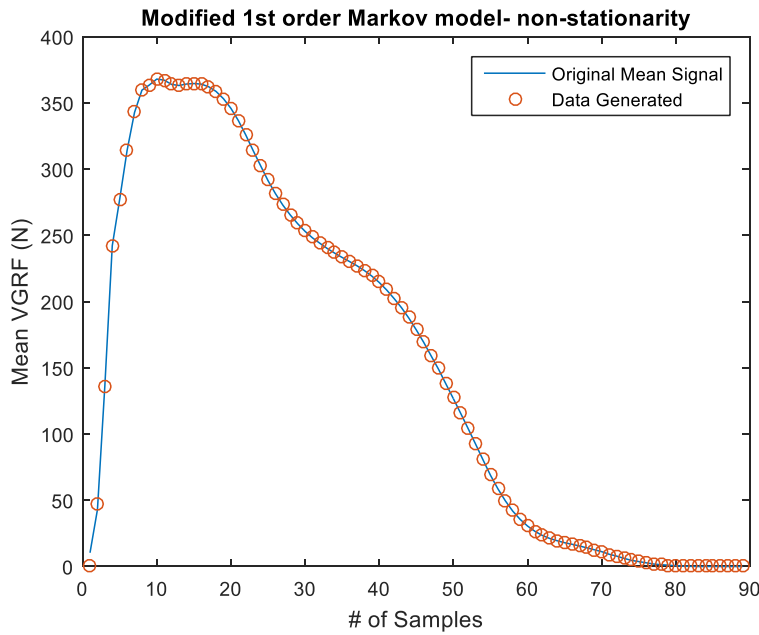


Figure 4.18: Data generated by the modified Markov-Model V.S. Raw Experimental Data

An acceptable data modelling as shown in Fig.4.18 is then reached using the new proposed model. The percentage of fitting increased to reach 99.76% on average. This result is generalized to cover all other sensors with variable percent of error but still are highly acceptable. A summary of the algorithm is expressed in Fig.4.19.

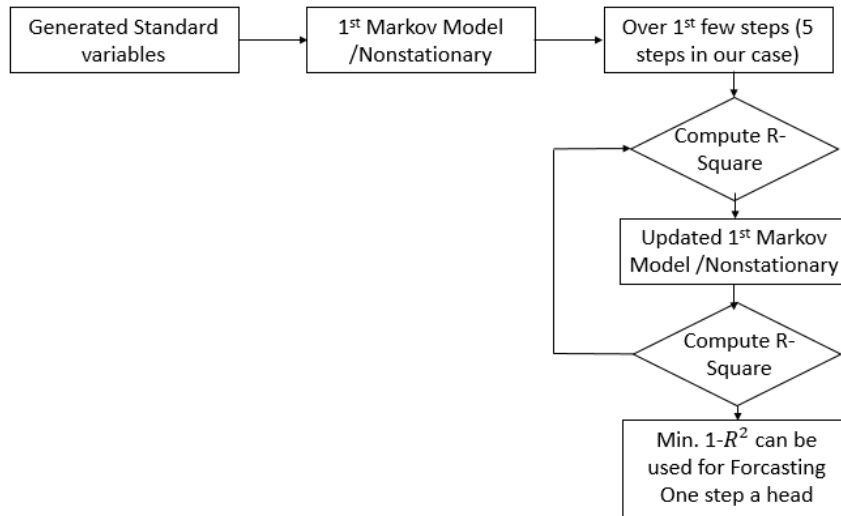


Figure 4.19. Algorithm for Modified Markov Model

4.13 Prediction of one step ahead in “Normal” & Parkinson”

After assessing time domain statistical properties of the Vertical Ground Reaction Force (VGRF) during moderate-pace walking, the aim is then eventually to create a reliable mathematical model of VGRF for normal and abnormal cases and that what have achieved so far. Predicting a one-step signal ahead in normal and Parkinson using the above model yields an important difference between them. The proposed model is able to predict in normal subjects better than the Parkinson subjects as shown in the Fig.4. 20.

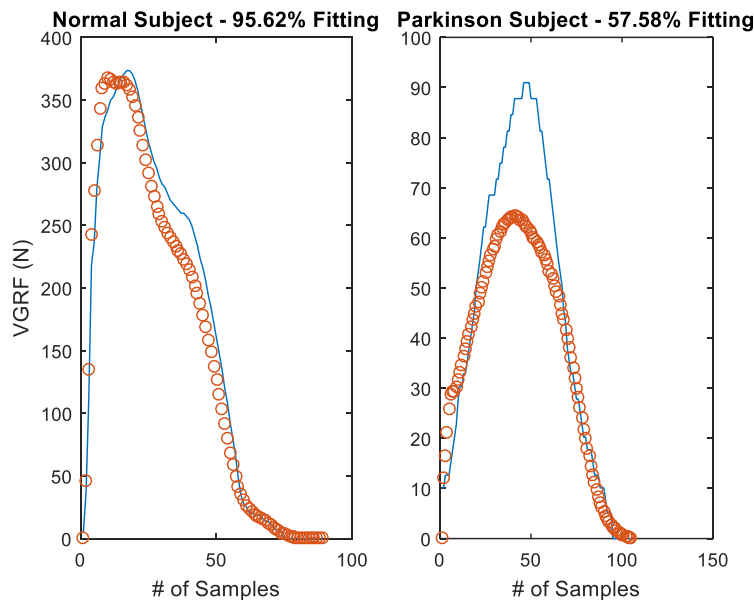


Figure 4.20: Forecasting Normal and Parkinson Gaits.

Fig.4.20 shows a 95.62 percentage of fit in the predicted normal gait signals while the model experienced a hard moments in having an appropriate prediction in Parkinson gait where the fit is around 58%. This can be justified by the previous observation in Fig.4.8 where the gait signals in Parkinson experience great variability.

4.14 DISCUSSION & CONCLUSION

First, the stride interval variability affect the signal analysis certainly its frequency content. Second, Steeper slope of VGRF measured from normal than from Parkinson. Third, the incidence of a stochastic deterministic level function is shown by the non-stationarity in mean and variance. In other words heteroskedasticity appeared in the walking gait VGRF signals. Fourth, the cross correlation between sensors suggest a model as the sum of certain deterministic (stationary and non-stationarity) [91] and stochastic (fluctuation) signals. Most importantly, the rate of decay of

the autocorrelation part forms an indicator of the memory type (range of dependence) that forms an indicator to whether the gait is normal or abnormal. In addition, focusing on those non-stationary signals by starting with stochastic trend stationary processes as assumed model, wherein the process has stationary behavior around such trend. This time series modeling will yield the advantage of Generalized Autoregressive Conditional Heteroskedasticity (GARCH).

Autoregressive Moving Average (ARMA (5, 5)) linear model is conducted on VGRF [93]. However this technique is fit for stationary time series signals and therefore periodicities are not desirable. It is worthy that VGRF are assumed to be cyclostationary [32] and nonstationary as on this chapter. Furthermore, the several combination of orders must be conducted then the best model will be chosen based on verification tests like Maximum likelihood rule. In another research the linear and polynomial regression models are being used and tested by Normalized Root Mean Square Error. However, the linear model didn't capture the peak forces and the polynomial didn't capture the dynamic patterns in force profiles. In order to increase estimation accuracy, the writer suggests to have different fitting methods for better explaining of the unique patterns in force profiles, and thus [94]. Another work on modelling VGRFs signals is introduced by the fourth order polynomial with additional two parameters. However, this technique requires the location of the local maxima in the actual VGRF data [95]. Therefore, the model will capture a huge error when both feet are in contact with the ground (i.e. no aerial phase). That is why, building models based on historical data is helpful specifically when it comes also to the type of foot: normal, low, and high-arch foot [91]. Research shows that this would affect the pattern of VGRF [96] making it difficult to have a common model generalized over different human gaits. This chapter presented

a novel modelling technique of VGRF signals that overcome the stated problems and preserves the fact being nonstationary. The technique is summarized on a modified first order Markov model based on nonstationary characteristics. It has been evaluated on normal gait signal and proved its potential in having a good prediction. However, it is hardly estimated the Parkinson gaits which suggests a higher order must be implemented. As a future work, the model will be verified over all sensors by finding a unique multi-sensor array model. On the other hand, the model generated should take into consideration the time quantization of the gait and thus the stride interval and also adopt the lognormal model into the proposed model based on the mentioned observation.

CHAPTER 5

GENERAL CONCLUSION AND PERSPECTIVES

In this chapter, we will wrap up this thesis with main results being obtained from the previous work. Previous chapters treated VGRF in time, frequency and space separately or in combination of two. Frequency- spatial characteristics will be easily obtained using multiway analysis like parallel factor analysis (PARAFAC) that contribute in identifying Parkinson elderly gait. Multiway modelling of human VGRF is not engaged yet. This analysis requires different measurements underneath the foot.

5.1 Summary: The Main Results of this Research

A strict relation between the frequency content of the signal and the way a subject moves is recorded. The frequency of the signal is shown to be high at heel-strike and at the toe-off. In addition, the frequency opposes the change of VGRF which produces it as a trying to retain the body in balance and not falling. In control subjects, higher frequency at instants of heel-strike and toe-off compared to patients is registered. However, the frequency content as a whole in Parkinson gait subjects tends to increase (i.e. the more they correspond to the impact peak), but the peaks and the valleys tend to be much more muted. Furthermore, we proved that traditional filters like Butterworth filter can eliminate a vital part of the signal's content. New adaptive filtering model is being proposed based on EMD. On the other hand, we have focused on eliminating turning points in the gait signals that impact their content by synchrosqueezing the time frequency

representation. Synchrosqueezing helped in spotting Active and Passive peaks in the gait signal. This would help in signal separation. In addition, as normalization and filtering are handled from statistical point of view, we showed that there could be other non-quantifiable parameters that one should take them into consideration when handling signals from different subjects. As many other parameters, cognitive task are hard to be filtered or normalized. We suggest in such cases to come up with features based on inter-subject analysis. For instance, the variation in the COP and energy distribution difference from one stride into another stride are used as features.

The total VGRF from array of sensors is widely used in literature. In our work we proved that the first four principal components, derived from PCA applied into the array of signals derived from different locations underneath both feet, counts for 94% of the total variance in VGRF signals. This is a good indicator that most of the data structure can be captured in three or four underlying dimensions. However, more attention to which sensor is chosen must be made to enhance analysis. This is especially recommended when building an acquisition system. This study shows the sensor located at the inner arch of the insole of the foot (i.e. at the mid foot) near the axis of the center of body holds the most pertinent information for classification. This could help more in using such sensor location to model walking with a 3D-link dynamics as one foot is in contact with ground while the other is in swing phase. This mid-sensor helped us with simple statics (mean and standard deviation) to prove that the signal is nonstationary.

Certain Parkinson subjects have the ability to synchronize their steps while experimenting and this is detected by variation in the COP. This will mislead us in building classifiers as their gait looks pretty like a normal subject. We proved that the movement of feet is uniform when

walking due to the distribution of loads between the feet. Therefore, imbalance is due to irregular distribution of loads between the feet. In a simpler way, pressure distribution between feet differs when a subject is affected with disease like Parkinson. This is more obvious in diseased subjects where their metabolic system is affected. In addition, the center of pressure variation between different gait steps was a good indicator of the type of gait. A decision tree for the used algorithm is developed and proved to work well. For instance, unbalanced gait corresponds to pathological subjects. However, balanced gait could be relevant to normal or pathological subjects. Differentiating between pathological subjects and normal subjects when they both exhibit balanced gait become easier due to the verified hypothesis that is derived from analysis of the database. Removing the unbalanced gait, allows the use of simple features like correlation to differentiate between normal subjects and Parkinson subjects. With linear models a classification of 90% with a 100% accuracy is achieved. A 100 % classification with quadratic discriminant analysis can be achieved. However, we didn't point out such a result in this thesis as the goal is to increase the database size and then we can generalize this conclusion. Then a gait signature is introduced. We recommended to increase the array of sensors to improve this signature.

This bipedal locomotion is an evoked response sensitive to the initial conditions of the nonlinear dynamical stimuli signals or perturbations which make them very difficult to predict within short intervals of time into future. A novel model technique is introduced using a modified version of Nonstationary first order markov model. Results show that this model best predict normal gait subject with 95.6% and fairly do in Parkinson gaits with 58 %.

5.2 Introduction to the Future Work:

We have proven that summing signals stemmed from all sensors is not a good practice. It's better to treat them as a single entity. Thus, dynamical changes of VGRF underneath both feet must be processed in time, frequency, and space. VGRF signals are captured in time domain, Synchrosqueezing of short time Fourier transform is then obtained for each sensor location to build three-way Time-Frequency-Space VGRF tensor (TFS-VGRF). A good separation of the three main events during gait is attained. A comparison between normal and Parkinson gait is then conducted. The results will be tested on experimental database obtained from 600 elderly participants walked at their self-selected normal speed. The database is obtained collaboratively as a teamwork between Laboratory of Signal Analysis and Industrial Processes (LASPI) and the University Hospital Center (CHU) of Saint-Étienne. However, a more innovative approach is to be followed using tensor methods.

Multi-way analysis techniques keep the structure of the multidimensional data dimensions. They are so called tensor methods formed of different tools like Tucker decomposition, Parallel factor analysis (PARAFAC) and Incrementalization. The objective is then to decompose arrays into set of loadings and scores which provide a condensed description way of data. Multi-way methods provides more adequate, robust and interpretable models than other models like given by PCA. However, PARAFAC is still a special case of Tucker3 which is a case in 2-way PCA as shown in Fig.5.1 below. However, this specificity of PARAFAC put it under bounded constraints even it requires fewer degree of freedom.

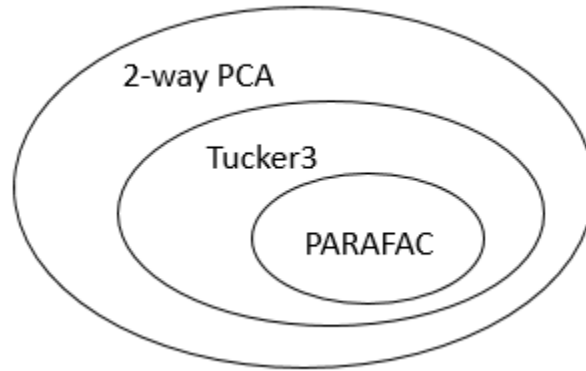
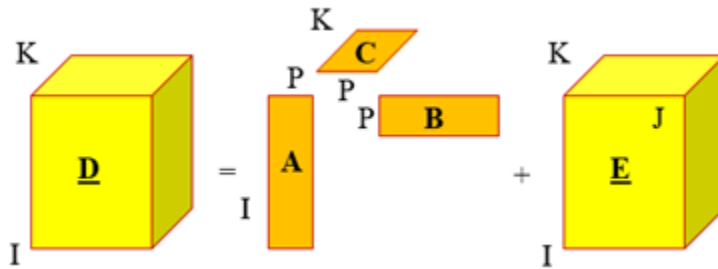


Figure 5.1: PARAFAC a special case of 2-way PCA

PARAFAC (also known tensor rank decomposition or canonical polyadic decomposition (CPD)) method attempts to decompose a three-way data into a set of trilinear terms (the product of three significantly smaller matrices) and a residual array:



$$\underline{D} = \sum_{p=1}^P x_p \otimes y_p \otimes z_p + \underline{E} \quad (5.1)$$

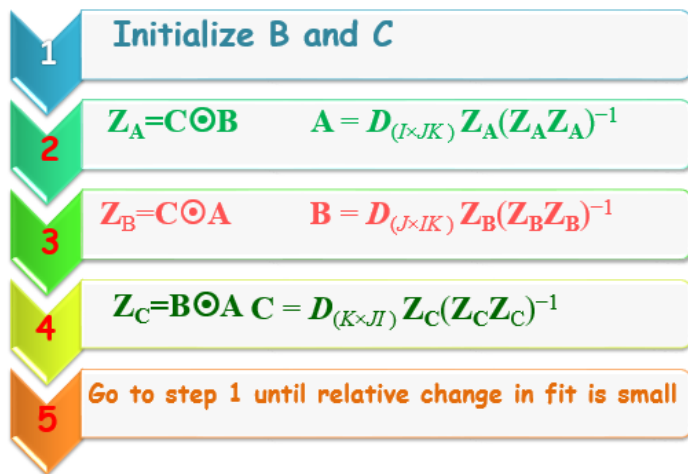
$$d_{ijk} = \sum_{p=1}^P a_{ip} b_{jp} c_{kp} + e_{ijk} \quad (5.2)$$

Where $i = 1 \dots I$; $j = 1 \dots J$; $k = 1 \dots K$

d_{ijk} stands for the point of i^{th} sensor at the j^{th} variable on the time mode and at the k^{th} variable on the frequency mode. The variability that not included in the model is denoted by residual e_{ijk} . Small “p” represents the number of the PARAFAC component. Each PARAFAC component will end up with I a-scores: one for each sensor, J b-values: one for each time and K c-values: one for each frequency.

The general PARAFAC is based on the alternating least squares (ALS) algorithm and can be summarized as follows:

Given: \underline{D} of size $I \times J \times K$



In this part, both set of 8 signals from both right and left foot will be considered.

$$x = [x_1(t), x_2(t) \dots x_{16}(t)]^T$$

Each variable in x is made up of 12000 observations sampled at 100 Hz.

5.3 PARAFAC Outcomes:

Footedness is important in studies of hemisphere lateralization. Studies work on development of scale for measuring foot preference. We have 16 data set captured from 16 sensors each 8 are distributed underneath each foot. PARAFAC has one strong feature to answer some important questions that highly would benefit in gait analysis, classification and prediction. Now the data are arranged into five locations underneath the foot as segmented in Fig.5.2:

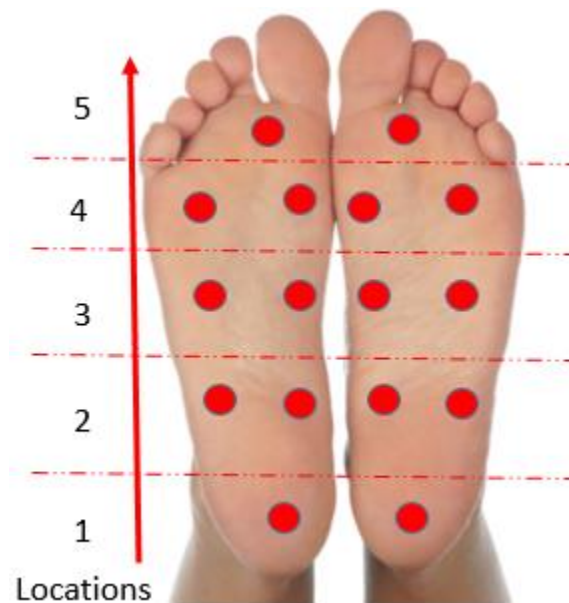


Figure 5.2: Foot being segmented into 5 locations

In this manner one can understand the type of foot strike: Rear foot strike (heel strike): *landing on the heel*, Midfoot Strike: *simultaneous landing on both heel and ball of the foot*, fore foot strike: *landing on the ball of the foot*. In addition to know the footedness of certain subject, i.e. the preference of a particular foot. It has been known that general population are right-footedness [98]. Such tests required too many analysis and laboratory work. For instance, Leg

preference is hypothesized to be dependent on the nature of the required test to be performed [98]. Anteroposterior floor oscillations are being used to test foot dominance to achieve postural stability and this done at various frequencies [99]. Other researchers consider the handedness and footedness are correlated, but it has been shown that they are partially correlated and footedness must be considered as a standalone variable [100].

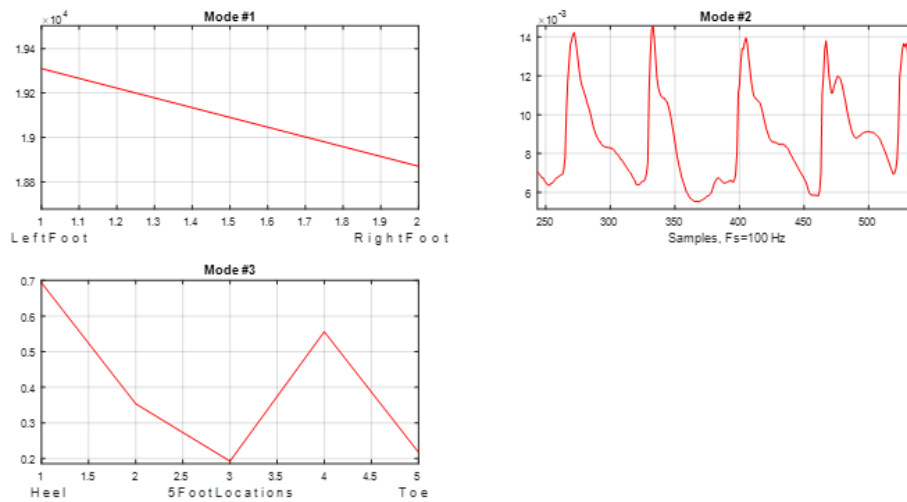


Figure 5.3: PARAFAC Model of a randomly chosen subject. Mode#1, 2 and 3 reflect the footedness, time domain signal and the type of foot strike respectively.

The mid-sensors are averaged to get VGRF distributed over 5 locations in both right and left feet. Performing PARAFAC analysis over the right and left foot as one dimension and the 5 sensors as another dimension in addition to VGRF over time in the third dimension end up with Fig.5.3 after choosing only one component. In this way one can capture the most important loadings and scores dedicated over both feet and sensors distribution. Fig.5.3 clearly indicate in the mode#1 that this subject is left-footed and mode # 3 indicate that this subject is loyal to rear foot strike. This agrees with VGRF signal obtained in mode#3 which is positively skewed.

Performing for another subject the PARAFAC model as shown in Fig.5.4 indicate that the gait of this subject is right-footed with a midfoot foot strike.

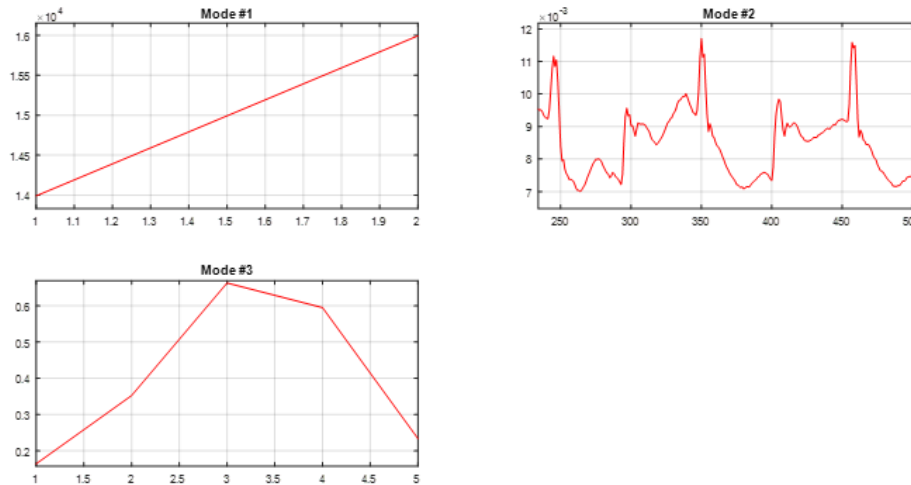


Figure 5.4: PARAFAC Model of a randomly chosen subject. Mode#1, 2 and 3 reflect the footedness, time domain signal and the type of foot strike respectively.

We have assumed that two patterns must be obtained one for the left and the other for the right foot. A third pattern will be capturing the overlapping in gait data while walking. However, there should be consistency when considering sensors locations underfoot. That's why, As we believe that averaging is also is not a good practice between the mid sensors because of the difference in the location and the foot structure, we will handle the heel and toe as one set of sensors and the sensors is between as another set. Considering the same subject in Fig.5.3 but now with two components gives Fig.5.5 with PARAFAC. Mode#3 convey the fact that this subject is with rear foot strike. However, Mode#1 shows two components with opposite slanted lines. Examining VGRF components obtained in Mode #3 shows that part of the second component is highly correlated with the first component while the other portion is negatively correlated. Adding other component lead all the components to be correlated and therefore no additional information

can be captured. So when dealing with VGRF from different sensors underneath both feet, the first component is enough to summarize the most important information in both feet.

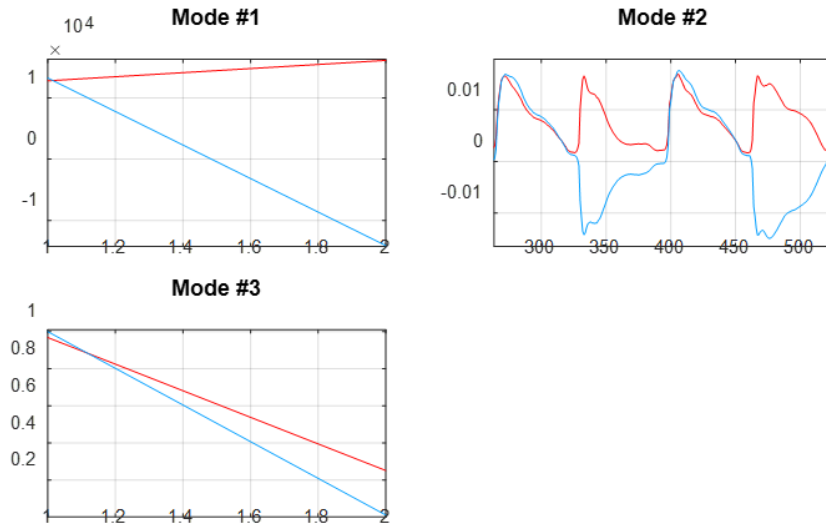


Figure 5.5: PARAFAC Model for the same gait obtained in Fig.5.3 but only with the heel and toe sensors.

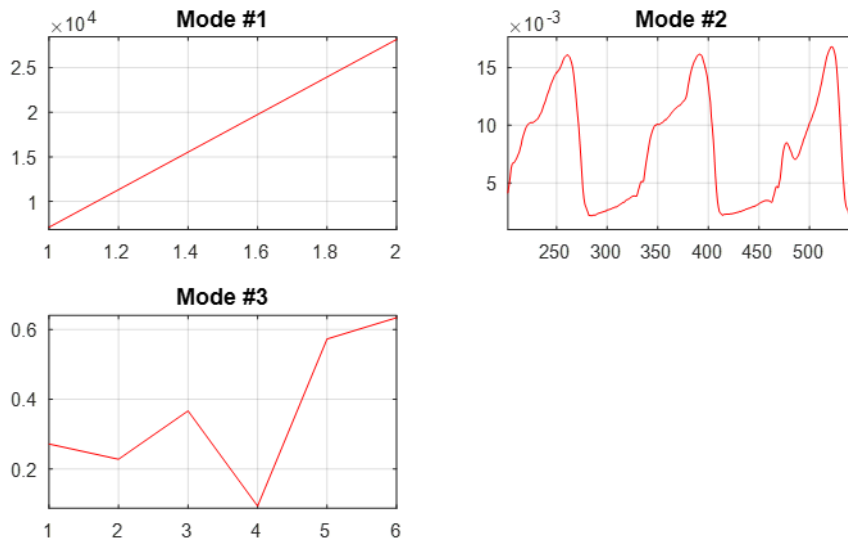


Figure 5.6: PARAFAC Model for the same gait obtained in Fig.5.3 but only with the heel and toe sensors

Now considering the sensors locations 2, 3 and 5 yields the PARAFAC model in Fig.5.6. It indicates that after the heel get in contact with the ground the foot strikes at location 5.

In summary, PARAFAC provided important information concerning the footedness and the type of foot strike of a certain subject. At least it classify subjects with commonalities before further analysis. Most importantly as gait forces are captured from multi-sensor system, PARAFAC had provided a summarized information with only one component. It is therefore useful in analysis of variance.

5.4 PARAFAC Summarizes Information from Multi-Sensors :

We have proved previously that all sensors underneath the foot share most of obvious information. For instance the fundamental frequency is the same underneath all locations of the same foot and this is also similar to the contrary foot. However, Parkinson subjects could have some variability between right and left feet. As a result, 3 components will be chosen. One component corresponds to most variability captured from left foot, the other is from the right foot and one component represent the overlapping between the two feet. Fig.5.7 indicate the three-way PARAFAC procedure being implemented.

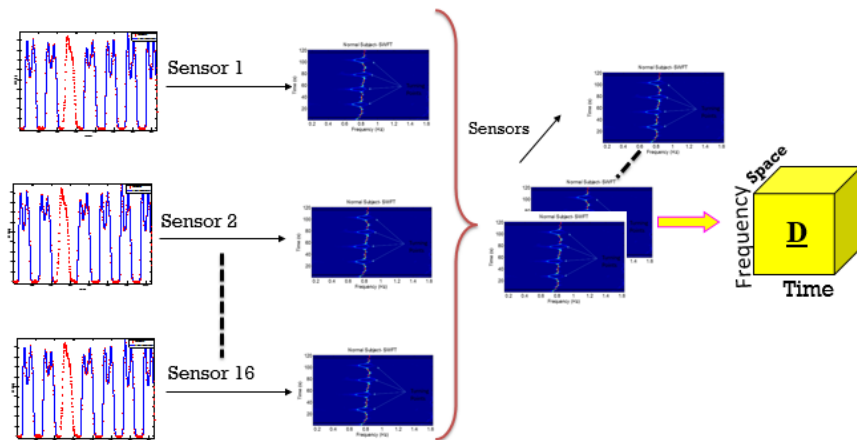


Figure 5.7: PARAFAC Model for the all sensors underneath both feet.

Now, all 5 locations VGRF signals underneath both foot are summarized in three components on each domain. For instance, Fig.5.8 illustrates this point:

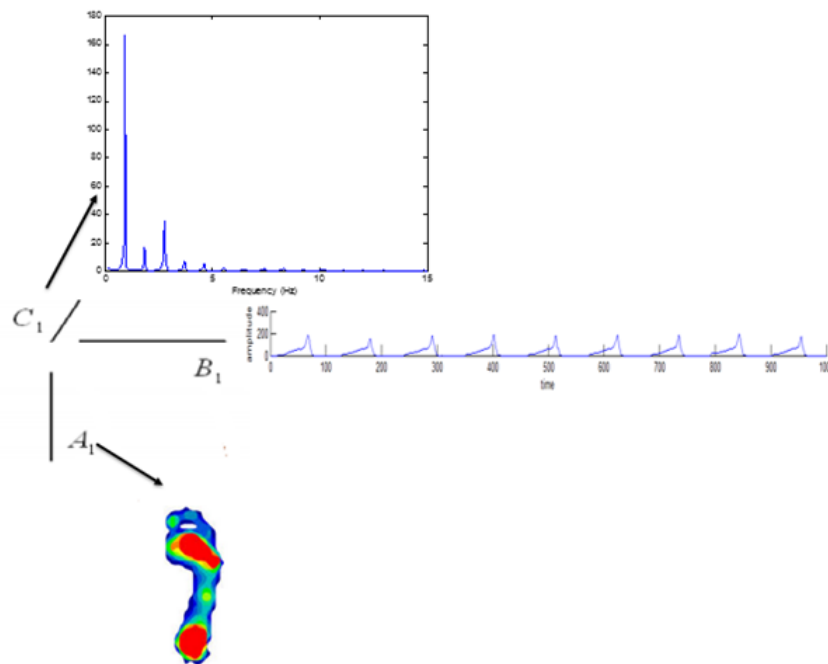


Figure 5.8: First component after conducting the PARAFAC Model for the all sensors underneath both feet.

A superficial analysis will be provided here and we will not dwell too much into details. This is because a more deep interpretations must be conducted.

5.4.1 Space Mode

The loadings for underneath different feet locations is shown in Fig.5.9 for both normal and Parkinson. The left graphs indicate both real and imaginary part while the right graph indicate only the real part over locations indicated in Fig.5.2. In the normal subject there is an indication that there is no need to three components. This is because the right and left foot load distributions are the same. This has been verified on the previous chapter. However, three components obtained in the Parkinson subject do indicate a difference between the obtained three components in this mode of loadings.

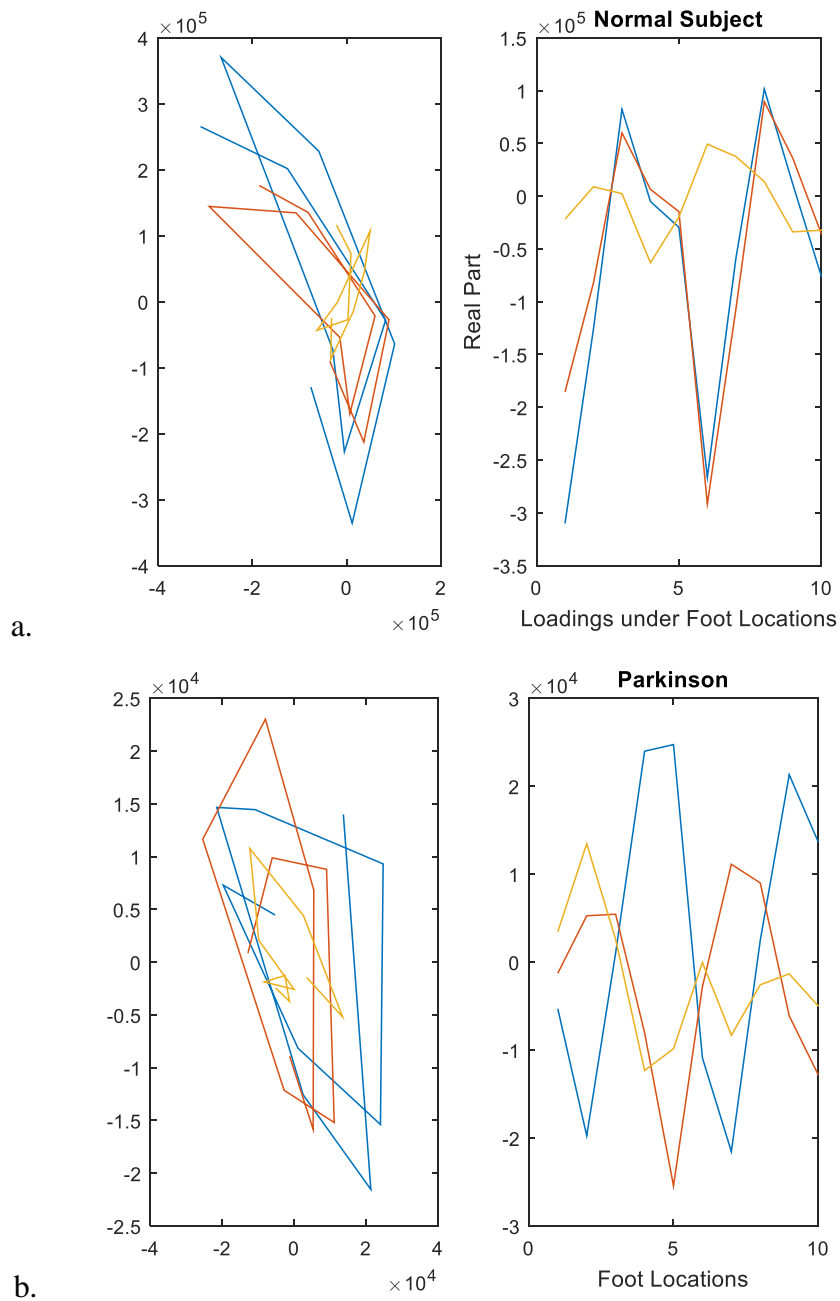


Figure 5.9: Loadings Under both Feet for a normal subject (a) and Parkinson subject (b)

5.4.2 Time Mode

Three components obtained as a summary of forces in both feet is shown in Fig.5.10.

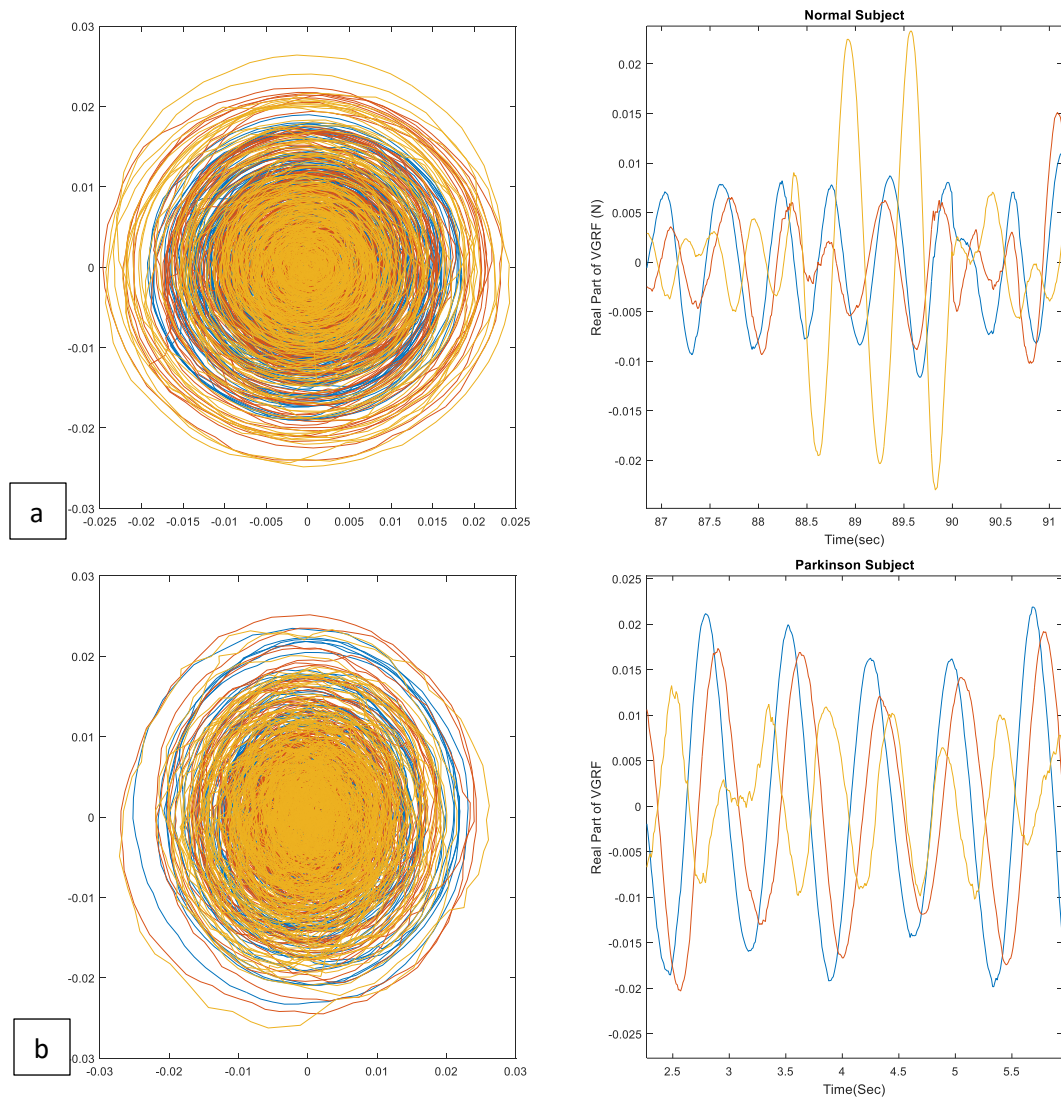


Figure 5.10: VGRF component both Feet for a normal subject (a) and Parkinson subject (b)

5.4.3 Frequency Mode

A summary in frequency domain is also obtained as in Fig.5.11. Variations in the frequency content is spotted to be higher in Parkinson gait than normal gait.

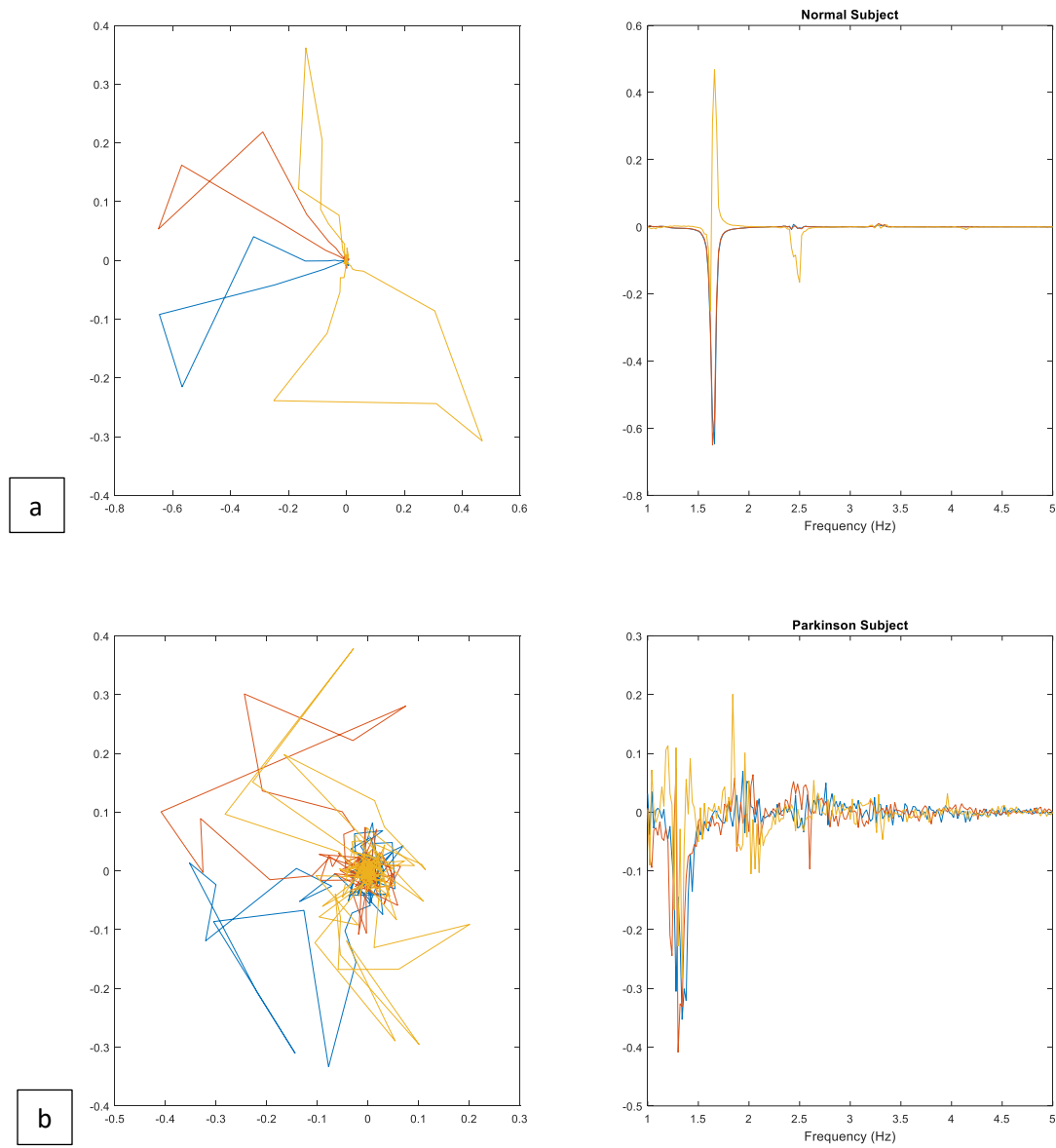


Figure 5.11: Loadings Under both Feet for a normal subject (a) and Parkinson subject (b)

5.5 PARAFAC Classify both Normal and Parkinson :

Conducting the PARAFAC model on both subjects over the synchrosqueezed STFT shows two components that are different from each other. In Fig.5.12 the model is conducted over all

foot locations and Fig.5.13 is a result only of model conducted under the inner arch of left foot.

This is done to give a much more clear view of this difference:

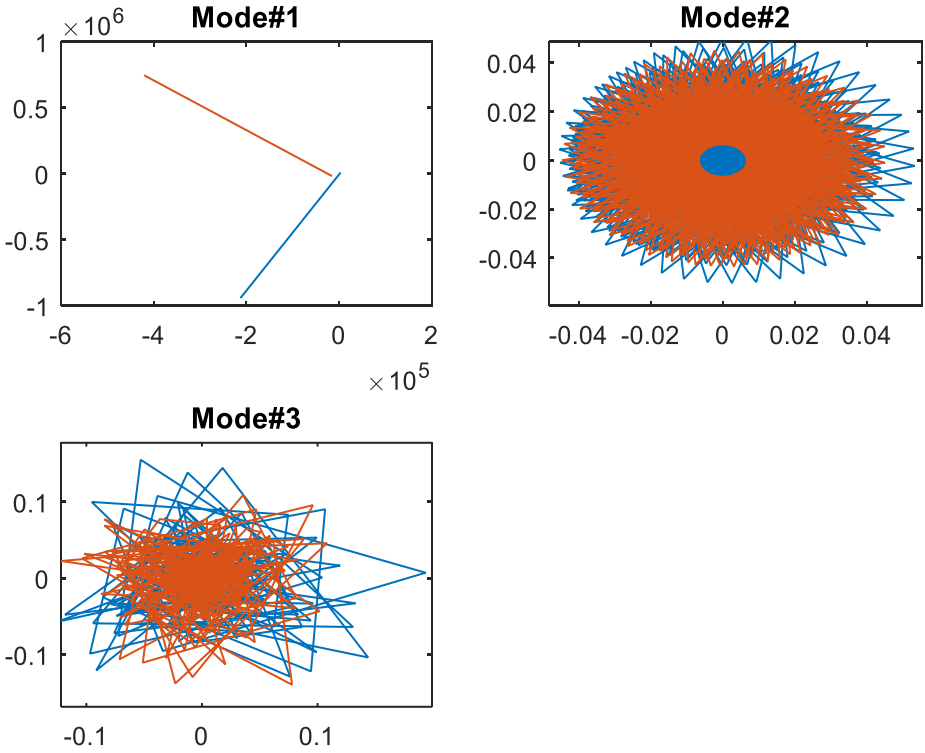


Figure 5.12: PARAFAC Model conducted on both normal and Parkinson subject over all foot locations.

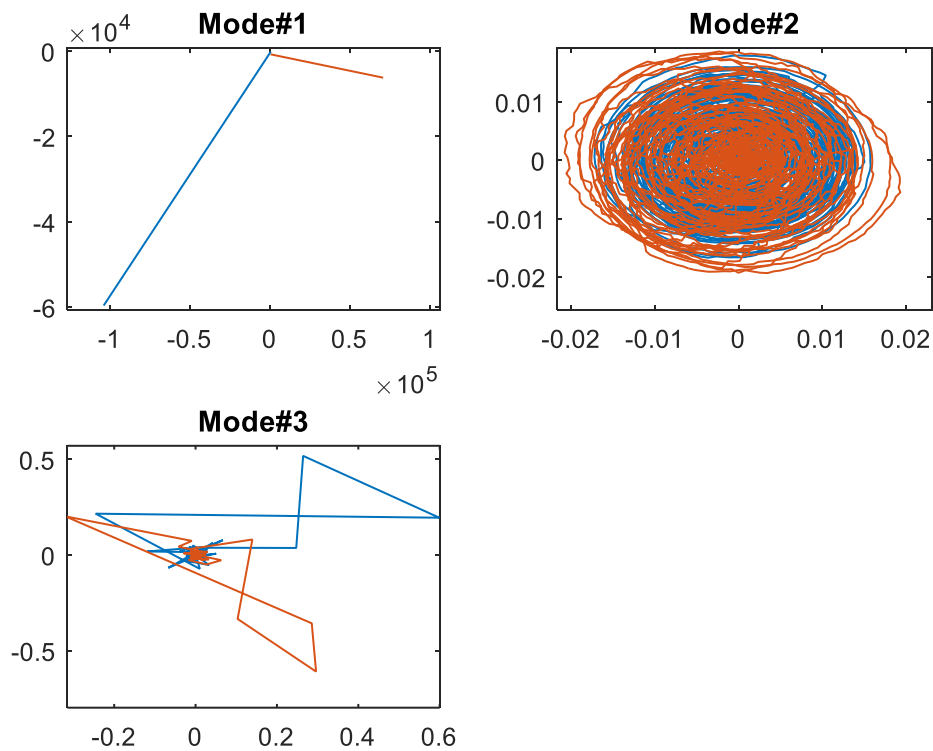


Figure 5.13: PARAFAC Model conducted on both normal and Parkinson subject under the inner arch of the left foot.

5.6 Discussion :

PARAFAC seems to be a good tool if used appropriately. More attention must be given to the number of components being used. Then it is important to find a tool to spot which component correspond to which situation. For instance it is important to differentiate components corresponds to left or right foot, or components that reflect Parkinson or normal gait... and so on. Most importantly, this three-way analysis provide an overall point of view to all traditional domain of analysis. It summarizes them and give the most relevant information.

REFERENCES

- [1] O. Beauchet, G. Allali, G. Berrut, C. Hommet, V. Dubost and F. Assal, "Gait analysis in demented subjects: Interests and perspectives," *Neuropsychiatr Dis Treat.*, vol. 4(1), no. PMCID: PMC2515920, p. 155–160, 2008 February.
- [2] C. Basdogan and F. M. Amirouche, "Nonlinear Dynamics of Human Locomotion: From the Perspective of Dynamical Systems Theory," in *Engineering Systems Design and Analysis Conference*, 1996.
- [3] M. Sobotka, "Hybrid Dynamical System Methods for Legged Robot Locomotion with Variable Ground Contact. Ph.D. thesis," Institute of Automatic Control Engineering, Technische Universität München, 2007.
- [4] R. L. Williams II, "Engineering Biomechanics of Human Motion," in *NotesBook Supplement for ME 4670 / BME 5670*, Ohio University, Dr. Bob Productions, 2014.
- [5] C. L. Vaughan, B. L. Davis and J. C. O'Connor, *Dynamics of human gait*, second edition, Cape Town, South Africa: Kiboho publishers, 2009.
- [6] J. W. Skinner, R. Roemmich, S. Amano, E. Stegemoller, L. Altmann and H. C. J., "FREQUENCY DOMAIN ANALYSIS OF GROUND REACTION FORCE DOES NOT DIFFERENTIATE BETWEEN HYPERKINETIC AND HYPOKINETIC MOVEMENT DISORDERS," University of Florida, Gainesville, FL, USA, 2012.
- [7] J. M. Hausdorff, "Gait variability: methods, modeling and meaning," *Journal of NeuroEngineering and Rehabilitation*, no. doi:10.1186/1743-0003-2-19, pp. 2-19, 20 Jul 2005.
- [8] A. H. Khandokerl, D. Lai, R. K. Begg and M. Palaniswamil, "A Wavelet-Based Approach for Screening Falls Risk in the Elderly using Support Vector Machines," ee.unimelb.edu.au. 2Biomechanics Unit, Centre for Ageing, Rehabilitation, Exercise and Sport, Victoria University, VIC8001, Australia, 2006.
- [9] D. H. Gates and J. B. Dingwell, "PERIPHERAL NEUROPATHY DOES NOT ALTER THE FRACTAL DYNAMICS OF GAIT STRIDE INTERVALS," University of Texas, Austin, TX, USA, 2006.

- [10] T. Amin and D. Hatzinakos, "Determinants in Human Gait Recognition," *Journal of Information Security*, vol. Scientific Research, no. <http://dx.doi.org/10.4236/jis.2012.32009> , pp. 77-85, February 20, 2012.
- [11] S. Ramamoorthy and B. J. Kuipers, "Qualitative Hybrid Control of Dynamic Bipedal Walking," in *Robotics Proceedings*, MIT Press, Cambridge, Massachusetts, 2007, 2007.
- [12] V. Ergović, "Models and methods for locomotion analysis of lower limbs," IBM Croatia, Miramarska 23, 10000 Zagreb, [Online]. Available: http://www.fer.unizg.hr/_download/repository/ergovic_KDI.pdf.
- [13] A. I. Bazin and M. S. Nixon, "Probabilistic combination of static and dynamic gait features for verification," School of Electronic and Computer Science, University of Southampton, SO17 1BJ, UK, 2005.
- [14] D. S. Bloswick and D. B. Chaffin, "AN ERGONOMIC ANALYSIS OF THE LADDER CLIMBING ACTIVITY," *International Journal of Industrial Ergonomics*, Elsevier, vol. 6, pp. 17-27, 1990.
- [15] M. Jeffry. F. Research, "Gait in Parkinson's Disease," National Institutes of Health, National Parkinson Foundation, and the Parkinson's Disease Foundation , 2005. [Online]. Available: <http://www.physionet.org/>.
- [16] W. Niu, T. Feng, C. Jiang and M. Zhang, "Peak Vertical Ground Reaction Force during Two-Leg Landing: A Systematic Review and Mathematical Modeling," *BioMed Research International*, Hindawi, vol. 2010, p. 10 pages, 2014.
- [17] A. Pouliot-Laforte, L.-N. Veilleux, F. Rauch and M. Lemay, "Validity of an accelerometer as a vertical ground reaction force measuring device in healthy children and adolescents and in children and adolescents with osteogenesis imperfecta type I," *J Musculoskelet Neuronal Interact* , vol. 14, no. 2, pp. 155-161, 2014.
- [18] S. Boozari, A. A. Jamshidi, M. Ali Sanjari and H. Jafari, "Effect of Functional Fatigue on Vertical Ground-Reaction Force in Individuals With Flat Feet," *Journal of Sport Rehabilitation*, Human Kinetics, Inc., vol. 22, pp. 177-183, 2013.
- [19] Chau, T. (2001). A review of analytical techniques of gait data. Part2: neural network and wavelet methods. Elsevier- *Gait and Posture*, 102-120.

- [20] I. R. Vega and S. Sarkar, "Experiments on Gait Analysis by Exploiting Nonstationarity in the Distribution of Feature Relationships," Computer Science and Engineering Department, University of South Florida, Tampa, FL, 2002.
- [21] K. Šušmáková, "Nonlinear statistical analysis of human gait dynamics, msc thesis," faculty of mathematics, physics and informatics , Comenius University ,Bratislava ,Department of Biophysics and Chemical Physics , 2003.
- [22] P. Terrier and O. Dériaz, "Kinematic variability, fractal dynamics and local," *journal of neuroengineering and rehabilitation*, no. BioMed Central, pp. 8-12, 2011.
- [23] M. F. del Olmo and J. Cudeiro, "Temporal variability of gait in Parkinson disease: effects of a rehabilitation programme based on rhythmic sound cues," *Elsevier , Parkinsonism and Related disorders*, no. Neuroscience and Motor control group (Neurocon), Department de Medicina-INEF-Galicina, Universidad se A Coruna, 15006 A coruna, pp. 25-33, 2005.
- [24] T. E. Lockhart, R. Soangra, J. Zhang and X. Wu, "Wavelet based automated postural event detection and activity classification with single IMU (TEMPO)," *Biomed Sci Instrum, PMID: PMC3755105*, vol. 49, p. 224–233, 2013.
- [25] S. WINIARSKI and A. R. KUCHARSKA, "Estimated ground reaction force in normal and pathological gait," *Acta of Bioengineering and Biomechanics*, vol. 11, January 19th, 2009.
- [26] D.A. Winter, "Biomechanics and Motor control of Human Gait: Normal, Elderly and Pathological," *Journal of Biomechanics*, Vol. 25, No.8, p.949. Waterloo, Ontario, 1991.
- [27] H. Yu and T. S. Gyan, "Towards a Methodology for the Differential Analysis in Human Locomotion: A Pilot Study on the Participation of Individuals with Multiple Sclerosis," *Scientific Research*, vol. 5, pp. 20-26, October 2012.
- [28] D. Sanderson, "school of human kinetics biomechanics 1," the university of british columbia, 2004. [Online]. Available: faculty.educ.ubc.ca/sanderson/courses/HKIN151/Impulse/constant.htm. [Accessed 2016].
- [29] T. Minamisawa, H. Sawahata, K. Takakura and T. Yamaguchi, "Characteristics of temporal fluctuation of the vertical ground reaction force during quiet stance in Parkinson's disease," *Gait & Posture*, vol. 35, no. 2, pp. 308-311, February 2012.
- [30] T. Takahashi, K. Ishida, D. Hirose, Y. Nagano, K. Okumiya, M. Nishinaga, Y. Doi and H. Yamamoto, "vertical ground reaction force shape is associated with gait parameters, timed up and go, and functional reach in elderly females," *J Rehabil Med*, vol. 36, p. 42–45, 2004.

- [31] T. Marasović, M. Cecić and V. Zanchi, "Analysis and Interpretation of Ground Reaction Forces in Normal Gait," Biomechanics and Control Systems Faculty of Electrical Engineering, Mechanical Engineering and Naval Architecture University of Split Ruđera Boškovića bb, 2009 .
- [32] K.Sabri, M.ElBadaoui, F.Guillet, A.Belli, G.Millet and J.Morin, "Cyclostationary Modeling of Ground Reaction Force Signals," France, Saint etaine ,Signal Processing 90(4):1146-1152, April 2010.
- [33] M. AM, M. EF, A. MC and N. J., "Principal component analysis of vertical ground reaction force: a powerful method to discriminate normal and abnormal gait and assess treatment.," PubMed - indexed for MEDLINE, 2006.
- [34] A. Muniz and J. Nadal, "Application of principal component analysis in vertical ground reaction force to discriminate normal and abnormal gait," *ELSEVIER*, vol. 29, no. 1, p. 31–35, January 2009.
- [35] K. Sabri, M. E. Badaoui and F. Guillet, " Blind Separation of Ground Reaction Force Signals, LASPI, Universit´e Jean Monnet," *Applied Mathematical Sciences*, vol. 6, no. 53, p. 2605–2624, 2012.
- [36] N. Sterqiou, G. Giakas, J. E. Byrne a and V. Pomeroy, "Frequency domain characteristics of ground reaction forces during walking of young and elderly females," *Clinical Biomechanics*, vol. 17, p. 615–617, July 2002.
- [37] J. T. Worobets and D. J. stefanyshyn, "Normalizing vertical ground reaction force peals to body weight in heel-toe running," Human performance Laboratory, Faculty of Kinesiology, University of Calgary, 1990.
- [38] K. Fournier, K. Radonovich, M. Tillman and J. Chow, "GROUND REACTION FORCES DURING THE STANCE PHASE OF GAIT OF YOUNG AUTISTIC CHILDREN," University of Florida, Gainesville, FL, USA, 2006 .
- [39] B. Raja, R. Neptune R and S. Kautz A, "Quantifiable patterns of limb loading and unloading during hemiparetic gait: Relation to kinetic and kinematic parameters," *JRRD*, vol. 49, no. 9, p. 1293–1304, 2012.
- [40] J. W. Wannop, J. T. Worobets and D. J. Stefanyshyn, "Normalization of Ground Reaction Forces, Joint Moments, and Free Moments in Human Locomotion," *Journal of Applied Biomechanics*, vol. 28, pp. 665-676, 2012.

- [41] M. E. Taylor, M. M. Ketels, K. Delbaere, S. R. Lord, A. S. Mikolaizak and J. C. T. Close, "Gait impairment and falls in cognitively impaired older adults: an explanatory model of sensorimotor and neuropsychological mediators," *Age and Ageing* , vol. 41, p. 665–669, 2012.
- [42] M. Dubey, A. Wadhvani and S. Wadhvani, "Gait Based Vertical Ground Reaction Force Analysis for Parkinson's Disease Diagnosis Using Self Organizing Map," *International journal of Advanced Biological and Biomedical Research* , vol. 1, no. 2322 - 4827, pp. 624-636, 2013.
- [43] B. Kluitenberg, S. Bredeweg W Bredeweg, S. Zijlstra, W. Zijlstra and I. Buist, "Comparison of vertical ground reaction forces during overground and treadmill running. A validation study," Kluitenberg et al. *BMC Musculoskeletal Disorders* , 2012.
- [44] R. Kram, T. M. Griffin, J. M. Donelan and Y. Hui Chang, "Force treadmill for measuring vertical and horizontal ground reaction forces," *Journal of Applied Physiology*, vol. 85, pp. 764-769, 1998.
- [45] A. v. d. Borget and J. d. Koning, "ON OPTIMAL FILTERING FOR INVERSE DYNAMICS ANALYSIS," in *Proceedings of the IXth Biennial Conference of the Canadian Society for Biomechanics*, Vancouver, 1996.
- [46] F. Mawase, T. Haizler, S. Bar-Haim and A. Karniel, "Kinetic adaptation during locomotion on a split belt treadmill," *J Neurophysiol*, vol. 109, no. 10.1152, p. 2216 –2227, 2013.
- [47] Y. Wang and K. Watanabe, "Limb Dominance Related to the Variability and Symmetry of the Vertical Ground Reaction Force and Center of Pressure," *Journal of Applied Biomechanics*, vol. 28, pp. 473-478, 2012.
- [48] J. Perttunen, "Foot Loading in Normal and Pathological Walking," *Studies in Sport, Physical Education and Health*, ISSN 0356-1070; 83, University of Jyväskylä, 2002, 86 p. , 2002.
- [49] T. Khajah and G. Hou, "Parameter identification for vertical ground reaction forces on feet while running," *International Sports Engineering Association*, Springer Link , vol. 18, no. 4, pp. 217-226, 19 July 2015.
- [50] Browning, R. C., Baker, E. A., Herron, J. A. and Kram, R. "Effects of obesity and sex on the energetic cost and preferred speed of walking". *Journal of Applied Physiology* 100(2), p. 390–398. doi:10.1152/jappphysiol.00767.2005, 2006.
- [51] J. Dingwell and L. Marin, "Kinematic variability and local dynamic stability of upper body motions when walking at different speeds." *Journal of Biomechanics*, vol. 39, no. 3, p. 444–452, 2006.

- [52] Malatesta, D., Simar, D., Dauvilliers, Y., Candau, R., Saad, H., Préfaut, C. and Caillaud, C. "Aerobic determinants of the decline in preferred walking speed in healthy, active 65- and 80-year-olds". *European Journal of Physiology* 447 (6): 915–921. doi:10.1007/s00424-003-1212-y. PMID 14666424, 2004.
- [53] H. Kang and J. Dingwell, "Separating the effects of age and walking speed on gait variability.," *Gait Posture*, 2008 May;27(4):572-7. Epub 2007 Sep 4.
- [54] J. M. Hausdorff, M. E. Cudkowicz, R. Firtion, F. Y. Wei and A. L. Goldberger, "Gait Variability and Basal Ganglia Disorders: Stride-to-Stride Variations of Gait Cycle Timing in Parkinson's Disease and Huntington's Disease," *Movement Disorders* , vol. 13, no. 3, pp. 428-437, 1998.
- [55] D. A. Winter, "Human balance and posture control during standing and walking," *Gait&Posture*, vol. 3, pp. 193-214, 1995.
- [56] J. HS, H. J, Y. WJ, J. B and P. KS, "Classification of Parkinson gait and normal gait using Spatial-Temporal Image of Plantar pressure.," *IEEE Eng Med Biol Soc.* 4672-5. doi: 10.1109/IEMBS.2008.4650255., 2008.
- [57] R. A. Kenny, C. N. Scanaill and M. McGrath, "Falls Prevention in the Home: Challenges for New Technologies," Trinity College , Intel, Ireland, 2012.
- [58] T. Iluz, E. Gazit, T. Herman, E. Sprecher, M. Brozgol, N. Giladi, A. Mirelman and J. M. Hausdorff, "Automated detection of missteps during community ambulation in patients with Parkinson's disease: a new approach for quantifying fall risk in the community setting," *Journal of NeuroEngineering and Rehabilitation* , pp. 11-48, 3 April 2014.
- [59] T. E. Lockhart, J. C. Woldstad and J. L. Smith, "Effects of age-related gait changes on the biomechanics of slips and falls," *Ergonomics* , vol. 46, no. 12, p. 1136–1160, 2003.
- [60] J. B. Casebolt, S. Yoon, S. Shin and Y.-H. Kwon, "biomechanical comparison of elderly gait during elevation changes," Texas Woman's University, Denton, TX, USA, 2006.
- [61] I. Melzer, I. Shtilman and N. Rosenblatt, "Reliability of voluntary step execution behavior under single and dual task conditions," *Journal of NeuroEngineering and Rehabilitation*, Vols. 4-16, 29 May 2007.
- [62] M. N. BENJUYA and J. KAPLANSKI, "Postural stability in the elderly: a comparison between fallers and non-fallers," *Age and Ageing* , vol. 33, p. 602–607, 2004.

- [63] M. L. Callisaya, L. Blizzard, M. D. Schmidt, K. L. Martin, J. L. Mcginley, L. M. Sanders and V. K. SRikanth, "Gait, gait variability and the risk of multiple incident falls in older people: a population-based study," *Age and Ageing* , vol. 40, p. 481–487, 2011.
- [64] J. KULMALA, A. VILJANEN, S. SIPILA, S. PAJALA, O. PARSSINEN, M. KAUPPINEN, J. KAPRIO and T. RANTANEN, "Poor vision accompanied with other sensory impairments as a predictor of falls in older women," *Age and Ageing* , vol. 38, p. 162–167 , 2009.
- [65] J. H. Challis, S. L. Winter and D. Quig, "postural stability in the young and elderly as a consequence of perturbations," Biomechanics Laboratory, Department of Kinesiology, The Pennsylvania State University, University Park, PA, USA, 2006 .
- [66] K.-C. Siu, V. Lugade, L.-S. Chou, P. v. Donkelaar and M. Woollacott, "secondary task effect on gait stability during obstacle clearance in older adults," Department of Human Physiology, University of Oregon, Eugene, Oregon, U.S.A, 2006 .
- [67] O. BEAUCHET, V. DUBOST, G. ALLALI, R. GONTHIER, R. HERMANN and R. W. KRESSIG2, "Faster counting while walking' as a predictor of falls in older adults," *Age and Ageing* , vol. 36, p. 418–423 , 9 March 2007.
- [68] I. Melzer, I. Kurz1, D. Shahar, M. Levi and L. Oddsson, "Application of the voluntary step execution test to identify elderly fallers," *Age and Ageing* , vol. 36, p. 532–537, 2007.
- [69] L. Z. Rubenstein and K. R. Josephson, " Falls and Their Prevention in Elderly People: What Does the Evidence Show?," *Med Clin N Am* , vol. 90, p. 807–824, 2006.
- [70] S. Turner, R. Kisser and W. Rogmans, "Falls among older adults in the EU-28: Key facts from the available statistics," EuroSafe: European Association for injury prevention and safety promotion, Amsterdam , Amsterdam , 2015.
- [71] A. M. Spellbring, Assessing elderly patients at high risk for falls: A reliability study. *J Nurs Care Quality* 6(3):30-35, 1992.
- [72] Murray CJL, Lopez AD, editors. The global burden of disease. Boston: The Harvard School of Public Health; p. 201–46; 1996.
- [73] P. Jérôme , French National Health at Home center (CNR Santé à Domicile et Autonomie). <http://www.cnr-sante.fr/2012/10/technologies-de-detection-de-chute-des-personnes-agees/?PHPSESSID=d5fmmts2cp14c3q2v26uduk6i4,2012>

- [74] Le Figaro France, "The falls in the elderly are common and cause serious complications", <http://sante.lefigaro.fr/mieux-etre/accident/chutes-personnes-agees/quels-chiffres>
- [75] JA .Stevens , PS .Corso , EA .Finkelstein , TR. Miller : The costs of fatal and non-fatal falls among older adults. Stevens JA, Corso PS, Finkelstein EA, Miller Inj Prev. Oct;12(5):290-5, 2006.
- [76] K.Jane, Falls among elderly 'cost NHS & pound;4.6m a day' , Independent, <http://www.independent.co.uk/life-style/health-and-families/health-news/falls-among-elderly-cost-nhs-pound46m-a-day-2006411.html>, Monday 21 June 2010.
- [78] C. Junsheng, Y. Dejie and Y. Yu, "Research on the Intrinsic mode function (IMF) criterion in EMD method," Hunan University, 2006.
- [79] D. Iatsenko, P. V. E. McClintock and A. Stefanovska, "Linear and synchrosqueezed time-frequency representations revisited. Part I: Overview, standards of use, related issues and algorithms.," in Department of Physics, Lancaster University, Lancaster LA1 4YB, UK, arXiv:1310.7215v2, 25 May 2014.
- [80] S. D. Stearns and D. . R. Hush, Digital Signal Processing with Examples in MATLAB®, Second Edition, Boca Raton, Florida 33431: CRC Press LCC, 2002.
- [81] R. H. Herrera, J. Han and M. Van der Baan, "Applications of the synchrosqueezing transform in seismic time-frequency analysis," GEOPHYSICS, vol. 79, no. 11, p. V55–V64, MAY-JUNE 2014.
- [82] M. S. Pepe, "Estimation and comparison of receiver operating characteristic curves," The Stata Journal, vol. 9, no. 1, p. 1–16, 2009.
- [83] Ng .Andrew, Machine Learning, Stanford University, Course code CS229. Available at <http://cs229.stanford.edu>, Spring 2016.
- [84] Lecture notes on forecasting by Robert Nau at Fuqua School of Business Duke University, Available at: http://people.duke.edu/~rnau/Slides_on_ARIMA_models--Robert_Nau.pdf
- [85] D. Powell W, B. Long, C. Milner E and S. Zhang, "Effects of Vertical Loading on Arch Characteristics and Intersegmental Foot Motions," *Journal of Applied Biomechanics*, vol. 28, no. 2012 Human Kinetics, Inc., pp. 165-173, 2012.
- [86] Alkhatib, R., Diab, M., Moslem, B., Corbier, C., & ElBadaoui, M. "Classification of Ground Reaction Forces Based on Non Stationary Analysis", Proceedings of the International Conference on Computer Vision and Image Analysis, IEEE ICCVIA 2015, pp. 1-4 , Soussa, Tunisia, Jan. 2015

- [87] C. Laughton and I. McClay, "Ground reaction force variables as predictors of lower extremity shock in forefoot and rearfoot strike patterns," in *asbweb.org*, 2000.
- [88] J. Hunter P, R. Marshall N and P. McNair J, "Relationships Between Ground Reaction Force Impulse and Kinematics of Sprint-Running Acceleration," *JOURNAL OF APPLIED BIOMECHANICS*, vol. 21, no. 2005 Human Kinetics Publishers, Inc., pp. 31-43, 2005 .
- [89] M. Tramontano, S. Bonni, C. A. Martino, F. Marchetti, C. Caltagirone, G. Koch and A. Peppe, "Blindfolded Balance Training in patients with Parkinson Disease: a sensory-motor strategy to improve the gait.," *BioMed Research International*, 2015 , Article ID 716042, 8 pages, 2015.
- [90] H. N. Chia Min Lim, T. Tzen Vun Yap and C. Ching Ho, "Gait Analysis and Classification on Subjects with Parkinson's Disease," *Jurnal Teknologi (Sciences & Engineering)*, vol. 72:1, no. eISSN 2180-3722, pp. 1-6, 2015 .
- [91] D. B. Fineberg, P. Asselin, N. Y. Harel, I. Agranova-Breyter, S. D. Kornfeld, W. A. Bauman and A. M. Spungen, "Vertical ground reaction force-based analysis of powered exoskeleton-assisted walking in persons with motor-complete paraplegia," *J Spinal Cord Med.* , vol. 36, no. 4, p. 313–321, 2013 .
- [92] R. Alkhatib, C. Corbier, M. El Badawi, B. Moslem, M. Diab, "Sensor's Ground Reaction Force Behaviour for Both Normal and Parkinson Subjects - a Qualitative Study", 37th Annual International Conference of the IEEE Engineering in Medicine and Biology Societ. Mico-Milan Conference Center – Milan, Italy, August 25-29 2015.
- [93] J. Garza-Ulloa, "Sensor Validation using Linear Regression for Error Detection between prediction data behavior and acquired data applied on sensing vertical Ground Reaction Forces on Human Gait Analysis.," *International Test and Evaluation Association (ITEA) White Sands Missile Range*, pp. 24-27 , 2012.
- [94] S. Lee and T. J. Armstrong, "CPWR Final Report," in *Field Tool for On-Site Biomechanical Analysis During Ladder Climbing*, University of Michigan , The Center for Construction Research and Training, 2014, pp. 13-14. I. S. Jacobs and C. P. Bean, "Fine particles, thin films and exchange anisotropy," in *Magnetism*, vol. III, G. T. Rado and H. Suhl, Eds. New York: Academic, 1963, pp. 271–350.
- [95] T. Anthony, E.W. Roshana, "Biomechanics of Running and Walking, Issue 43 of Dolciani Mathematical Expositions," in *Mathematics and Sports*, contributor: Mathematical Association of America, MAA, 2010, 2010, p. 324.

- [96] Y. Yorozu, M. Hirano, K. Oka, and Y. Tagawa, "Electron spectroscopy studies on magneto-optical media and plastic substrate interface," *IEEE Transl. J. Magn. Japan*, vol. 2, pp. 740–741, August 1987 [Digests 9th Annual Conf. Magnetism Japan, p. 301, 1982].
- [97] N. A. Krasnegor, D. M. Rumbaugh and R. L. Schiefelbusch, "Biological and Behavioral Determinants of Language Development," ISBN 978-1-317-78389-3, Psychology Press., 2014, p. 182.
- [98] J. Velotta, J. Weyer, A. Ramirez, J. Winstead and R. Bahamonde, "RELATIONSHIP BETWEEN LEG DOMINANCE TESTS AND TYPE OF TASK," *Portuguese Journal of Sport Sciences, Biomechanics in Sports*, vol. 29, no. 11 , pp. 1035-1038, 2011.
- [99] T. Kiyota and K. Fujiwara, "Dominant side in single-leg stance stability during floor oscillations at various frequencies," *Journal of Physiological Anthropology* , vol. 33, no. 25, pp. 2-9, 2014.
- [100] J. Chapman, L. Chapman and J. Allbn, "The Measurement of Foot Preference," *Pergamon Journals: Neuropsychologia* , vol. 25, no. 3, pp. 579-584, 1987.

LIST OF PUBLICATIONS

JOURNALS:

IN PROGRESS: R.Alkhatib, M.Diab, C.Corbier, M.El Badawi, B.Moslem "Simplified gait analysis and classification for early detection of Parkinson", *Physiological Measurement, IOP Science*, submitted Article reference: PMEA-101332

R.Alkhatib, M.Diab, C.Corbier, M.El Badawi "Prediction of Human Gait - Vertical Ground Reaction Force", *International Journal of Enhanced Research in Science Technology & Engineering*, Vol. 5 Issue 2, Pp. 206-216, ISSN: 2319-7463, February-2016. <http://www.erpublications.com/>

R.Alkhatib, M.Diab, B.Moslem, M.El Badawi, C.Corbier," gait - ground reaction force sensors selection based on roc curve evaluation", *The 4th Int'l Conf. on Signal and Image Processing (CSIP 2015Mar.)*. Paper ID: CSIP2015Mar_80008, *Scientific Research Publishing (SRP)* , "Journal of Computer and Communications" (ISSN:2327-5219), California (US), article acceptance: 2014-12-28, Vol. 3, 13-19, 2015.

INTERNATIONAL CONFERENCES:

M.Diab, R.Alkhatib, B.Moslem ,C.Corbier, M.El Badawi, "Synchrosqueezing Characterize Non-Stationary Signals: Application on Gait-Vertical Ground Reaction Force", *Global Summit on Computer and Information Technology (GSCIT'2016)*, IEEE. Sousse, TUNISIA, 16-18-July, 2016, Accepted Article.

K.Hiba, M.Diab, B.Moslem ,R.Alkhatib, C.Corbier, M.El Badawi, "Frequency Content Analysis of Gait -Vertical Ground Reaction Force", *Third International Conference On Advances In Biomedical Engineering (ICABME15)*, IEEE. EMB, Doctoral School of Sciences and Technology (EDST) and the Faculty of Engineering Lebanese University (LU), Hadat-Beirut, Lebanon, September 16-18, 2015.

R.Alkhatib, C.Corbier, M.El Badawi, B.Moslem, M.Diab,"Sensor's Ground Reaction Force Behaviour for Both Normal and Parkinson Subjects- a Qualitative Study", *37th Annual International Conference of the IEEE Engineering in Medicine and Biology Societ. Mico-Milan Conference Center – Milan, Italy, August 25-29 2015*.

Rami Alkhatib, Mohamad Diab, Bassam Moslem, Christophe Corbier, Mohamed El Badaoui. "Classification of Ground Reaction Forces Based on Non Stationary Analysis", *Proceedings of the International Conference on Computer Vision and Image Analysis, IEEE ICCVIA 2015*, pp. 1-4 , Soussa, Tunisia, Jan. 2015.

NATIONAL CONFERENCES:

R. Alkhatib, M. El Badawi, C. Corbier, B. Moslem, M. Diab, "Gait-Ground Reaction Force Signals- Balancing Parameters", 21st LAAS International Science Conference, pp. 95-98, Beirut, Lebanon, April 2015.

R. Alkhatib, M. Diab, B. Moslem, M. El Badawi, C. Corbier, "Non Stationary Analysis of Gait-Ground Reaction Force Signals", LAAS20, International Science Conference, pp. 56-59, Beirut, Lebanon, March 2014.